AN ABSTRACT OF THE THESIS OF

Mingdong Huang for the degree of Doctor of Philosophy

in Chemistry Presented on Februry 19, 1993.

TITLE: Synthesis and Structure of Transition Metal Siloxy Compounds.

Abstract approved: Redacted for Privacy

Dr. Carroll W. DeKock

In this thesis work, several triphenylsiloxy compounds were synthesized through direct silylation of silver metallates by triphenylchlorosilane. This synthesis method has the advantages that the product isolation is simple; the products are relatively pure; and the extent of the reaction is easy to monitor. The reactions of $MoO_2(OSiPh_3)_2$ with various reagents were studied. With Lewis bases L, simple adducts were formed: $MoO_2(OSiPh_3)_2(L)_n$ (n = 1 for L = $OPPh_3$ and 2,2'-bipyridine). In the study of the oxygen atom transfer reactions of $MoO_2(OSiPh_3)_2$ with trialkylphosphines, an interesting compound, $MoO_2(OSiPh_3)_2(PPh_3)$, was isolated and characterized by X-ray diffraction methods. $MoO_2(OSiPh_3)_2$-(PPh_3) has a distorted trigonal bipyramidal configuration around Mo center and is the first example that contains Mo(VI)-Phosphine bond. This compound is a direct evidence to support a mechanism of oxygen atom transfer reaction where the first step was considered to be the attack of a phosphine on a metal center instead of an oxo atom in the metal-oxo moiety. An EHMO (Extended Hückel Molecular Orbital) calculation was performed on a model compound of $MoO_2(OSiPh_3)_2(PPh_3)$ to explore the nature

of the Mo(VI)-Phosphine bond. The structure of a Zn compound was also reported in this thesis as a product of reaction between $MoO_2(OSiPh_3)_2$ and diethylzinc. The structure has several features: a Zn trimer with both three- and four-coordinate Zn atoms; two Zn-ethyl bonds which are air-stable.

M-O-Si bond angles has long been a subject of discussions. Both electronic and steric factors have been suggested to explain the M-O-Si bond angles. By summarizing all available data in the literature, this thesis work found a correlation between the M-O-Si angles and the O...O separation of two neighboring triphenylsiloxy ligands in $\{M(OSiPh_3)_2\}$ type complexes, and suggested that the steric factor plays a more important role in determing M-O-Si bond angles in this particular case.

Synthesis and Structure

of

Transition Metal Siloxy Compounds

by

Mingdong Huang

A THESIS

submitted to

Oregon State University

in partial fulfillment of
the requirements of the
degree of

Doctor of Philosophy

Completed Februry 19, 1993

Commencement June, 1993

APPROVED:

Redacted for Privacy

Professor of Chemistry in charge of major

Redacted for Privacy

Head of Department of Chemistry

Redacted for Privacy

Dean of Graduate School

Date thesis is presented: February 19, 1993

Prepared by: Mingdong Huang

ACKNOWLEDGEMENTS

I would like to express my appreciation to the many people who gave me indispensable help during my four years in Oregon State University. It has been an honor to be associated with Prof. Carroll W. DeKock. His guidance, encouragement, and patience contributed greatly to my personal and professional growth and is greatly appreciated.

I am deeply indebted to my family, especially my wife, Yumei, whose love, understanding and support during my study in OSU were invaluable to me.

Many thanks are extended to Prof. Douglas Keszler, Prof. Kevin P. Gable and Prof. James Krueger for their guidance and productive discussion on my thesis work; to Kathleen Schaffers for her help in X-ray diffraction study; to John Archibald, Roger Kohnert, and Christine Pastorek for the help each has given.

I am grateful to the Department of Chemistry at OSU for its financial support for my education at OSU.

TABLE OF CONTENTS

TABLE OF CONTENTS
(Cont'd)

LIST OF FIGURES

LIST OF TABLES

Synthesis and Structure of Transition Metal Siloxy Compounds

Chapter 1

Introduction to Oxo Siloxy Chemistry

This thesis work focuses on the preparation of transition metal oxo triphenylsiloxy (Ph_3SiO-) complexes, and the reactions of one of the triphenylsiloxy compound, $MoO_2(OSiPh_3)_2$, with a variety of reagents. The products are studied by X-ray diffraction methods.

The aspects of several branches in inorganic chemistry that relate to this thesis work will be addressed in this chapter. These include alkoxide chemistry, the chemistry of the compounds that contain steric-demanding ligands, and the chemistry of metal-ligand multiple bonds, especially metal oxo double bonds.

1-1. Alkoxy and siloxy chemistry

Transition metal alkoxide [$M(OR)_x$] chemistry has been a very active area in inorganic chemistry in the past twenty years [1].

The empirical formulas of homoleptic metal alkoxide $[M(OR)_x]$ is, in general, not the molecular formula because the metal strives to attain its preferred coordination number by alkoxide bridge formation. Thus, oligomeric structures, $[M(OR)_x]_n$, where n represents the degree of oligomerization, are often found both in the solid state and in solution. The value of n depends on the nature of the metal and the steric properties of R. The species present in solution may not be the same as that found in the solid state and the nature of the solvent and temperature can lead to complex equilibria.

Bradley [1e] formulated a structural theory for the oligomerization of metal alkoxides based on the premise that the observed structures represent a compromise of opposing forces --- an enthalpic drive to form the maximum number of M-O bonds by alkoxide bridge formation and an entropic drive to minimize aggregation. He also pointed out in 1967 that metal oxide alkoxide polymers $[MO_x(OR)_{(y-2x)}]_n$ bridge the gap between the oligomeric alkoxides $[M(OR)_y]_m$ and the macromolecular metal oxides $[M_2O_y]_\infty$. Similarly, the metal oxides trialkylsiloxides $[MO_x(OSiR_3)_{(y-2x)}]_n$ may be regarded as intermediate between the oligomeric metal trialkylsiloxides $[M(OSiR_3)_y]_m$ and the mineral silicate macromolecules.

Chisholm [1d,2] published a series of papers entitled "Metal Alkoxides. Models for Metal Oxides". He also pointed out [3] the alkoxide clusters that contain metal-metal bonds are analogues to the cluster subunits found in the solid-state structures of reduced metal oxides. For example [3], the $[W_4(OEt)_{16}]$ cluster contains the same $[M_4(\mu_3\text{-}O)_2(\mu\text{-}O)_4O_{10}]$ unit found in the $[Ba_{1.14}Mo_8O_{16}]$ structure.

Besides as a model for metal oxides, the metal oxo siloxides are also considered as a model for the surface of silica-supported catalysts. One example is Feher's compound [11], the vanadium-containing polyhedral oligometallasilsesquioxanes (POMSS), which imitate the "three-legged" surface species on the silica-supported vanadium-catalyst.

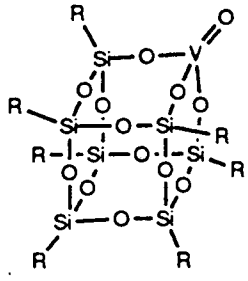

Another impetus for the development of alkoxide (siloxide) [12] complexes comes from the idea that they may be useful as molecular precursors to unusual materials such as superconducting oxides via the hydrolytic sol-gel process. Such molecular precursors guarantee dispersion of metal sources at the molecular level and provide uniform reaction sites for the reaction. Also, alkoxide (siloxide) complexes can provide chemically more robust alternatives to the more common cyclopentadienide complexes in organometallic and catalytic applications.

There are many interesting features of alkoxides and siloxides [3]. Alkoxides and siloxides are both uninegative π donors, π^x, where $0<x<4$, and thus can stabilize high-oxidation-state metal centers in which vacant metal d_π orbitals are present: e.g., the d_0 metal complexes $[Mo(OMe)_6]$. The alkoxide ligand is electronically flexible in that the π^x can vary

as a function of the M-O-C angle; i.e., as the angle approaches 180°, x approaches 4 if the metal has available vacant dπ orbitals. The M-O-C angles (and also M-O-Si angles for siloxides) are influenced by steric and electronic factors at the metal center. Sterically demanding RO ligands will commonly have large M-O-C angles. If there are filled metal dπ orbitals, these will be raised in energy by the presence of alkoxide ancillary ligands. The M-O-Si bond angles in siloxides are also influenced by both electronic and steric factors. Chapter 2 will address this issue.

It is nearly always possible to arrive at an 18-valence-electron count for early-transition-metal alkoxides complexes by invoking dπ-pπ bonding, although it is important to note that the electrons involved in π bonding are ligand-centered. The LUMO's of metal alkoxide complexes are metal-centered (d orbitals) and therefore the compounds usually behave as coordinatively unsaturated species and are labile toward Lewis base uptake.

Metal alkoxide complexes are inherently more substitutionally labile, being susceptible to both nucleophilic attack at the metal center and electrophilic attack at oxygen, provided steric factors are not limiting. Dissociation of OR^- in nonpolar hydrocarbon solvents has never been established and does not present an important reaction pathway for alkoxide complexes.

The combinations of the alkyl groups of alkoxides offers the possibility to tune the degree of oligomerization, the solubility, as well as steric and electronic factors [1]. The siloxy ligand further extends the range of possibilities for the "OR" group. By suitable choice of alkoxy and siloxy group, steric access to the metal may be made substrate-selective. This parallels the common use of specific PR_3 or η-C_5R_5 ligands to control access to the metal coordination sphere in organometallic chemistry.

1-2. Sterically-demanding ligands

The chemistry of compounds that contain sterically-demanding ligands has long been a subject of substantial research [1a]. Some examples of steric-demanding ligands are: OR (where R = adamantyl, bis(t-butyl)methoxyl (OCH-tBu$_2$) [1a]), and $OSiR_3$ (where R = phenyl, t-butyl [4]), as well as amido ($NHSiBu^t_3$ [5], $N(SiMe_3)_2$) and imido NAr (Ar = 2,6-diisopropylphenyl) [6] ligands.

Bulky ligands can reduce or eliminate the possible oligomerization, increase the solubility in organic solvents, stabilize unusually low coordination numbers, and often lead to interesting structural features and reactivity [5]. Among some compounds with interesting structural features are unbridged binuclear hydride complexes, $[(^tBu_3SiO)_2MH_2]_2$ (M = Nb, Ta) [7], $[(^tBu_3SiNH)Ti]_2(\mu\text{-}NSi^tBu_3)_2$ [5] containing a short Ti-Ti bond, and three-coordinate third row compounds, $[Os(=N\text{-}2,6\text{-}^iPr_2(C_6H_3))_3]$ [6a], $[(^tBu_3SiO)_2W{=}NBu^t]$ [4b], and $Ta(OSi^tBu_3)_3$ [4a].

By using steric-demanding ligands, unusual η^2-pyridine, η^2-benzene, and ketyl adducts have been characterized, activations of molecular oxygen, molecular hydrogen, carbon monoxide [4a], and carbon-hydrogen bonds [8] have been explored.

The thermolyses of $(^tBu_3SiNH)_3ZrR$ complexes has been shown to generate a highly reactive transient, $(^tBu_3SiNH)_2Zr{=}Nsi^tBu_3$, capable of carbon-hydrogen bond activation [8]. The capture of alkanes by the electrophilic, three-coordinate d^0 zirconium center, in particular the subsequent addition of RH to the $Zr{=}Nsi^tBu_3$ functionality, may be relevant to the oxidation of hydrocarbons by metal oxides, since the imido and oxo group are isoelectronic.

The reactions of $(^tBu_3SiO)_3Ta$ [4a] is a good example of the chemistry induced by coordination unsaturation. $Ta(OSiBu^t_3)_3$ was made through the reduction of $(^tBu_3SiO)_3TaCl_2$ by Na/Hg in THF at room temperature (eq. 1). A cryoscopic molecular weight determination in benzene was consistent with a monomeric formulation. An X-ray diffraction study revealed a sterically favorable trigonal (D_{3h}) arrangement of the tri(tert-butyl)siloxy groups, which is consistent with a singlet ground state ($^1A_1'$), provided both electrons of tantalum occupy the d_{z2} orbital.

$$(^tBu_3SiO)_3TaCl_2 \xrightarrow[\text{THF, 25°C, 2h}]{\text{Na/Hg, -2NaCl}} (^tBu_3SiO)_3Ta \qquad \ldots(1)$$

The d^2 Ta(III) metal center in $(^tBu_3SiO)_3Ta$ is a strong reductant, which is capable of cleaving dioxygen (eqn. 2), dinitrogen (eqn. 3), numerous C-X (X = O, S, halide, etc.) bonds, and most interestingly, carbon monoxide, CO, to form well defined products $(^tBu_3SiO)_3Ta{=}O$ and $[(^tBu_3SiO)_3Ta]_2(\mu\text{-}C_2)$ (eqn. 4).

$$(^tBu_3SiO)_3Ta + O_2 \xrightarrow{\text{benzene, } 25^\circ C} (^tBu_3SiO)_3Ta{=}O \qquad \ldots(2)$$

$$(^tBu_3SiO)_3Ta + H_2 \xrightarrow{\text{benzene, } 25^\circ C} (^tBu_3SiO)_3TaH_2 \qquad \ldots(3)$$

$$(^tBu_3SiO)_3Ta + \tfrac{1}{2}CO \xrightarrow[\text{benzene}]{25^\circ C} \tfrac{1}{2}(^tBu_3SiO)_3Ta{=}O + \tfrac{1}{4}[(^tBu_3SiO)_3Ta]_2(\mu\text{-}C_2) \qquad \ldots(4)$$

$[(^tBu_3SiO)_3Ta]_2(\mu\text{-}C_2)$ is a tantalum dimer bridged by a dicarbide, $-C{=}C-$, unit. Chemical characterization provided further evidence for the existence of the dicarbide bridge. The hydrolysis of the tantalum dimer produces C_2H_4 and $(^tBu_3SiO)_3Ta{=}O$ through cleavage of the dicarbide bridge (eqn. 5).

$$[(^tBu_3SiO)_3Ta]_2(\mu\text{-}C_2) \xrightarrow[\text{THF-}d_8,\ 110^\circ C,\ 15h]{\text{excess } H_2O} C_2H_4 + 6\,^tBu_3SiOH + Ta_2O_5 \qquad \ldots(5)$$

An intermediate (1) has been suggested to account for the formation of $[(^tBu_3SiO)_3Ta]_2(\mu\text{-}C_2)$. It can be seen from 1 that the coordination unsaturation of the parent compound, $(^tBu_3SiO)_3Ta$, is crucial for the

formation of 1, which is made possible by using the sterically demanding and yet electronically flexible ligand $^tBu_3SiO^-$.

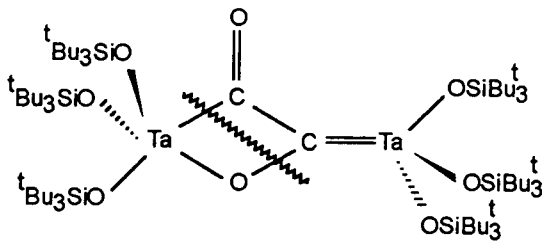

(1)

In this thesis work, a relative bulky siloxy ligand, triphenylsiloxy (Ph_3SiO^-), was used. Indeed, it stabilizes a tetrahedral $(MoO_2)^{2+}$ unit, which is relatively rare among a large number of Mo complexes [9].

1-3. Chemistry of Metal-ligand multiple bonds

This thesis work benefits very much from an excellent book entitled "Metal-Ligand Multiple Bonds, The Chemistry of Transition Metal Complexes Containing Oxo, Nitrido, Imido, Alkylene, or Alkylidyne Ligands" by William A. Nugent and James M. Mayer [10]. The book covers the literatures prior to 1988. The materials are very well organized and is quite readable. Many examples in the following brief review on metal oxo chemistry are taken from the book.

One important and long-standing application of metal oxo derivatives is their use as oxidants in organic synthesis. The traditional oxidants include chromium(VI), $KMnO_4$, RuO_4, and OsO_4. Moreover, the need for more efficient and selectitve oxidizing agents continues to provide

an impetus for research in this area. Pyridium chlorochromate (PCC) and pyridinium dichromate (PDC) represent examples of novel oxidants that have gained widespread acceptance among organic chemists.

Our understanding of the mechanisms by which oxo derivatives oxidize olefins has increased considerably in the last decade. Historically, such reactions had been viewed as an electrophilic attack of the oxo-metal moiety on an electron-rich olefinic π system. In 1977 Sharpless et al. published a thought-provoking paper in which they pointed out that such a mechanism was incompatible with the then-prevalent notion of charge control. Instead they proposed that these reactions proceed through prior coordination of the olefin and collapse of the resultant complexes to an oxametallacyclic intermediate. For the reduction of M=O moiety by a trialkylphosphine, they pointed out that the attack of a phosphine on a metal-oxo moiety (typically polarized M^{+}-O_{-}) was also inconsistent with a charged-controlled process and suggested that the phosphine made a direct attack to the metal center. The triphenylphosphine adduct of $MoO_2(OSiPh_3)_2$ containing a Mo-P bond, which was found in this thesis work, is a support for this mechanism (See Chapter 3 for further details).

These advances in mechanistic understanding have been accompanied by exciting developments in oxidation chemistry itself. Mayer [13] has succeeded in rationally designing ruthenium-oxo complexes that will catalytically oxidize a variety of organic substrates when continually reoxidized at the anode of an electrochemical cell. Osmium-based systems

have been developed for the asymmetric oxidation of olefins to diols; excellent chemical and optical yields have been achieved.

Nature also utilizes metal-oxo complexes in a ubiquitous series of important enzymes. Examples include the cytochrome P-450 family containing an oxo-porphyrin system and "oxo-transferases" which contains molybdenum-oxo bonds and involve both oxidative and reductive processes. Recently, significant advances have been made in developing model systems that mimic the transformation of oxo-transferase (see Chapter 3).

Metal-oxo species are also present on the surface of industrially important heterogeneous catalysts (see Chapter 4). For example bismuth molybdate catalysts are used for the oxidation of C4's to butadiene and for the oxidation of propylene to acrolein. Similarly, iron molybdate catalysts are utilized for the oxidation of methanol to formaldehyde. A variety of evidence suggests that it is the terminal oxo groups on the catalyst surface that are directly involved in the catalytic chemistry. Supported metal-oxo compounds also form the basis of commercial catalysts for olefin metathesis [10].

During the past decade, organometallic chemists have begun to appreciate the ability of the oxo ligand to stabilize high oxidation states. This stabilization has been applied to the synthesis of both σ and π organotransition metal derivatives, for example, of vanadium(V), molybdenum(VI), tungsten(VI), and rhenium(VII). Several of these are shown in the following.

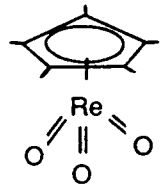

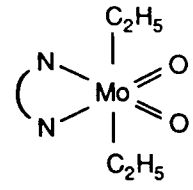

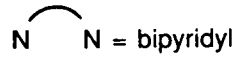

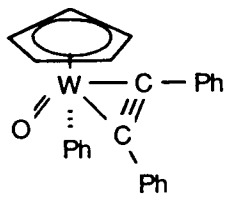

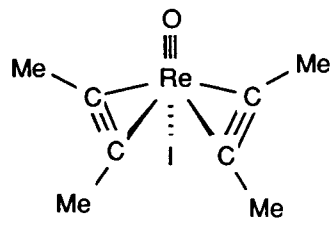

In the subsequent chapters, the preparation of dioxobis(triphenylsiloxy)molybdenum, $MoO_2(OSiPh_3)_2$, and its reactions with various reagents, and the characterization (primarily by X-ray diffraction methods) of the products will be covered. Chapter 2 deals with the preparation of triphenylsiloxy compounds and the addition reactions of $MoO_2(OSiPh_3)_2$. Also discussed in the chapter is a correlation between M-O-$SiPh_3$ angles in $\{M(OSiPh_3)_2\}$ type compounds with the O...O separation between two neighboring triphenylsiloxy groups. Chapter 3 discusses the Oxygen Atom Transfer reactions between $MoO_2(OSiPh_3)_2$ and trialkylphosphines and oxygen atom transfer reaction mechanisms. The reactions of $MoO_2(OSiPh_3)_2$ with alkylating reagents ($ZnEt_2$ and $SnMe_4$) and the structure of an interesting

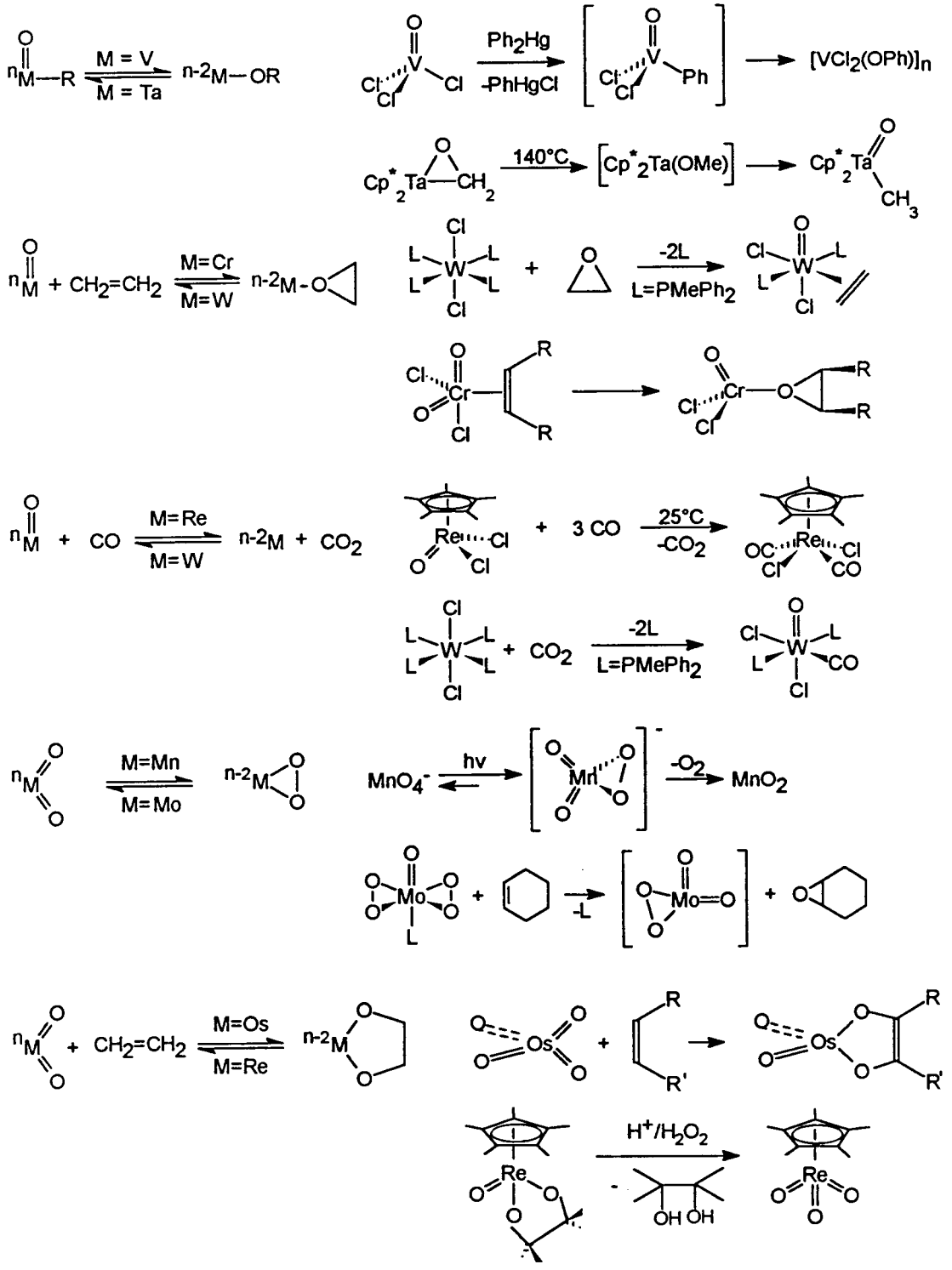

Figure 1-1. Summary of some transformations of metal oxo complexes.

Zn compound as a product of the reactions are included in Chapter 4. Chapter 5 describes some attempts on the "inorganic version" of the Wittig reaction, i.e., the reactions of $MoO_2(OSiPh_3)_2$ with ylides $Ph_3P^+C(CH_3)_2^-$ and $Ph_3P^+CH_2^-$. The structure of a hexamolybdate is also discussed in this chapter.

1-4. References

1. some review papers on alkoxide chemistry: (a) Mehrotra, R.C. "Transition-metal alkoxides", in *Adv. in Inorg. and Radiochem.* **1983**, *26*, 269-335. (b) Bradley, D.C.; Mehrotra, R.C.; Gaur, D.P. "*Metal Alkoxides*", Academic Press, New York, **1978**. (c) Bradley, D.C., and Fischer, K.J., "Alkoxides, Mercaptides, Dialkylamides and Phosphides", *MTP Int. Rev. Sci. Gen. Chem. Transition Met.* **1972**, *5*, 65-91. (d) Chisholm, M.H. "Metal Alkoxides: Model for Metal Oxides", in *Inorg. Chem. Toward the 21st Century*, ACS Symposium, series 211, Ed. M.H. Chisholm, ACS, Washington, D.C., **1983**. (e) Bradley, D.C. "Metal Oxides Alkoxide (Trialkylsiloxide) Polymers", *Coord. Chem. Rev.* **1967**, *2*, 299-318.

2. Chacon, S.T.; Chisholm, M.H.; Eisenstein, O.; Huffman, J.S. *J. Am. Chem. Soc.* **1992**, *114(22)*, 8497-8509, and references therein.

3. Chisholm, M.H.; Clark, D.L.; Hampden-Smith, M.J.; Hoffman, D.H., "Alkoxide Clusters of Molybdenum and Tungsten as templates for Organometallic Chemistry: Comparison with Carbonyl Clusters of the Later Transition Elements", *Angew. Chem. Int. Ed. Engl.* **1989**, *28*, 432-444.

4. (a) Neithamer, D.R.; LaPointe, R.E.; Wheeler, R.A.; Richeson, D.S.; Van Duyne, G.D.; Wolczanski, P.T. *J. Am. Chem. Soc.* **1989**, *111*, 9056-9072. (b) Eppley, D.F.; Wolczanski, P.T.; Van Duyne, G.D. *Angew. Chem. Int. Ed. Engl.* **1991**, *30(5)*, 584--585. (c) Weidenbruch, M.; Pierrard, C.; Pesel, H.; *Z. Naturforsch.* **1978**, *33b*, 1468-1471.

5. Cummins, C.C.; Schaller, C.P.; Van Duyne, G.D.; Wolczanski, P.T.; Chan A.W.E.; Hoffmann, R. *J. Am. Chem. Soc.* **1991**, *113*, 2985-2994 and reference therein.

6. (a) Anhaus, J.T.; Kee, T.P.; Schofield, M.H.; Schrock, R.R. *J. Am. Chem. Soc.* **1990**, *112*, 1642-1643. (b) Chao, Y.-W.; Rodgers, P.M.; Wigley, D.E.; Alexander, S.J.; Rheingold, A.L. *J. Am. Chem. Soc.* 1991, *113*, 6326-6328.

7. (a) Toreki, R.; La Pointe, R.E.; Wolczanski, P.T. *J. Am. Chem. Soc.* **1987**, *109*, 7558-7560. (b) La Pointe, R.E.; Wolczanski, P.T. *J. Am. Chem. Soc.* **1986**, *108*, 3535-3537.

8. Cummins, C.C.; Van Duyne, G.D.; Schaller, C.P.; Wolczanski, P.T. *Organometallics* **1991**, *10*, 164-170.

9. Wilkinson, G. Ed. "*Comprehensive Coordinative Chemistry*", Vol. 4, Pergamon Press, **1987**.

10. Nugent, W.A. and Mayer. J.M. "*Metal-Ligand Multaiple Bonds, The Chemsitry of Transition Metal Complexes Containing Oxo, Nitrido, Imido, Alkylidene, or Alkylidyne Ligands*", John Wiley & Sons, New York, **1988**.

11. Feher, F.J.; Walzer, J.F., *Inorg. Chem.* **1991**, *30*, 1689.

12. For example: McGeary, M.J. et.al., *Inorg. Chem.* **1991**, *30*, 1723.

13. Mayer, B.A.; Thompson, M.S.; Meyer, T.J. *J. Am. Chem. Soc.* **1980**, *102*, 2310-2312.

Chapter 2

Syntheses and Addition Reactions of Triphenylsiloxy Compounds

2-1. Introduction

In this thesis work, the triphenylsiloxy ligand was chosen because its bulkiness may increase the solubility of siloxy compounds, prevent the possible formation of oligomers, and increase the reactivity of siloxy complexes by creating coordinative unsaturation on the central metal atom. As is shown in Chapter 1, the coordinative unsaturation of low-coordination-number complexes leads to some unusual reactions.

This chapter will discuss the common synthetic routes for triphenylsiloxy compounds, including a new synthetic method for triphenylsiloxy compounds employed in this thesis work, and report the synthesis and crystal structures of some triphenylsiloxy compounds including $MoO_2(OSiPh_3)_2$. The results of the addition reactions of $MoO_2(OSiPh_3)_2$ will also be discussed. Factors that determine the angles of M-O-$SiPh_3$ linkages in triphenylsiloxy compounds have long been a subject of intense discussion. This chapter points out, by correlating a molecular structural parameter to the M-O-Si angle, that steric effects play an important role in determining the M-O-Si angle for complexes containing more than one triphenylsiloxy ligand.

2-2. Synthesis of triphenylsiloxy compounds

There are many ways [1] to synthesize triphenylsiloxy compounds. The following reactions summarize most of the synthetic routes used in the literature to prepare triphenylsiloxy compounds:

$$Y[N(SiMe_3)_2]_3 + 3\ Ph_3SiOH \xrightarrow{\text{toluene, } 0^\circ C} [Y(OSiPh_3O)_3]_n \quad \ldots(1)$$

$$\{Co[N(SiMe_3)_2]_2\}_2 + 4\ Ph_3SiOH \xrightarrow{THF} [Co(OSiPh_3)2(THF)_2]_2 \quad \ldots(2)$$

$$(C_5H_5)_2Pb + Ph3SiOH \xrightarrow{r.t.} Pb(OSiPh3)_2 \xrightarrow{\text{heating}} Pb_4(OSiPh_3)_6O + (Ph_3Si)_2O \quad \ldots(3)$$

$$(C_5H_5)_2Zr(CH_3)_3 + Ph_3SiOH \longrightarrow (C_5H_5)_2Zr(OSiPh_3)_3\ [2] \quad \ldots(4)$$

$$AlMe_3 + Ph_3SiOH \xrightarrow{\text{THF, } 0^\circ C} Al(OSiPh_3)_3(THF) \quad \ldots(5)$$

$$TiCl_4 + Ph_3SiOH \xrightarrow{\text{acetic acid, } 100^\circ C} Ti(OSiPh_3)_4 \quad \ldots(6)$$

$$VO(OPr^i)_3 + 3\ CH_3CO_2SiPh_3 \longrightarrow VO(OSiPh_3)_3 + 3\ CH_3CO_2Pr^i \quad \ldots(7)$$

$$Al(OPr^i)_2(acac)_2 + 4\ Ph_3SiOH \longrightarrow 2\ Al(OSiPh_3)_2(acac) \quad \ldots(8)$$

$$CrO_3 + Ph_3SiOH \xrightarrow{\text{boiling } CCl_4} CrO_2(OSiPh_3)_2 \quad \ldots(9)$$

$$(NH_4)_2Ln(NO_3)_5 + NaOSiPh_3 \xrightarrow[\text{Ln = Ce, Nd, Pr, Y}]{\text{THF, r.t.}} [Ln(OSiPh_3)_3(THF)_3](THF)\ [3] \quad ...(10)$$

One common method to prepare metal triphenylsiloxy compounds is through alcoholysis of reactive transition metal compounds with triphenylsilanol. Usually very reactive precursors are used, e.g. metal amides (eqns. 1 and 2), metal alkyls (eqns. 1, 4 and 5), and metal chlorides (eqn. 6). If the alkoxy compounds are readily available, the ligand exchange reactions are a good way to prepare the corresponding triphenylsiloxy compounds. In reactions 7 and 8, isopropoxyl groups in $VO(OPr^i)_3$ and $Al(OPr^i)_2(acac)_2$ are replaced by triphenylsiloxy groups, and the configurations around the metal ions are preserved. One difficulty with the above two synthetic strategies is that sometimes the starting metal compounds like $Y[N(SiMe_3)_2]_3$, $\{Co[N(SiMe_3)_2]_2\}_2$, $(C_5H_5)_2Pb$, and $Al(OPr^i)_2(acac)_2$, are themselves difficult to make. In some cases, synthesis of alkoxides of lanthanide using the metal halides as starting materials have been shown to form alkoxide complexes that incorporate oxide and halide ligands [3]. Synthesis directly from simple inorganic salts or metal oxides is rare (eqns. 9 and 10). Reaction 10 is typical of the reaction of ammonium nitrate metal complexes with anionic reagents of this type and has been observed previously in reactions of $(NH_4)_2Ce(NO_3)_5$ (abbreviated as CAN) with $Na(C_5H_5)$ [4] and with sodium alkoxides [5].

In this thesis work, a synthetic strategy of direct silylation was employed. As shown in the following equation, the metal-oxo moiety of the metal oxide is directly silylated by triphenychlorosilane.

$$L_nM{=}O + Ph_3Si^+ \longrightarrow (L_nM\text{-}OSiPh_3)^+ \qquad \ldots(11)$$

The silver salts of metallates were employed as precursor. The use of the silver salt facilitates the reactions by eliminating silver chloride. Other kinds of ANHYDROUS salts, like sodium or potassium salts, may also work, but have not been tried. The silver salt is easy to dry in a 50°C vacuum oven overnight.

The following is a summary of the preparation of triphenylsiloxy compounds by direct silylation in this work.

$$\underset{\text{excess}}{Ag_2CrO_4} + Ph_3SiCl \xrightarrow[\text{r.t. 2 days,-AgCl}]{\text{1,2-dichloroethane}} \underset{86\%}{(Ph_3SiO)_2CrO_2} \qquad \ldots(12)$$

$$\underset{\text{excess}}{Ag_2MoO_4} + Ph_3SiCl \xrightarrow[80°C,\ \text{overnight}]{\text{1,2-dichloroethane}} \underset{94\%}{(Ph_3SiO)_2MoO_2} \qquad \ldots(13)$$

$$\underset{\text{excess}}{Ag_2WO_4} + Ph_3SiCl \xrightarrow[\text{reflux overnight}]{\text{1,2-dichloroethane}} \text{No Reaction} \qquad \ldots(14)$$

$$\underset{\text{excess}}{AgVO_3} + Ph_3SiCl \xrightarrow[\text{reflux overnight}]{\text{1,2-dichloroethane}} \underset{92\%}{(Ph_3SiO)_3VO} + V_2O_5 \qquad \ldots(15)$$

2-2-1. Reaction conditions

There are many factors that influence the reaction which include the solvent, reaction time and temperature, and stoichiometry of the reactants.

The choice of the solvent is very important since direct silylation is a heterogeneous reaction. The initial requirements for the solvent are that it be anhydrous (Ph_3SiOH and the triphenylsiloxy compounds are hygroscopic); non-reductive (since many metal oxides are oxidative); and that it have good product solubility. 1,2-dichloroethane was a good choice because it is easily dried; non-reductive (compared to, e.g., ethanol); good solubility (compared to toluene etc.); and has a wide reaction temperature range (b.p. = 80°C, compared to b.p. of 1,2-dichloromethane of only 40°C).

Usually vigorous stirring, heating (or refluxing) and extended reaction time are needed for the reaction since direct silylation is a heterogeneous reaction.

In all silylation reactions, an excess amount of silver metallate was used. This ensures the total consumption of Ph_3SiOH by silver metallate so that the only species left in the liquid phase, provided the reaction time is long enough to make the reaction complete, will be the triphenylsiloxy compound, which is then easily recovered.

It is interesting to note that in the synthesis of $MoO_2(OSiPh_3)_2$, a small amount of acetonitrile in 1,2-dichloroethane is needed to avoid the formation of a deep bluish solution which contains mostly $(Ph_3Si)_2O$ and metal oxide, instead of the triphenylsiloxy compound $MoO_2(OSiPh_3)_2$. This phenomenon may be explained by assuming that the acetonitrile saturates the inner coordination sphere of Mo thus protecting the Mo-$OSiPh_3$ bond from attack by Ph_3Si^+ (eqn. 16), and preventing the intramolecular elimination of $(Ph_3Si)_2O$ (eqn. 17). Use of pure acetonitrile or THF also leads to the same results.

$$L_nM\text{-}OSiR_3 + R_3Si^+Cl^- \longrightarrow L_nM\text{-}Cl + (R_3Si)_2O \quad \ldots(16)$$

$$MoO_2(OSiPh_3)_2 \longrightarrow \text{"}MoO_3\text{"} + (Ph_3Si)_2O \quad \ldots(17)$$

2-2-2. Advantages of direct silylation

The advantage of this strategy is that the product isolation is very simple, the products are relatively pure, and the extent of the silylation can be easily monitored. Since the only species left in the liquid phase is the triphenylsiloxy compound, the triphenylsiloxy product is easy to extract by simply filtering and drying the filtrate. This procedure assumes that moisture is excluded and reaction conditions are carefully controlled. If so, the product can be used for subsequent reactions without further purification. To monitor the extent of the reaction, a drop of the reaction mixture was taken from the reaction flask and filtered through a small filter (a small Pasteur pipette filled

with a flock of glass wool). The filtrate was applied to the surface of a KBr plate. After allowing the solvent to evaporate in the dry box, the IR spectrum was taken. A band at 542 cm^{-1} which characterized the Si-Cl stretching was monitored. The disappearance of the 542cm^{-1} absorption indicates the end of the reaction (complete consumption of Ph_3SiCl).

There are a few examples of the direct silylation in the literature applied to the synthesis of trimethylsilyl compounds (eqn. 18) [6].

$$AgReO_4 + (CH_3)_3SiCl \xrightarrow{25°C,\ -AgCl} (CH_3)_3SiOReO_3 \qquad ...(18)$$

The compound $MoO_2(OSiPh_3)_2$ is the first molybdenum(VI) triphenylsiloxy compound prepared in this manner, $VO(OSiPh_3)_3$ and $CrO_2(OSiPh_3)_2$ have been prepared by other synthetic routes. Although there are other methods [7] to prepare $VO(OSiPh_3)_3$, the current method has the advantage that the starting materials are easily available, and that the product is easy to isolate and purify. The yield is high based on Ph_3SiCl, although it is low (31%) based on silver vanadate.

It is worthwhile mentioning here that while Ph_3SiCl silylates 3 V=O bonds in the (VO_4) tetrahedron to form $VO(OSiPh_3)_3$, the reaction between $(^tBu)_3SiOH$ and V_2O_5 gives a dimer $(^tBu_3SiO)_2VO\text{-}O\text{-}VO(OSi^tBu_3)_2$ with only two V=O bonds being silylated [8]. This is a reflection of the greater steric bulkiness of $^tBu_3SiO$ over Ph_3SiO. The cone angle of $^tBu_3Si$ (187°) is significantly larger than that of Ph_3Si (150°) [9].

2-2-3. Reactivities of metallates towards Ph_3SiCl

The reactivity of metallates towards Ph_3SiCl displays an interesting pattern. It was found in this study that while $CrO_2(OSiPh_3)_2$ can be prepared from the reaction of silver chromate with Ph_3SiCl at room temperature, higher temperatures (83°C) are required for silver molybdate to react with Ph_3SiCl. For silver tungstate, no reaction with Ph_3SiCl was observed even at 110°C for 15 hours. Because this direct silylation is a heterogeneous reaction, the lattice energies of the silver metallates are very important in determining the reactivity for direct silylation. On the basis of metal ionic radii, it can be expected that going from silver chromate to tungstate the lattice energy of the silver metallates gradually decreases. This is supported by the solubility product data of silver metallates in aqueous solution: $7.1x10^{-13}$, $6.4x10^{-12}$, and $5.2x10^{-10}$ at 25°C for silver chromate, molybdate, and tungstate, respectively [10]. It is interesting to note that although the tungstate has the lower lattice energy (higher solubility), it does not react with triphenylchlorosilane at all! There must be other factors that play an important role in determining the reactivity. Metal oxo bond strength is one of the factors which is parallel to the reactivity of the silver metallate silylation reactions. W=O bond strength, 150KCal/Mole in WO_3, is greater than the Mo=O bond strength, 141Kcal/mole in MoO_3 [11], which in turn is greater than that of Cr=O bond (102.6±7.0 KCal/mole for diatomic Cr-O species [12]).

Silver perrhenate and manganate have low lattice energies as indicated by the solubility product $8.0x10^{-5}$ and $1.6x10^{-3}$, respectively [10]. Re-O and Mn-O bonds (149.2±20.0 and 96.3±10.00Kcal/mole for diatomic species [12], respectively) may be compared to that of V-O, Mo-O, W-O diatomic species with bond strengths 149.8±4.5, 133.9±5.0, 160.6±10 KCal/mole [12], respectively. Both trimethylsilyl pertechnate and perrhenate have been prepared by direct silylation of $(CH_3)_3SiCl$ on the corresponding silver metallates [13].

One of the advantages of using Ph_3Si^{+1} instead of $(CH_3)_3Si^{+1}$ [15,16] for direct silylation is that for Ph_3SiCl the side reaction of the loss of $(R_3Si)_2O$ either by the attack of R_3Si^+ on M-$OSiPh_3$ moiety shown in eqn. 16 or by intramolecular extrusion from $\{M(OSiR_3)_2\}$ moiety (eqn. 17) can be reduced due to the relative bulkiness of Ph_3Si- compared to the $(CH_3)_3Si$- group.

However, the decomposition of $MoO_2(OSiPh_3)_2$ to hexaphenyldisilanol, $(Ph_3Si)_2O$, is still the primary side reaction of the preparation of $MoO_2(OSiPh_3)_2$. Actually, $(Ph_3Si)_2O$ was also quite often seen in the reactions of $MoO_2(OSiPh_3)_2$ with various reagents (see subsequent chapters). In the preparation of $MoO_2(OSiPh_3)_2$, some measures were taken to reduce the side reactions, which included the use of a large volume of solvent; the use of aluminum foil to wrap the reaction vessel to avoid light; and the temperature control avoid overheating the reaction mixture.

The use of a more bulky ligand tri(tert-butyl)siloxy in the place of triphenylsiloxy may overcome the side reaction to $(R_3Si)_2O$.

2-3. IR characterization of triphenylsiloxy compounds

IR spectra are very useful in the characterization of triphenylsiloxy compounds since the absorptions of Si-Ph group are constant and characteristic [17,18]. At least five sharp bands are seen in the aromatic C-H stretching region (3100 to 3000 cm^{-1}) of the infrared. The characteristic overtone and combination bands of monosubstituted benzene ring are present in the 2000-1750 cm^{-1} region. Bands characteristic of Si-Ph are the phenyl ring absorptions found at about 1590m, 1490w, 1430m, and 1119s cm^{-1}. The 1430 cm^{-1} is one of most useful bands for detecting phenyl on silicon. Probably the most characteristic band for Si-Ph is the strong band at about 1119 cm^{-1} from a planar ring vibration which has some Si-C stretch character. It is affected by the electronegativity of the other groups on silicon. The strong bands at 750 to 690 cm^{-1} region is the out-of-plane hydrogen vibration of the phenyl group, and are quite constant among different triphenylsiloxy compounds. Si-O-Si stretching of $(Ph_3Si)_2O$ is found at 1095 cm^{-1} with medium intensity.

The molybdenum-dioxo stretching region of $MoO_2(OSiPh_3)_2$ shows a complex pattern: 949 (weak, shoulder), 931 (weak, shoulder), 896 (strong, broad) cm^{-1}, probably due to the overlap of Mo=O stretching and Si-O-Mo stretching bands.

2-4. Addition reactions of $MoO_2(OSiPh_3)_2$ with Lewis bases

$MoO_2(OSiPh_3)_2$ is both a coordinatively and electronically unsaturated compound. It can easily add Lewis bases to saturate its coordination sphere.

$$MoO_2(OSiPh_3)_2 + OPPh_3 \xrightarrow{\text{r.t.}} (Ph_3SiO)_2MoO_2(OPPh_3) \quad ...(19)$$

$$MoO_2(OSiPh_3)_2 + 2,2'\text{-bipy} \longrightarrow (Ph_3SiO)_2MoO_2(2,2'\text{-bipy}) \quad ...(20)$$

$MoO_2(OSiPh_3)_2(2,2'\text{-bipy})$ has been structurally characterized by single crystal X-ray diffraction in this thesis work (Fig. 2-3).

2-5. Structural features of triphenylsiloxy compounds

2-5-1. Structural characterization of triphenylsiloxy compounds

Crystal structure of $MoO_2(OSiPh_3)_2$: The structure of $MoO_2(OSiPh_3)_2$ was determined by single crystal X-ray diffraction. The structure of $MoO_2(OSiPh_3)_2$ and some selected bond angles and lengths are shown in Figure 2-1. $MoO_2(OSiPh_3)_2$ has a tetrahedral configuration around the Mo center, which is relatively rare since most monomeric Mo compounds are six-coordinate [20]. The four-coordinate bis(alkoxy)dioxomolybdenum type compounds $MoO_2(OR)_2$ tend to oligomerize for R = methyl, ethyl, propyl, etc.. The current evidence is that oligomerization rates are greater for

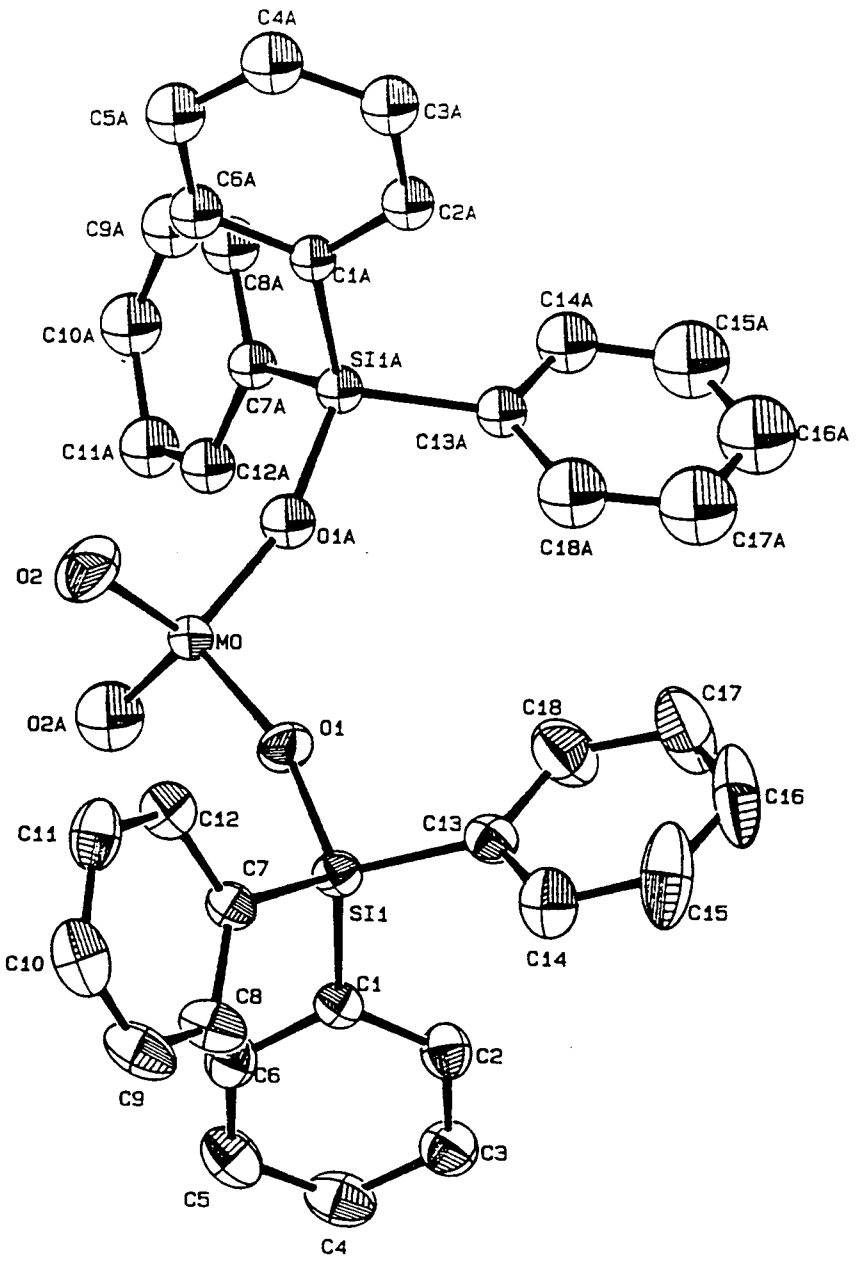

Figure 2-1. ORTEP drawing of the structure of $MoO_2(OSiPh_3)_2$. Selected bond lengths (Å) and bond angles (deg): Mo-O(1) = 1.815(5), Mo-O(2) = 1.692(7), Si(1)-O(1) = 1.669(6); O(2)-Mo-O(2) = 106.4(5), O(1)-Mo-O(1) = 110.(4), O(1)-Mo-O(2) = 109.9(3), O(1A)-Mo-O(2) = 110.3(3), Mo-O(1)-Si(1) = 163.6(4). H atoms are omitted for clarity.

smaller R groups [21]. The existence of the discrete four-coordinate structure for $MoO_2(OSiPh_3)_2$ suggests that the steric bulkiness of the triphenylsiloxy group prevents oligomerization.

There is a two-fold axis in $MoO_2(OSiPh_3)_2$ through the Mo atom and bisecting the O(1)-O(1A) linkage. The $\{MoO_2\}^{2+}$ unit is typical of that in four coordinate Mo dioxo compounds. Mo-O(1)-Si(1) linkages are almost linear (163.6(4)°), on the contrary, one Cr-O-Si linkage in the analogue $CrO_2(OSiPh_3)_2$ [21] is bent (133.1(6)°, 162.7(7)°). The Mo-O-Si linkages in $MoO_2(OSiPh_3)_2(PPh_3)$ with a trigonal bipyramidal structure are bent (143.9(4)°, 138.7(4)°).

Crystal structure of $VO(OSiPh_3)_3$: An ORTEP drawing is shown in Figure 2-2. The coordination geometry around V is nearly tetrahedral with the O-V-O angle spanning the range of 107.8-111.2°. The V-O-Si angles are 145.4, 154.7, and 156.6°, respectively. Feher has reported a crystal structure for $VO(OSiPh_3)_3.0.5C_6H_6$ [22] at -90°C. Their crystal of $VO(OSiPh_3)_3$ was grown from benzene solvent and contained one benzene molecule per unit cell. Feher's $VO(OSiPh_3)_3$ structure has an O...O separation (see the following section on the discussion of M-O-Si angles), V-O-Si angles, and Si-O bond lengths which average 2.858(2)Å, 154.6(1)°, and 1.653(2)Å, respectively. The averaged V-O-Si bond angle (154.6(1)°) is slightly larger than that in our $VO(OSiPh_3)_3$ compound (152.2(4)°), which corresponds to a slightly wider O...O separation in $VO(OSiPh_3)_3.0.5C_6H_6$. Other aspects of the two structures are very close to each other.

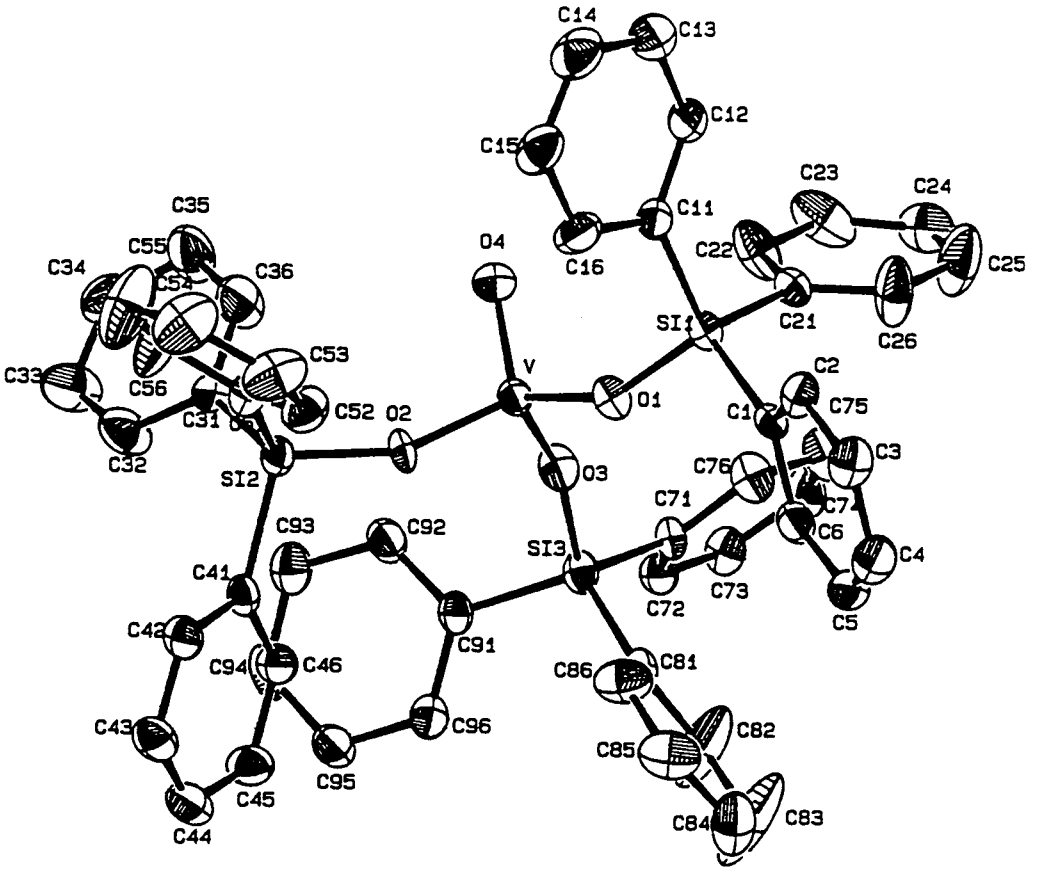

Figure 2-2. ORTEP drawing of $VO(OTPS)_3$. Selected bond lengths (Å) and bond angles (deg): V-O1 = 1.742(6), V-O2 = 1.740(6), V-O3 = 1.737(6), V-O4 = 1.566(7), Si1-O1 = 1.649(7), Si2-O2 = 1.650(6), Si3-O3 = 1.643(7); V-O1-Si1 = 145.4(4)°, V-O2-Si2 = 154.7(4)°, V-O3-Si3 = 156.6(5)°, O1-V-O2 = 110.5(3)°, O1-V-O3 = 107.8(3)°, O1-V-O4 = 109.0(4)°, O2-V-O3 = 111.2(3)°, O2-V-O4 = 110.0(3)°, O3-V-O4 = 108.1(4)°. H atoms are omitted for clarity.

Crystal structure of $MoO_2(OSiPh_3)_2$(2,2'-bipy): $MoO_2(OSiPh_3)_2$(2,2'-bipy) has octahedral coordination. The two oxygen atoms, one Mo atom, and 2,2'-bipyridine form an equatorial plane. Two triphenylsiloxy groups occupy the axial positions (Fig. 2-3).

2,2'-bipyridine is a very useful ligand to stabilize transition metal compounds in high oxidation states [23], especially high oxidation state organometallic compounds containing M-C bonds [24,25]. Tables 2-1 and 2-2 list some structural data of some selected transition metal 2,2'-bipyridine compounds.

Table 2-1. Comparison of bond distances of $MoO_2(OSiPh_3)_2$(2,2'-bpy) with some selected 2,2'-bipyridine complexes

bond	distance, Å		complexes	reference
Mo=O	1.68(2)	1.75(2)	$MoO_2(OSiPh_3)_2$(bpy)	this work
	1.64(2)	1.83(2)	MoO_2Br_2(bpy)	[26]
	1.707(2)	1.708(2)	$MoO_2(Me)_2$(bpy)	[27]
	1.709(3)	1.706(3)	$MoO_2(Np)_2$(bpy)	[28]
W=O	1.715(3)	1.728(3)	$WO_2(Me)_2$(bpy)	[29]
Mo-X	1.91(2)	1.98(3)	$MoO_2(OSiPh_3)_2$(bpy)	this work
(X=axial atom)	2.189(3)	2.194(2)	$MoO_2(Me)_2$(bpy)	[27]
	2.237(5)	2.235(5)	$MoO_2(Np)_2$(bpy)	[28]
W-C	2.195(4)	2.194(5)	$WO_2(Me)_2$(bpy)	[29]
Mo-N	2.37(2)	2.36(3)	$MoO_2(OSiPh_3)_2$(bpy)	this work
	2.45(2)	2.26(2)	MoO_2Br_2(bpy)	[26]
	2.314(2)	2.346(2)	$MoO_2(Me)_2$(bpy)	[27]
	2.348(4)	2.317(4)	$MoO_2(Np)_2$(bpy)	[28]
	2.243(6)	2.249(6)	$Mo(CO)_3$(bpy)(dipyam)	[30]
W-N	2.302(4)	2.333(3)	$WO_2(Me)_2$(bpy)	[29]

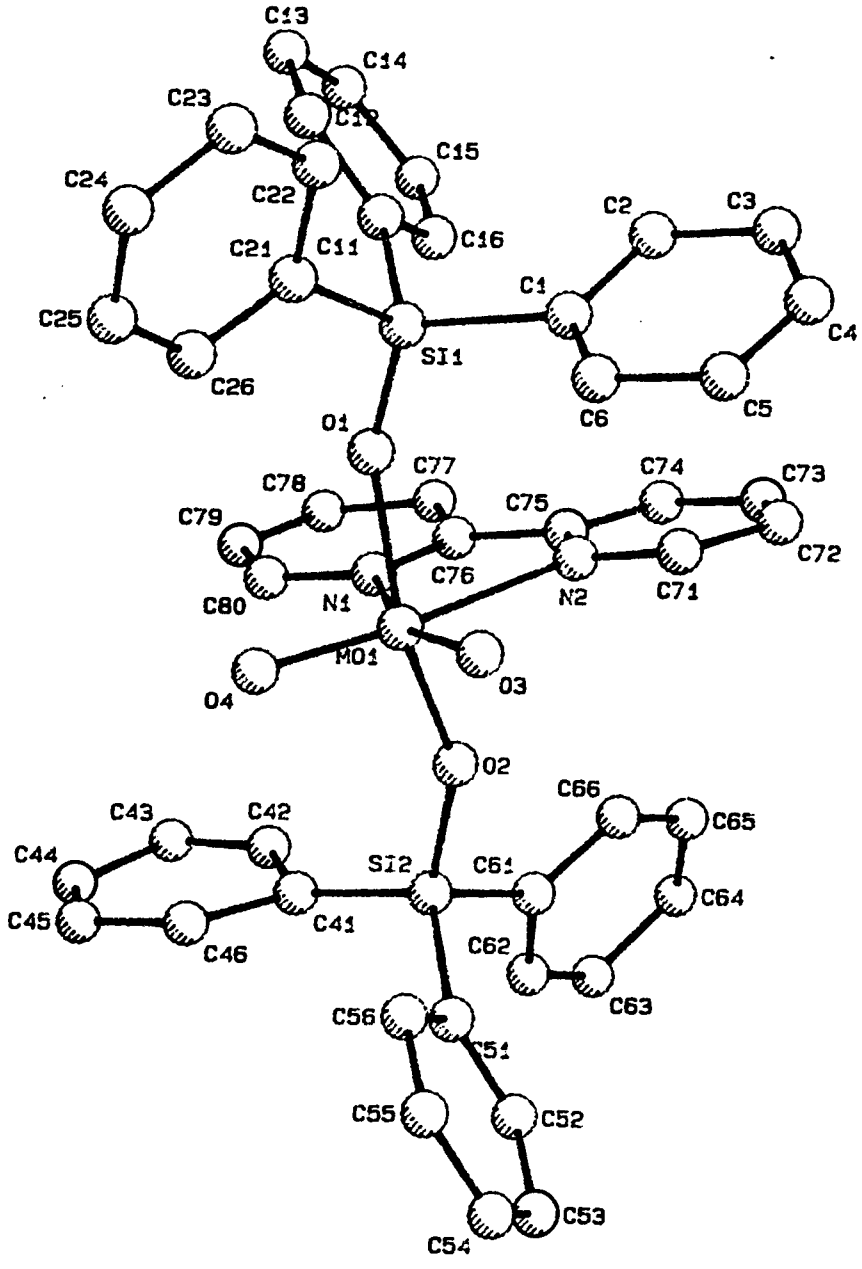

Figure 2-3. Structure of $MoO_2(OSiPh_3)_2$(2,2'-bpy). Selected bond lengths and bond angles in Å or deg. Mo-O1 1.98(3), Mo-O2 1.91(2), Mo-O3 1.75(2), Mo-O4 1.68(2), Mo-N1 2.37(2), Mo-N2 2.36(3), Si1-O1 1.51(3), Si2-O2 1.74(3); O1-Mo-O2 152.9(6)°, N1-Mo-N 268.6(5)°, O3-Mo-O4 107.0(7)°, O1-Mo-O3 99.9(9)°, O1-Mo-O4 97(1)°, O1-Mo-N1 78.5(9)°, O1-Mo-N2 81.0(8)°, O2-Mo-O3 97(1)°, O2-Mo-O4 98.6(8)°, O2-Mo-N1 77.9(7)°, O2-Mo-N2 78(1)°, Mo-O1-SI1 152(2)°, Mo-O2-SI2 151(2)°.

Table 2-2. Comparison of bond angles of $MoO_2(OSiPh_3)_2$(2,2'-bpy) with some selected 2,2'-bipyridine complexes

angle	value(deg)	molecule	reference
O-Mo-O	107.0(7)	$MoO_2(OSiPh_3)_2$(bpy)	this work
	103.3(9)	MoO_2Br_2(bpy)	[26]
	110.20(9)	$MoO_2(Me)_2$(bpy)	[27]
	110.0(2)	$MoO_2(Np)_2$(bpy)	[28]
O-W-O	108.8(2)	$WO_2(Me)_2$(bpy)	[29]
X-Mo-X	152.9(6)	$MoO_2(OSiPh_3)_2$(bpy)	this work
(X=axial	159.7(1)	MoO_2Br_2(bpy)	[26]
atom)	149.0(1)	$MoO_2(Me)_2$(bpy)	[27]
	145.8(2)	$MoO_2(Np)_2$(bpy)	[28]
C-W-C	149.6(2)	$WO_2(Me)_2$(bpy)	[29]
N-Mo-N	68.6(5)	$MoO_2(OSiPh_3)_2$(bpy)	this work
	66.9(6)	MoO_2Br_2(bpy)	[26]
	68.40(6)	$MoO_2(Me)_2$(bpy)	[27]
	68.6(1)	$MoO_2(Np)_2$(bpy)	[28]
	72.2(2)	$Mo(CO)_3$(bpy)(dipyam)	[30]
N-W-N	68.8(1)	$WO_2(Me)_2$(bpy)	[29]

Note: dipyam = di-2-pyridylamine, $(C_5H_4N)_2NH$.

Again it can be seen from Tables 2-1 and 2-2 that the dioxo moieties are quite consistent among different compounds. The Mo-N(2,2'-bpy) bond lengths (~2.3Å) are almost the same among all MO_2X_2(2,2'-bpy) type compounds, but significantly longer than that of the Mo(0) complex $Mo(CO)_3$(2,2'-bpy)(dipyam) (2.247Å) [30]. This may be an indication of $d\pi$-π^* interaction in the latter complex [31].

It is interesting to note that in most octahedral dioxo transition metal compounds the metal center is always displaced from the center of its coordination octahedron and shifts toward the dioxo unit (Figure 2-3, O1-Mo-O2 = 152.9(6)°). This can be described from another point of view: the axial ligands always bend away from the dioxo unit and bend closer

to the 2,2'-bipyridine ligand (for $MoO_2(OSiPh_3)_2$(2,2'-bipy) compound). The following shows that while $ReCl_4$(2,2'-bipy) adopts a regular octahedral configuration for the center Re atom (C12-Re-C14 = 174.2(1)°), the W atom in WO_2Cl_2(2,2'-bipy) shifts toward the dioxo site significantly (C11-W-C12 = 158.5(1)°) [23]. Schrauzer and his coworkers [24] proposed that the highly distorted octahedral coordination geometry may suggest that molybdenum(VI) is in a $(5s)(6p)^3$ state of hybridization, giving rise to a tetrahedral coordination geometry of the $MoO_2(OR)_2$ moiety. Its interaction with the bipyridine ligand is comparatively weak and does not cause a rehybridization to a regular octahedral geometry. The phenomenon that the metal atoms displace from the centers of their coordination polyhedra is also quite common in polyoxometallates [32]

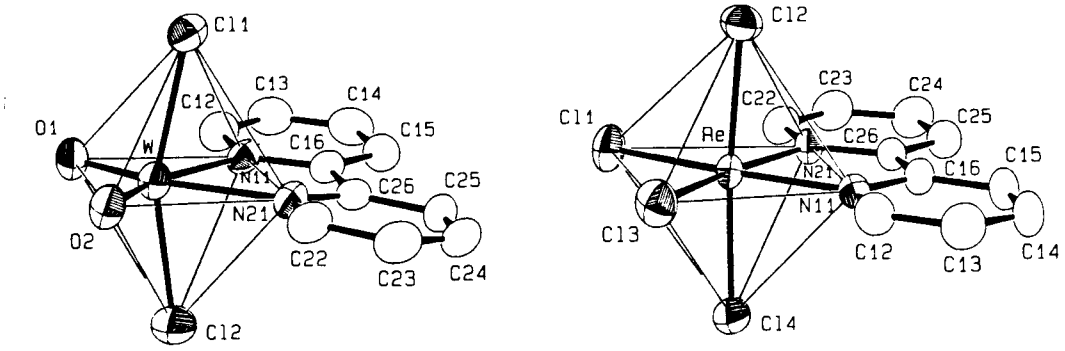

2-5-2. Comparison of triphenylsiloxy structures

A few conclusions can be drawn from a comparison of the dioxomolybdenum triphenylsiloxy structures (Table 2-3).

Table 2-3. The comparison of selected structural parameters of $MoO_2(OSiPh_3)_2$, $MoO_2(OSiPh_3)_2(PPh_3)$, and $MoO_2(OSiPh_3)_2$(2,2'-bpy) (in Å or deg)

Complexes	Mo=O	O=Mo=O	Mo-O(Si)	Si-O	Mo-O-Si
$MoO_2(OSiPh_3)_2$	1.690(6)	106.4(5)	1.815(5)	1.669(6)	163.6(4)
$MoO_2(OSiPh_3)_2(PPh_3)$	1.688(7)	110.0(4)	1.922(6)	1.638(7)	138.7(4)
	1.678(7)		1.903(6)	1.645(7)	143.9(7)
$MoO_2(OSiPh_3)_2$(2,2'-bipy)	1.68(2)	107.0(7)	1.91(2)	1.74(3)	151(2)
	1.75(2)		1.98(3)	1.51(3)	152(2)

The Mo-O(Si) bond length of $MoO_2(OSiPh_3)_2$ (1.95(2)Å av) is greater than that of five-coordinate $MoO_2(OSiPh_3)_2(PPh_3)$ (1.912(6)Å av) (see Chapter 3), which is in turn greater than the Mo-O bond length of $MoO_2(OSiPh_3)_2$(2,2'-bipy) (1.815(5)Å). The variation in the trend of Mo-O(Si) bond lengths was found to be correlated with the coordination number of the central Mo atom: 6 for $MoO_2(OSiPh_3)_2$(2,2'-bipy) > 5 for $MoO_2(OSiPh_3)_2(PPh_3)$ > 4 for $MoO_2(OSiPh_3)_2$. From an ionic point of view, the higher positive charge of Mo atom in $MoO_2(OSiPh_3)_2$ may account for the short Mo-O(Si) bond distance. However, the relatively low coordination number in $MoO_2(OSiPh_3)_2$ allows the triphenylsiloxy to approach more easily to the Mo center, which may also explain the short Mo-O(Si). These two effects work in the same direction, but it is difficult to say which one has dominant effect.

The Mo=O bond lengths and O-Mo-O bond angles in all these dioxomolybdenum triphenylsiloxides do not change significantly (Table 2-3),

which is consistent with the conclusion that $(MoO_2)^{2+}$ is a rigid structural unit [33].

2-5-3. M-O-$SiPh_3$ bond angles

The M-O-Si angle of triphenylsiloxy compounds has long been a topic of discussion in many papers. In the large number of metal triphenylsiloxy compounds, the M-O-Si angles span a range from 133.1° in $CrO_2(OSiPh_3)_2$ [21] to 177° in $[La(OSiPh_3)_3(THF)_3].THF$ [34]. Wide angles are often explained by $d\pi$-$p\pi$ bonding. For example, in $ZrCl_2(OSiPh_3)_2(DME)$ [35], the 171° Zr-O-Si angle was correlated with a short Zr-O bond distance and attributed to $d\pi$-$p\pi$ bonding. On the other hand, the wide Co-O-Si angles, 170.7° and 161.3° in $[Co(OSiPh_3)_2(THF)]_2$ [36], were ascribed to the increased steric crowding at the cobalt center as a result of THF coordination. In the explanation of the bent V-O-Si linkage in $VO(OSiPh_3)_3.0.5C_6H_6$, Feher [22] emphasized the electronic effect, i.e., the wider V-O-Si angle corresponding to a larger extent of $O(p\pi)\rightarrow V(d\pi)$ bonding.

Here a model is suggested to explain the non-linearity of the M-O-Si linkage. The M-O-$SiPh_3$ linkage prefers a linear disposition, since, as has been pointed out, a linear Si-O-Si linkage is a general characteristic of disiloxanes with bulky electron withdrawing organic substituents at the silicon atoms [37]. This has been explained in terms of $d\pi$-$p\pi$ bonding between Si and O atoms and the electron withdrawing nature of the phenyl group in $SiPh_3$, which reduces the lone pair electron

density around the O atom. The possible $d\pi$-$p\pi$ bonding in M-O, as in the case of $ZrCl_2(OSiPh_3)_2(DME)$ [35], will further increase this effect to make the M-O-Si linkage linear.

The question then arises as to why M-O-Si linkages in some metal triphenylsiloxy complex systems are non-linear. We suggest that steric repulsion accounts for bent M-O-Si linkages. Considering a triphenylsiloxy complex containing the $M(OSiPh_3)_x$ unit, where $x \geq 2$, define O atoms around the metal center as the inner coordination layer, and the $SiPh_3$ groups as the outer coordination layer. While the O atoms of Ph_3SiO in the inner coordination sphere are strongly fixed relative to the metal center and other atoms in the inner coordination layer, the steric repulsion of the outer layer phenyl tails of the triphenylsiloxy groups causes one or more M-O-Si linkages to bend. In other words, the disposition of the Ph_3Si groups in the outer coordination layer relative to the inner coordination layer determines the M-O-Si bond angle.

A parameter that can be used to measure the steric repulsion between two neighboring triphenylsiloxy groups is the distance between the two oxygen atoms of the triphenylsiloxy groups. If the O...O distance is relatively short, the phenyl tails of the triphenylsiloxy groups will repel each other leading to a bent M-O-Si linkage. Table 2-4 gives both the O...O distances and M-O-Si bond angles for some compounds containing neighboring triphenylsiloxy groups. Figure 2-4 plots the M-O-Si angles against the O...O separation. It can be seen from the plot that the M-O-Si angles correlate well with the O...O distance.

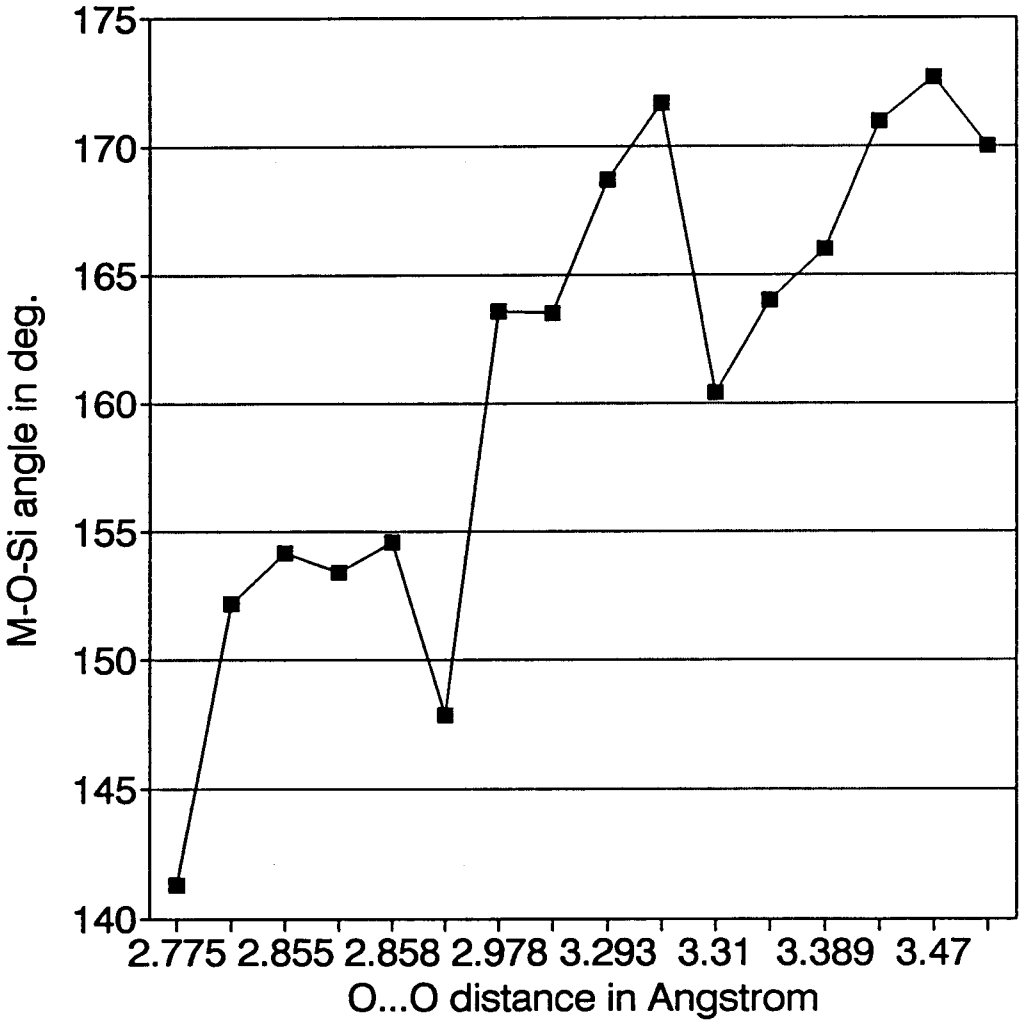

Figure 2-4. The relationship between M-O-Si angles (°) and O...O distance of neighboring triphenylsiloxy Oxygen atoms (Å). . . . . .

Table 2-4. O...O distance (Å), Si-O distance (Å), and M-O-Si angles (°) for selected triphenylsiloxy compounds.

	O...O	M-O-Si	Si-O(Å)	ref.
$MoO_2(OSiPh_3)_2(PPh_3)$	2.714	141.3°	1.641	this work
$VO(OSiPh_3)_3$	2.834	152.2°	1.647	this work
$Al(OSiPh_3)_3(THF)$	2.86(3)	153(4)°	1.606	[38]
$Al(acac)(OSiPh_3)_2$	2.855	154.2°	1.615	[39]
$VO(OSiPh_3)_3.0.5C_6H_6$	2.858	154.6°	1.653	[22]
$CrO_2(OSiPh_3)_2$	2.880	147.9°	1.60	[21]
$Al(OSiPh_3)_3(H_2O)(THF)$	3.31(9)	160.4(3)°	1.586	[38]
$MoO_2(OSiPh_3)_2$	2.978	163.6°	1.669	this work
$Y(OSiPh_3)_3(OP(^nBu)_3)_2$	3.125	163.5°	1.593	[40]
$[Y(OSiPh_3)_4(DME)]^{-1}$	3.293	168.7°	1.584	[40]
$Y(OSiPh_3)_3(THF)_3$	3.303	171.7°	1.580	[41]
$[Ce(OSiPh_3)_2(\mu\text{-}OSiPh_3)]_2$	3.367	164.0°	1.623	[42]
$[Co(OSiPh_3)_2(THF)]_2$	3.389	166.0°	1.592	[43]
$(DME)ZrCl_2(OSiPh_3)_2$	3.439	171.0°	1.65	[35]
$La(OSiPh_3)_3(THF)_3$	3.470	172.7°	1.597	[40]
$Y_2(OSiPh_3)_6$	3.492	170.0°	1.610	[44]

Most of the experimental facts can be explained by using this idea, for instance, M-O-Si is linear in $MoO_2(OSiPh_3)_2$ but bent in its chromium analogue $CrO_2(OSiPh_3)_2$. The O...O distance in the chromium analogue (2.880Å), compared to that of $MoO_2(OSiPh_3)_2$ (2.978Å), gives rise to a strong repulsion between the phenyl rings of the two Ph_3SiO groups. For $MoO_2(OSiPh_3)_2$, only a slight steric crowding may occur in the outer coordination layer at 2.978Å for the O...O distance, so that the Mo-O-Si linkage is close to linear. In compound $MoO_2(OSiPh_3)_2(PPh_3)$, the coordina-

tion of PPh_3, although weak, pushes the O...O distance closer (2.714Å) and forces the Mo-O-Si angle to an average of 141.3°.

It can be seen from Table 2-4 that the first row transition elements have a bent M-O-Si connection due to the relatively small metal cations. An exception is $[Co(OSiPh_3)_2(THF)]_2$ (166.0°) which can be explained by the large O...O separation (3.389Å). Lanthanum and yttrium triphenylsiloxy compounds always have almost linear M-O-Si linkage, due to a large O...O distance, which may be the result of the large ionic radii of the lanthanide ions.

The electronic effect of Si-O $d\pi$-$p\pi$ bonding does not appear to play a dominant role in determining M-O-Si angles. As can be seen from Table 2-4 that there is no obvious correlation between Si-O bond length and the M-O-Si angle.

2-6. Experimental

The operations were carried out under an atmosphere of purified nitrogen. Anhydrous 1,2-dichloroethane and acetonitrile were purchased from Aldrich, and purged with Ar for 15 minutes before use. All other solvents were dried and distilled before use by standard methods. Silver vanadate and silver molybdate were prepared from analytical grade silver nitrate and ammonium vanadate and sodium molybdate, respectively, and dried in an vacuum oven at 60°C for several days. Triphenylchlorosilane was purchased from the Petrach System (Huls-America, Inc.) and used as

received. All other reagents were reagent grade. Infrared spectra were recorded with a Nicholet 510P FTIR spectrometer, and NMR spectra with a AC-300 Bruker instrument. Deuterated solvents were purchased from Cambridge Isotope Laboratory. $CDCl_3$ was filtered through a neutral alumina column before use. Benzene-d^6 was stored over sodium metal. Elemental analysis were performed by Galbraith Laboratories, Knoxville, TN.

Synthesis of $MoO_2(OSiPh_3)_2$: In a typical synthesis, a flask loaded with Ag_2MoO_4 (2.38g, 6.33 mmol), Ph_3SiCl (2.44g, 8.29mmol), 40ml of 1,2-dichloroethane and about 1ml of acetonitrile was stirred and heated in a 82°C bath overnight yielding a bluish or cocoa-like solution. A bluish solution was recovered by filtration through Celite. Removal of the solvent under vacuum gave a white or sometimes slightly bluish solid. Yields based on Ph_3SiCl are typically >90%. Frequently the solid is pure enough for further reactions. If desired, it can be crystallized from n-hexane/1,2-dichloroethane or hot acetonitrile. The elemental analysis was consistent with the formula $MoO_2(OTPS)_2$. IR (KBr, cm^{-1}): 3070m, 3024m, 1588m, 1485m, 1428s, 1188w, 1119s, 948m, 933m, 886vs, 743m, 712s, 697s, 556m, 512s. NMR ($CDCl_3$/TMS): 7.5(dd, J=7, 2Hz, 2H), 7.46(tt, J=7, 2Hz, 1H), 7.33(t, J=7Hz, 2H).

$MoO_2(OSiPh_3)_2$ is a white or sometimes pale bluish solid, which is stable in air for several months. It is soluble in most organic solvents, except non-polar solvents like hexane. Once exposed to air, the 1,2-dichloroethane solution of $MoO_2(OSiPh_3)_2$ became bluish.

Synthesis of $VO(OSiPh_3)_3$: A mixture of $AgVO_3$ (0.490g, 2.37mmol) and Ph_3SiCl (0.700g, 2.37mmol) and 30ml of 1,2-dichloroethane was stirred and refluxed for 70 hours yielding a bluish solution. Filtration through Celite gave a pale yellowish solution, and from this solution 0.676g white solid was recovered upon solvent removal and n-hexane wash. The IR (909.6cm^{-1}, V=O), NMR, elemental analysis, and X-ray diffraction results of this solid confirmed that it is $VO(OSiPh_3)_3$. The yield is 93% based on Ph_3SiCl.

Synthesis of $MoO_2(OSiPh_3)_2(2,2'\text{-bpy})$: In a dry box, 876mg (1.23mmol) $MoO_2(OSiPh_3)_2$ and 209mg (1.34mmol) 2,2'-bipyridine were dissolved in 25ml of 1,2-dichloroethane. Four hours later some white solid precipitated out. The clear supernatant also afforded some crystals upon reducing the volume of solvent and cooling. The total weight of combined white solid was 1.009g. Yield based on $MoO_2(OSiPh_3)_2$ was 82%. Proton NMR (CD_2Cl_2, ppm): 9.05 (d, J=7Hz), 7.74 (dt, J=1.5, 7.7Hz), 7.44 (d, J=7.7Hz), 7.1-7.3 (m). FTIR (KBr, cm^{-1}): 3040m, 3020w, 1595m, 1474w, 1442m(2,2'-bpy), 1428s, 1115s, 928vs(Mo=O), 910vs(Mo=O), 738m 709s, 700s, 511s.

$MoO_2(OSiPh_3)_2(2,2'\text{-bpy})$ is an air-stable white solid, soluble in CH_2Cl_2 and pyridine, insoluble in 1,2-dichloroethane, THF, CH_3CN, and hexane.

The synthesis of $MoO_2(OSiPh_3)_2(OPPh_3)$: 0.462g (0.681mmol) $MoO_2(OSiPh_3)_2$ and 0.191g (0.687mmol) $OPPh_3$ were dissolved in 1,2-dichloroethane, and then mixed and allowed to cool to -15°C. Some white solid

(0.376g) was isolated the following day and was dried. Elemental analysis for $C_{54}H_{45}O_5PSi_2Mo$: Calcd. C 67.76%; H 4.74%, Measd. C 66.60%; H 4.64%. FTIR (KBr, cm^{-1}): 3050m, 3020w, 1589w, 1484w, 1437s($OPPh_3$), 1427s(Ph_3SiO), 1176m(P=O), 1150w, 1118s, 1004m, 992m, 925vs(Mo=O), 881vs (Mo=O), 744w, 725m, 711s, 697s, 539s, 508vs.

Crystallographic Studies: In all cases, X-ray reflection data were collected at 23°C in Rigaku AFC6R diffractometer equipped with graphite monochromated Mo K_α (λ = 0.71073Å) radiation. Three intense reflections were monitored every 300 reflections to check stability. No significant intensity loss was found in all cases. Crystallographic programs used were those of TEXSAN [45] installed on a microVAX, except direct method was SHELXS-86 [46]. All triphenylsiloxy compound have small absorption coefficients. Only an empirical absorption (DIFABS) was applied in call cases. All H atoms were included in calculated positions (C-H=0.95Å) in structure factor calculations. H parameters were not refined. Some selected crystallographic data are given in Table 2-5. Fractional coordinates and thermal factors are given in Tables 2-6 to 2-7. For the detailed descriptions of data collection and structure solve, see an example in Chapter 4.

$MoO_2(OSiPh_3)_2$. A colorless single crystal (0.2x0.2x0.5mm) of $MoO_2(OSiPh_3)_2$ crystallized from 1,2-dichloroethane and hexane mixed solvent, was coated in epoxy and mounted on a Rigaku AFC6R diffractometer. Unit cell parameters were determined from a least-squares fit of 19 accurately centered reflections ($27.8 < 2\theta < 31.7°$). The heavy

atom was located by the deconvolution of the Patterson pattern (PHASE [47]). The remaining atoms were expanded by DIRDIF program [48] and difference Fourier techniques. Anisotropic temperature factors were refined for all nonhydrogen atoms. The final structural factor was 4.4%. The largest residue on a final difference electron density map was 0.339 $eÅ^{-3}$.

$VO(OSiPh_3)_3$. Crystals suitable for an X-ray diffraction study were obtained by crystallization from mixed solvents of 1,2-dichloroethane and hexane. Unit cell parameters were determined from a least-squares fit of 15 accurately centered reflections ($20.5 < 2\theta < 23.7°$). The structure was solved by the combination of direct methods (SHELXS-86) and difference Fourier synthesis. Anisotropic temperature factors were refined for all nonhydrogen atoms. The final structural factors were 6.51% and 6.79% for R and R_w. The largest residue on a final difference electron density map was 0.269 $eÅ^{-3}$.

$MoO_2(OSiPh_3)_2$(2,2'-bpy). Unit cell parameters were determined from a least-squares fit of 15 accurately centered reflections ($22.26 < 2\theta < 29.24°$). (1 0 6), (2 0 4), and (3 2 2) reflections were used as standards to monitor the data collection. The structure was solved by the combination of direct method (SHELXS-86) and difference Fourier synthesis. Anisotropic temperature factors were refined for all nonhydrogen atoms. The final structural factors for R and R_w were 6.67% and 7.24%, respectively. The final difference electron density map was featureless with largest peak at 0.588 $eÅ^{-3}$.

Table 2-5. Crystallographic Data and experimental conditions for $MoO_2(OSiPh_3)_2$, $VO(OSiPh_3)_3$, and $MoO_2(OSiPh_3)_2(2,2'\text{-bpy})$

compounds	$MoO_2(OSiPh_3)_2$	$VO(OSiPh_3)_3$	$MoO_2(OSiPh_3)_2(2,2'\text{-bpy})$
empirical formula	$MoSi_2O_4C_{36}H_{30}$	$VSi_3O_4C_{54}H_{45}$	$MoSi_2O_4N_2C_{46}H_{38}$
formula weight	678.7416 amu	893.1451 amu	834.9282 amu
dimension, mm	0.2x0.2x0.5	0.2x0.2x0.3	0.1x0.2x0.4
crystal system	orthorhombic	triclinic	orthorhombic
lattice parameters	a = 19.556(7)Å	13.477(5)Å	a = 17.532(15)Å
	b = 34.187(4)Å	18.577(4)Å	b = 33.345(8)Å
	c = 9.748(5)Å	10.014(3)Å	c = 13.273(4)Å
		α = 98.66(3)°	
		β = 101.22(3)°	
		γ = 73.14(2)°	
V, Å^3	6517.3(3.6) Å^3	2341.7(1.4) Å^3	7781(10)Å^3
space group	Fdd2 (#43)	P-1 (#2)	Pbca (#61)
Z	8	2	8
D_{calc}, g cm-3	1.3833	1.2665	1.425
F(000)	2784	932	3440
μ (MoKα), cm^{-1}	4.9975	3.22	4.3386
temperature	23°C	23°C	23°C
diffractometer	Rigaku AFC6R		
radiation	MoKα (λ = 0.710690 Å) graphite monochromated		
$2\theta_{max}$	53.2°	53°	50°
data collection speed	16.0° min^{-1} in ω	16.0° min^{-1} in ω	16.0° min^{-1} in ω
scan method	ω-2θ	ω	ω
h k l limits	0,0,0 to 24,42,12	0,-23,-17,16,23,17	0,0,0 to 20,39,15
total no.of measd data	1921	6839	6007
no. observations (I>3σ(I))	1236	3011	1622
no. variables	194	559	261
residuals: R; R_w	0.044; 0.044	0.0651, 0.0679	0.0667; 0.0724
GOF	1.52	1.90	1.60
maximum shift	0.07	0.05	0.15
largest residual peak	0.339	0.269	0.588

Table 2-6. Positional parameters and B(eq) of non-Hydrogen atoms for $MoO_2(OSiPh_3)_2$

atom	x	y	z	B(eq)
Mo	0	0	0	3.42(4)
Si(1)	0.0935(1)	0.07143(6)	-0.1649(3)	3.6(1)
O(2)	-0.0577(3)	0.0219(2)	0.1038(8)	7.6(4)
O(1)	0.0417(3)	0.0364(2)	-0.1068(6)	4.6(3)
C(1)	0.1822(4)	0.0533(2)	-0.1504(9)	3.3(3)
C(2)	0.2192(5)	0.0423(2)	-0.265(1)	4.5(4)
C(3)	0.2855(5)	0.0285(3)	-0.256(1)	5.5(5)
C(4)	0.3146(4)	0.0258(3)	-0.129(1)	6.0(6)
C(5)	0.2809(5)	0.0358(3)	-0.014(1)	5.7(5)
C(6)	0.2140(4)	0.0501(2)	-0.025(1)	4.5(5)
C(7)	0.0803(4)	0.1154(2)	-0.0571(8)	3.6(4)
C(8)	0.1320(4)	0.1425(2)	-0.035(1)	5.1(5)
C(9)	0.1223(5)	0.1761(2)	0.039(1)	6.2(6)
C(10)	0.0610(6)	0.1842(3)	0.096(1)	6.1(5)
C(11)	0.0067(5)	0.1581(3)	0.077(1)	5.7(5)
C(12)	0.0169(4)	0.1245(2)	0.003(1)	4.6(4)
C(13)	0.0711(4)	0.0795(3)	-0.344(1)	4.0(4)
C(14)	0.0865(5)	0.1143(3)	-0.413(1)	5.8(6)
C(15)	0.0712(8)	0.1179(4)	-0.548(1)	9.4(8)
C(16)	0.0455(7)	0.0897(5)	-0.624(1)	9.6(9)
C(17)	0.0283(9)	0.0550(4)	-0.562(1)	9.7(9)
C(18)	0.0420(6)	0.0507(3)	-0.425(1)	7.6(7)

Table 2-7. Positional parameters and B(eq) for non-hydrogen atoms of $VO(OSiPh_3)_3$

atom	x	y	z	B(eq)
V	0.8186(1)	0.2116(1)	0.1653(2)	4.2(1)
Si(1)	0.5808(2)	0.2088(2)	0.1738(3)	4.3(2)
Si(2)	1.0198(2)	0.1956(2)	0.4182(3)	4.6(2)
Si(3)	0.8246(2)	0.3496(2)	-0.0043(3)	4.7(2)
O(1)	0.6921(5)	0.2331(4)	0.2043(6)	5.2(4)
O(2)	0.9083(4)	0.2216(4)	0.3127(6)	4.7(4)
O(3)	0.8174(5)	0.2718(4)	0.0477(6)	5.8(4)
O(4)	0.8483(6)	0.1285(4)	0.0961(7)	6.7(5)
C(1)	0.4872(7)	0.2860(6)	0.261(1)	4.1(5)
C(2)	0.4225(8)	0.2729(6)	0.341(1)	5.8(6)
C(3)	0.352(1)	0.3301(8)	0.404(1)	6.8(8)
C(4)	0.344(1)	0.4027(8)	0.389(1)	7.1(8)
C(5)	0.405(1)	0.4190(7)	0.310(1)	6.7(8)
C(6)	0.4775(8)	0.3611(7)	0.247(1)	5.6(7)
C(11)	0.6012(8)	0.1193(6)	0.244(1)	5.0(6)
C(12)	0.571(1)	0.0598(7)	0.172(1)	6.7(7)
C(13)	0.582(1)	-0.0060(8)	0.227(2)	9(1)
C(14)	0.628(1)	-0.0132(8)	0.361(2)	9(1)
C(15)	0.661(1)	0.0432(9)	0.436(1)	8(1)
C(16)	0.649(1)	0.1098(7)	0.378(1)	7.5(8)
C(21)	0.5331(8)	0.2012(6)	-0.013(1)	4.7(6)
C(22)	0.600(1)	0.1686(8)	-0.104(1)	8.1(9)
C(23)	0.564(1)	0.164(1)	-0.245(2)	10(1)
C(24)	0.462(2)	0.193(1)	-0.294(1)	9(1)
C(25)	0.398(1)	0.222(1)	-0.206(2)	14(1)
C(26)	0.433(1)	0.2273(9)	-0.066(1)	10(1)
C(31)	1.1243(8)	0.1382(6)	0.319(1)	4.8(6)
C(32)	1.221(1)	0.1446(8)	0.344(2)	9(1)
C(33)	1.302(1)	0.103(1)	0.276(2)	11(1)
C(34)	1.279(1)	0.0510(9)	0.174(2)	9(1)
C(35)	1.183(1)	0.039(1)	0.143(2)	12(1)
C(36)	1.106(1)	0.0828(9)	0.222(2)	10(1)
C(41)	1.0541(7)	0.2833(6)	0.499(1)	4.6(6)
C(42)	1.0856(8)	0.2970(6)	0.637(1)	5.8(7)
C(43)	1.114(1)	0.3606(8)	0.697(1)	7.0(8)
C(44)	1.110(1)	0.4146(7)	0.616(1)	7.2(8)
C(45)	1.079(1)	0.4036(7)	0.477(1)	6.6(8)
C(46)	1.0514(8)	0.3399(6)	0.419(1)	5.3(6)
C(51)	1.0012(9)	0.1443(6)	0.552(1)	5.6(6)
C(52)	0.915(1)	0.1672(7)	0.615(1)	7.1(8)
C(53)	0.907(1)	0.1350(9)	0.728(2)	9(1)
C(54)	0.989(2)	0.078(1)	0.776(2)	11(1)
C(55)	1.076(1)	0.054(1)	0.716(2)	14(1)
C(56)	1.081(1)	0.086(1)	0.606(2)	11(1)
C(71)	0.7753(7)	0.3489(6)	-0.191(1)	4.3(5)
C(72)	0.8239(8)	0.3718(6)	-0.277(1)	5.1(6)
C(73)	0.787(1)	0.3733(6)	-0.415(1)	5.8(7)
C(74)	0.699(1)	0.3521(7)	-0.467(1)	6.3(7)
C(75)	0.6456(9)	0.3287(7)	-0.383(1)	7.1(8)
C(76)	0.6871(9)	0.3261(7)	-0.245(1)	6.3(7)
C(81)	0.7398(8)	0.4304(6)	0.086(1)	5.2(6)
C(82)	0.696(1)	0.498(1)	0.030(1)	13(1)
C(83)	0.629(2)	0.559(1)	0.092(2)	19(2)
C(84)	0.608(1)	0.556(1)	0.217(2)	10(1)
C(85)	0.654(1)	0.493(1)	0.277(1)	8(1)
C(86)	0.719(1)	0.4318(7)	0.213(1)	8(1)
C(91)	0.9643(8)	0.3489(7)	0.033(1)	4.8(6)
C(92)	1.040(1)	0.2836(7)	0.014(1)	6.1(7)
C(93)	1.146(1)	0.2814(8)	0.043(1)	7.0(8)
C(94)	1.174(1)	0.348(1)	0.090(1)	6.7(8)
C(95)	1.101(1)	0.4135(7)	0.111(1)	6.5(8)
C(96)	0.9947(9)	0.4147(6)	0.083(1)	5.5(7)

Table 2-8. Positional parameters and B(eq) for non-hydrogen atoms of $MoO_2(OSiPh_3)_2(2,2'\text{-bpy})$

atom	x	y	z	B(eq)
Mo(1)	0.21619(8)	0.12625(6)	0.2494(4)	2.70(6)
Si(1)	0.2416(5)	0.1100(5)	-0.000(1)	3.3(6)
Si(2)	0.2542(3)	0.1394(4)	0.509(1)	2.1(5)
O(1)	0.236(1)	0.1048(9)	0.113(2)	3(1)
O(2)	0.2485(6)	0.145(1)	0.379(2)	3(1)
O(3)	0.160(1)	0.1679(6)	0.219(2)	6(1)
O(4)	0.156(1)	0.0900(6)	0.287(1)	3(1)
N(1)	0.329(1)	0.0887(6)	0.276(1)	1.4(5)
N(2)	0.326(2)	0.1638(8)	0.209(1)	4(1)
C(1)	0.253(1)	0.166(1)	-0.038(2)	1.4(8)
C(2)	0.316(1)	0.1788(6)	-0.093(2)	2.6(5)
C(3)	0.322(1)	0.2198(8)	-0.118(2)	5.0(6)
C(4)	0.260(1)	0.2446(8)	-0.096(2)	2.0(6)
C(5)	0.199(1)	0.2314(7)	-0.046(2)	3.5(5)
C(6)	0.195(1)	0.1896(7)	-0.020(2)	3.0(5)
C(11)	0.325(1)	0.0786(7)	-0.048(2)	1.9(5)
C(12)	0.317(1)	0.0502(8)	-0.124(2)	4.9(6)
C(13)	0.379(2)	0.0249(9)	-0.149(2)	7.2(8)
C(14)	0.447(2)	0.0312(8)	-0.100(2)	5.9(7)
C(15)	0.457(2)	0.0602(9)	-0.030(2)	6.1(8)
C(16)	0.394(2)	0.0832(8)	-0.009(2)	4.3(8)
C(21)	0.152(1)	0.0914(7)	-0.061(2)	2.4(6)
C(22)	0.138(1)	0.0994(6)	-0.166(2)	3.1(5)
C(23)	0.070(1)	0.0865(7)	-0.209(2)	4.3(6)
C(24)	0.014(1)	0.0687(7)	-0.151(2)	3.5(5)
C(25)	0.028(2)	0.0623(7)	-0.054(2)	4.4(6)
C(26)	0.095(1)	0.0731(7)	-0.006(2)	3.2(6)
C(41)	0.253(1)	0.089(1)	0.547(3)	3(1)
C(42)	0.314(2)	0.0628(8)	0.554(2)	5.0(7)
C(43)	0.315(1)	0.0239(8)	0.577(2)	4.4(6)
C(44)	0.244(2)	0.006(2)	0.596(4)	10(2)
C(45)	0.182(2)	0.025(1)	0.585(2)	6.4(8)
C(46)	0.184(1)	0.0661(7)	0.556(2)	3.9(6)
C(51)	0.176(1)	0.1692(8)	0.563(2)	2.9(6)
C(52)	0.185(1)	0.1943(7)	0.642(2)	3.2(5)
C(53)	0.126(1)	0.2178(7)	0.678(2)	4.1(5)
C(54)	0.057(1)	0.2161(6)	0.636(2)	4.1(5)
C(55)	0.046(1)	0.1912(7)	0.555(2)	3.4(6)
C(56)	0.104(2)	0.1677(7)	0.519(2)	3.2(6)
C(61)	0.349(2)	0.1586(7)	0.546(2)	2.9(6)
C(62)	0.374(1)	0.1551(6)	0.644(2)	3.1(5)
C(63)	0.445(1)	0.1664(6)	0.677(1)	2.9(5)
C(64)	0.496(1)	0.1849(7)	0.607(2)	3.1(5)
C(65)	0.469(2)	0.1902(7)	0.511(2)	3.6(5)
C(66)	0.397(1)	0.1775(7)	0.481(2)	3.6(6)
C(71)	0.326(1)	0.2006(8)	0.178(2)	5.0(6)
C(72)	0.392(1)	0.2226(7)	0.165(2)	4.2(5)
C(73)	0.458(2)	0.2041(7)	0.184(2)	5.3(6)
C(74)	0.466(2)	0.1654(7)	0.214(2)	5.0(6)
C(75)	0.397(1)	0.1447(7)	0.227(2)	3.5(6)
C(76)	0.396(1)	0.1028(7)	0.260(2)	3.4(5)
C(77)	0.464(2)	0.0784(7)	0.270(2)	5.8(6)
C(78)	0.448(1)	0.0391(8)	0.298(2)	5.2(6)
C(79)	0.382(1)	0.0237(7)	0.314(2)	4.7(6)
C(80)	0.323(1)	0.0498(7)	0.302(2)	4.2(6)

2-7. **References:**

1. Chisholm, M.H., in Wilkinson, G. Ed. *"Comprehensive Coordinative Chemistry"*, Vol 2, **1987**, Pergamon Press.

2. Babaian, E.A.; Hrncir, D.C.; Bott, S.G.; Atwood, J.L. *Inorg. Chem.* **1986**, *25*, 4818.

3. Gradeff, P.S; Yunlu, K.; Deming, T.J.; Olofson, J.M.; Doedens, R.J. *Inorg. Chem.* **1990**, *29*, 420.

4. Gradeff, P.S.; Yunlu, K.; Deming, T.J.; Olofson, J.M.; Ziller, J.W.; Evans, W.J. *Inorg. Chem.* **1989**, *28*, 2600-2604.

5. Gradeff, P.S.; Schreiber, F.G.; Brooks, K.C.; Sievers, R.E. *Inorg. Chem.* **1985**, *24*, 1110-1111. Gradeff, P.S.; Schreiber, F.G.; Mauermann, H. J. *Less-Common Met.* **1986**, *126*, 335-338. Evans, W.J.; Deming, T.J.; Ologson, J.M.; Ziller, J.W. *Inorg. Chem.* **1989**, *28*, 4027-4034.

6. Schmidt, M.; Schidbauer, H., *Inorg. Syn.* **1967**, *9*, 149.

7. Sekiguchi, S; Kurihara, A. *Bull. Chem. Soc. Jpn.* **1969**, *42*, 1453.

8. Weidenbruch, M; Pierrard, C.; Pesel, H. *Z. Naturforsch.* **1978**, *33b*, 1468.

9. Imyanitov, N.S. *Koordinatsionnaya Khimiya* **1985**, *11(9)*, 1171-8.

10. Linke, W. F. *"Solubilities"*, 4th. Ed., D. Van Nostrand Company, Inc., 1958. The K_{sp} data of silver molybdate manganate and perrhenate were estimated from their solubilities in water.

11. Glidewell, C. *Inorg. Chim. Acta* **1977**, *24*, 149-57 and references therein.

12. Pedley, J. B. and Marshall, E. M. *J. Phys. Chem. Ref. Data* **1984**, *12*, 967.

13. Schmidt, M.; Schmidbauer, H. *Inorg. Synth.* **1967**, *9*, 149. Nugent, W. A. *Inorg. Chem.* **1983**, *22*, 965.

16. Arzoumanian, H; Corao, C.; Krentzien, H.; Lopez, R.; Teruel, H. *J. Chem. Soc., Chem. Commun.* **1992**, 856.

17. Anderson, D.R. in *"Analysis of Silicone"*, Ed. by Smith, A.L., John Wiley & Sons, New York, **1974**.

18. Lipp, E.D. and Smith, A.L. in *"The Analytical Chemistry of Silicones"*, Ed. by Smith, A.L., John Wiley & Sons, New York, **1991**.

19. Wilkinson, G. Ed., *"Coordinative Chemistry Review"*, **1987**.

20. Kim, G.S. *Ph.D Thesis*, Oregon State University, 1989.

21. Stensland, B.; Kierkegaard, P. *Acta Chemica Scandinavica* **1970**, *24*, 211.

22. Feher, F. J.; Walzer, J. F. *Inorg. Chem.* **1991**, *30*, 1689

23. Herrmann, W.A.; Thiel, W.R.; Herdtweck, E. *Chem. Ber.* **1990**, *123*, 271-276.

24. Zhang, C.; Schlemper, E.O.; Schrauzer, G.N. *Organometallics* **1990**, *9*, 1016-1020. Schrauzer, G.N.; Hughes, L.A.; Stramach, N. *Organometallics* 1983, 2(4), 484-485. Zhang, C.; Schlemper, E.O.; Schrauzer, G.N. *Organometallics* **1990**, *9*, 1016.

25. Djafri, F.; Lai, R.; Pierrot, M.; Regnier, J. *Acta Crystallogr.* **1991**, *C47*, 1374-1376.

26. Fenn, R.H. *J. Chem. Soc. (A)* **1969**, 1764.

27. Schrauzer, G.N.; Hughes, L.A.; Strampach, N.; Robinson, P.R.; Schlemper, E.O. *Organometallics* **1982**, *1*, 44.

28. Schrauzer, G.N.; Hughes, L.A.; Strampach, N. *Organometallics* **1983**, *2(4)*, 481.

29. Zhang, C.; Schlemper, E.O.; Schrauzer, G.N. *Organometallics* **1990**, *9*, 1016.

30. Howie, R.A.; McQuillan, G.P. *J. Chem. Soc. Dalton Trans.* **1986**, 759

31. Cotton, F.A. and Wilkinson, G. "*Advanced Inorganic Chemistry*", 5th Ed. John Wiley & Sons, New York, p349, **1988**.

32. Pope, M.T. "*Heteropoly and Isopoly Oxometalates*", Springer-Verlag, New York, **1983**.

33. Nugent, W.A.; Mayer, J.M., *"Metal-Ligand Multiple Bonds"*, **1988**, John Wiley and Sons, Inc.

34. McGeary, M.J.; Coan, P.S.; Folting, K.; Streib, W.E.; Caulton, K.G. *Inorg. Chem.* **1991**, *30*, 1723.

35. Babaian, E.A.; Hrncir, D.C.; Bott, S.G.; Atwood, J.L. *Inorg. Chem.* **1986**, *25*, 4818.

36. Sigel, G.A.; Bartlett, R.A.; Decker, D. Olmstead, M.M.; Power, P.P. *Inorg. Chem.* **1987**, *26*, 1773.

37. Lukevics, E.; Pudova, O.; Sturkovich, R." *Molecular Structure of Organosilicon Compounds*", pp 191, Ellis Horwood Limited, Chichester, **1989**.

38. Apblett, A.W.; Warren, A.C.; Barron, A.R. Can. J. Chem. **1992**, *70*, 771.

39. Garbauskas, M.F.; Wwngrovius, J.H.; Going, R.C.; Kasper, J.S. *Acta Cryst*. **1984**, *C40*, 1536.

41. McGeary, M.J.; Coan, P.S.; Folting, K.; Streib, W.E.; Caulton, K.G. *Inorg. Chem*. **1989**, *28*, 3284.

42. Evans, W.J., Golden, R.E., Ziller, J.W. *Inorg. Chem*., **1991**, *30*, 4963.

43. Mais, R.H.B.; Owston, P.G.; Thompson, D.T. *J. Chem. Soc. (A)*, **1967**, 1735.

44. Coan, P.S., McGeary, M.J.; Lobkovsky, E.B.; Caulton, K.G. *Inorg. Chem*. **1991**, *30*, 3570.

Chapter 3

Oxygen Atom Transfer Reactions

3-1. Introduction [1]

The transition metal mediated oxygen atom transfer reaction is a reaction where the oxygen atom in M=O moiety is transferred to a substrate. By far, the most common reagents for oxygen atom abstraction are phosphines, PR_3, which reduce a wide range of metal-oxo complexes (eqn. 1).

$$L_nM{=}O + PR_3 \longrightarrow L_nM + R_3P{=}O \qquad \ldots(1)$$

An often-mentioned example of oxygen atom transfer reaction is the reduction of bis(diethyldithiocarbamate)dioxo molybdenum by triphpenylphosphine (shown in eqn. 2). Extensive research has shown two features of this chemistry. First, because molybdenum can be reoxidized to the +6 oxidation state with dioxygen, this reaction can be carried out using a catalytic amount of the molybdenum compound. Thus, the reaction has been studied as a prototypic oxometal-mediated air oxidation. Interest is

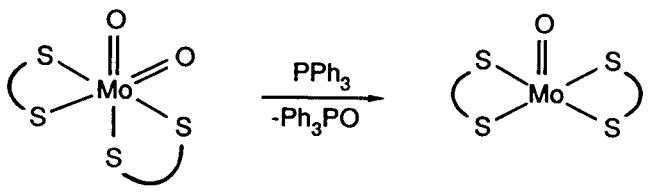

...(2)

S⌒S = diethyldithiocarbamate

further enhanced by the presumed relevance of this transformation to their "oxo transferase" family of molybdenum-containing enzymes.

In fact, oxygen atom transfer reactions have received considerable attention in recent years because of its importance as a fundamental step in a variety of industrial catalytic processes and enzymatic processes.

The selective oxidation of propylene to acrolein is a very important industrial process (eqn. 3). This process and the closely related ammoxidation of propylene (eqn. 4) have been the subject of extensive mechanistic investigations. As indicated in eqn. 3, selective propylene oxidation is promoted by a bismuth molybdate catalyst. Such catalysts contain multiply bonded oxo species, which were proposed to be directly involved in propylene oxidation. An important step in the mechanism of the propylene oxidation was suggested to be the oxygen atom transfer from molybdenum oxide catalyst to propyl cation. The molybdenum oxide catalyst is then regenerated by dioxygen, O_2, so as to furnish the whole oxygen transfer from O_2 to propylene..

$$CH_3CH{=}CH_2 + O_2 \xrightarrow[Bi_2O_3/MoO_3]{400^\circ C} CH_2{=}CHCH{=}O + H_2O \qquad ...(3)$$

$$CH_2{=}CHCH_3 + 1.5O_2 + NH_3 \xrightarrow[catalyst]{450^\circ C} CH_2{=}CHCH_2CN + 3H_2O \qquad ...(4)$$

Among other examples of the oxygen transfer reaction are the epoxidation of olefin by a number of high-valent metal oxo complexes and cis-dihydroxylation of alkenes [1].

Holm suggests a term "oxo-transferase" to describe a widely distributed family of molybdenum redox enzymes that promote the addition of an oxygen atom to, or its removal from a substrate [2]. These enzymes include hydroxylases such as xanthine oxidase (eqn. 5), aldehyde oxidase, and sulfite oxidase. Also included are formate dehydrogenases and reductases such as nitrate reductases [1]. It is now generally believed that these enzymes function, at least in some cases, by direct transfer of the oxo ligand to the organic substrate.

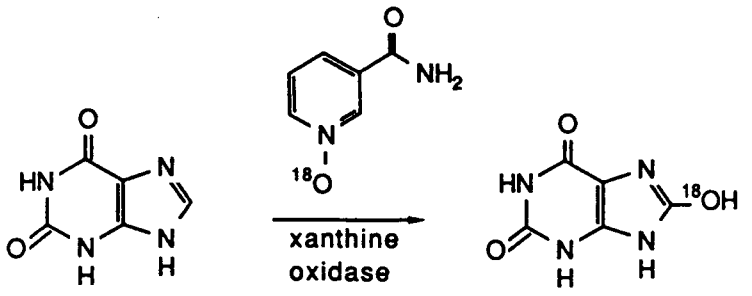

xanthine uric acid ...(5)

In an effort to model the enzymatic oxygen atom transfer reactions of oxygen transferases, a large number of molybdenum dioxo compounds has been synthesized and their chemistry with a variety of trialkylphosphines (eqn. 2) was extensively studied.

The thermodynamic studies on eqn. 2 (for triethylphosphine), in the solvent 1,2-dichloroethane, indicate that the process is substantially exoergonic with ΔH = -29.0±2.5 Kcal/mole [3]. A kinetic study by Holm and coworkers [4] gave the rate constants (in $M^{-1}sec^{-1}$) for the $MoO_2(S_2C\text{-}NEt_2)_2/PR_3$ system were shown to increase along the series Ph_3P (0.071), PPh_2Et (0.23), $PPhEt_2$ (0.43), PEt_3 (0.53), which is parallel to the reducing power of the trialkylphosphine.

Another contribution of Holm and coworkers is the development of molybdenum enzyme models containing sterically encumbered NS_2^- type ligands [5]. These ligands inhibit the formation of μ-oxo dimers shown in eqn. 6. Reaction with triphenylphosphine therefore proceeds cleanly, as shown in Figure 3-1.

$$MoO(dtc)_2 + MoO_2(dtc)_2 \longleftrightarrow Mo_2O_3(dtc)_4 \qquad \ldots(6)$$

(dtc = diethyldithiocarbamate)

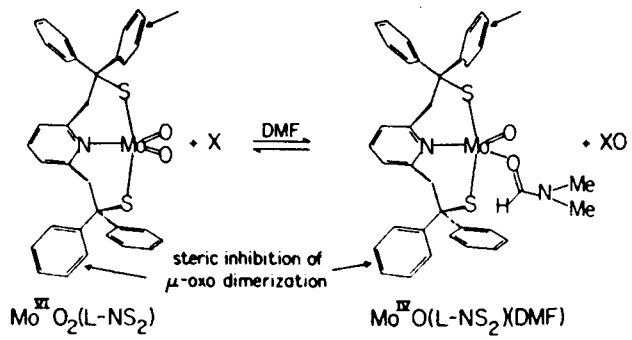

Figure 3-1. Use of bulky NS_2 ligands to promote clean oxo transfer uncomplicated by formation of μ-oxo dimer (X = PPh_3).

In this thesis work, the oxygen atom transfer reaction of $MoO_2(OSiPh_3)_2$ with trialkylphosphine was studied. It was hoped that the sterically bulky triphenylsiloxy would stabilize the possible highly reactive, three-coordinate Mo(IV) compound $MoO(OSiPh_3)_2$. In the study, this compound, however, was not obtained. A five-coordinate Mo(VI) triphenylphosphine compound, containing the first-observed Mo(VI)-P bond was instead isolated. It is astonishing that triphenylphosphine does not reduce the $Mo(VI)O_2$ moiety and the Mo(VI)-phosphine bond is stable enough to undergo an X-ray diffraction study. This chapter will discuss the synthesis and the X-ray structure of $MoO_2(OSiPh_3)_2(PPh_3)$ and its implication in the mechanism of the oxygen atom transfer reaction. An Extended Huckel Molecular Orbital (EHMO) calculation was also performed to a model compound of $MoO_2(OSiPh_3)_2(PPh_3)$ to obtain some insight into the stability of the Mo(VI)-phosphine bond.

3-2. Oxygen Atom Transfer Reaction and Crystal Structure of $MoO_2(OSiPh_3)_2(PPh_3)$

The starting compound $MoO_2(OSiPh_3)_2$ was prepared as described in the previous chapter. It was then reacted with several trialkylphosphine in 1,2-dichroethane. The results are summarized in the following equations:

$$MoO_2(OSiPh_3)_2 + PEt_3 \longrightarrow OPEt_3 + \{Mo\} + (Ph_3Si)_2O \quad ...(7)$$

$$MoO_2(OSiPh_3)_2 + PBu^n_3 \longrightarrow OPBu^n_3 + \{Mo\} + (Ph_3Si)_2O \quad ...(8)$$

$$MoO_2(OSiPh_3)_2 + PPh_3 \longrightarrow MoO_2(OSiPh_3)_2(PPh_3) \quad ...(9)$$

The reactions of $MoO_2(OSiPh_3)_2$ with the stronger reducing trialkylphosphine (PEt_3 and PBu^n_3) gives a deep reddish mixture. The mixture was shown to contain $(Ph_3Si)_2O$, $R_3P{=}O$ and a deep reddish oily solid. This deep reddish oily solid was identified as a reduced polyoxometallate, as it contains no hydrocarbon signals in either the NMR or the FTIR. The Mo=O stretching bands in the FTIR were very strong.

Only the reaction with triphenylphosphine (eqn. 9) gives a well characterized compound $MoO_2(OSiPh_3)_2(PPh_3)$, which is the adduct of the parent compound and triphenylphosphine as determined by an X-ray diffraction study. The structure of $MoO_2(OSiPh_3)_2(PPh_3)$ and some selected bond lengths and bond angles from an X-ray diffraction study are shown in Figure 3-2. Final fractional coordinates are given in Table 3-2.

$MoO_2(OSiPh_3)_2(PPh_3)$ has a distorted trigonal bipyramidal configuration around the Mo atom. The oxo atoms and the one triphenylsiloxy oxygen atom occupy the equatorial plane. The Mo atom is not coplanar with the equatorial ligands, but is slightly moved (by 0.276Å) toward the axial triphenylsiloxy group. The axial triphenylsiloxy group is displaced from the axial position toward the equatorial triphenylsiloxy group. This causes the four oxygen atoms in the inner coordination layer to be in a quasi-tetrahedral setting. It is noteworthy that the equatorial Mo-O(Si) bond length (1.922(6)Å) is longer than the axial one (1.903(6)Å). We will address this issue in the section on theoretical studies.

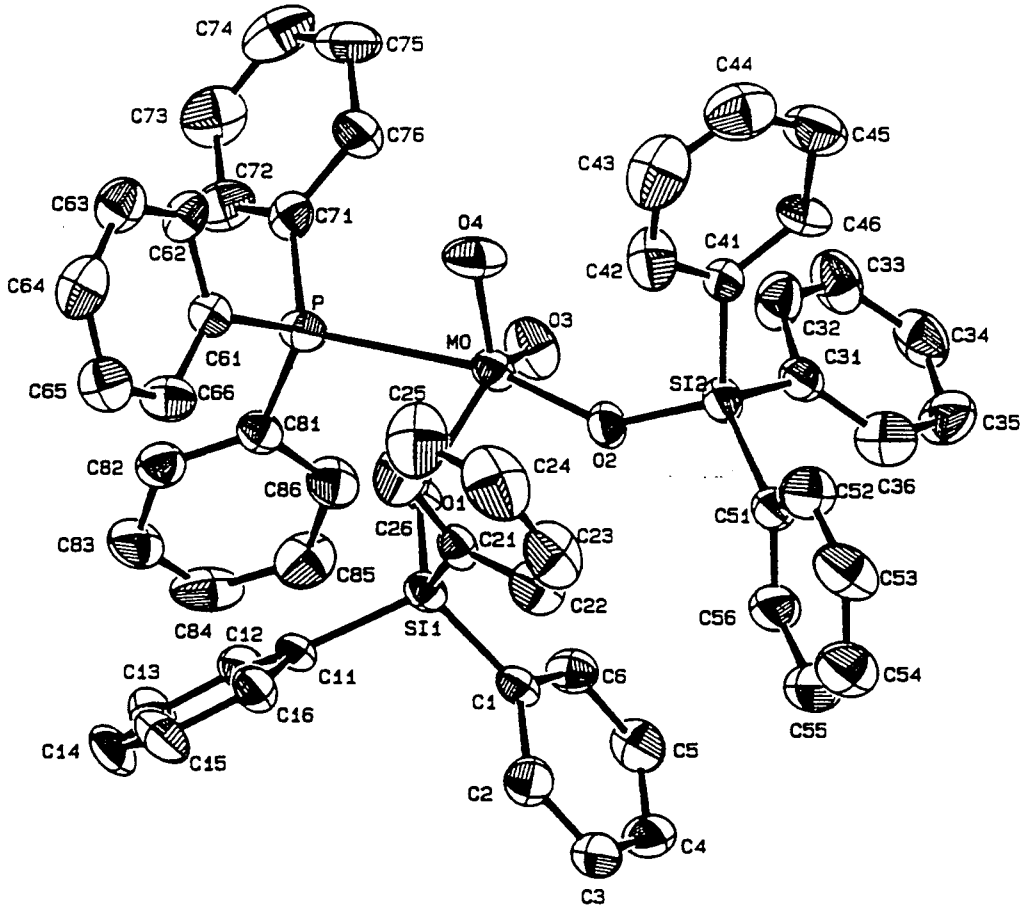

Figure 3-2. An ORTEP view of the structure of $MoO_2(OSiPh_3)_2(PPh_3)$. Selected bond lengths (Å) and bond angles (deg): Mo-P 2.759(3), Mo-O(1) 1.922(6), Mo-O(2) 1.903(6), Mo-O(3) 1.688(7), Mo-O(4) 1.678(7), P-O(1) 2.961(7), P-O(3) 3.071(7), P-O4 3.071(7); P-Mo-O(1) 76.2(2)°, P-Mo-O(2) 166.5(2)°, P-Mo-O(3) 83.7(3)°, P-Mo-O(4) 83.8(3)°, O(1)-Mo-O(2) 90.4(3)°, O(1)-Mo-O(3) 119.3(3)°, O(1)-Mo-O(4) 123.5(3)°, O(2)-Mo-O(3) 104.2(3)°, O(2)-Mo-O(4) 103.3(3)°, O(3)-Mo-O(4) 110.0(4)°, Mo-O(1)-Si(1) 138.7(4)°, Mo-O(2)-Si(2) 143.9(4)°. Hydrogen atoms are omitted for clarity.

The bond angle of the Mo dioxo bonds O=Mo=O (110.0°) in $MoO_2(OSiPh_3)_2(PPh_3)$ is close to that of the parent tetrahedral compound (106.4°). The Mo=O bond lengths (1.638(7), 1.678(7)Å) are comparable to the corresponding Mo=O bond lengths in $MoO_2(OSiPh_3)_2$ (1.690(6) Å). It appears that the structural parameters of the $\{MoO_2\}^{+2}$ unit are not sensitive to the uptake of triphenylphosphine from these structural data. This is also true for the uptake of 2,2'-bipyridine by $MoO_2(OSiPh_3)_2$ to form $MoO_2(OSiPh_3)_2(2,2'\text{-bpy})$ (see Chapter 2). These results are in contrast to those from the infrared spectra for $MoO_2(OSiPh_3)_2(PPh_3)$ (Fig. 3-3). The infrared spectra shows that ν(Mo=O) for $MoO_2(OSiPh_3)_2(PPh_3)$ at 898, 873 cm^{-1} are significantly lower than 948, 932, and 885 cm^{-1} of the parent compound, which may suggest that the Mo=O bond strength in $MoO_2(OSiPh_3)_2(PPh_3)$ is weaker than Mo=O in $MoO_2(OSiPh_3)_2$.

The most interesting structural feature of $MoO_2(OSiPh_3)_2(PPh_3)$ is the coordination of the phosphine atom to the parent compound $MoO_2(OSiPh_3)_2$. To our knowledge, no Mo(VI) compounds coordinated by alkyl or aryl P compounds have been observed. The Mo-P distance here is 2.759(3)Å. For comparison, Mo(IV)-P bond lengths in $MoOCl_2(PMe_2Ph)_3$ are 2.500, 2.541, and 2.588(3)Å [6], Mo(II)-P in $MoBr_2(CO)_3\{Ph_2P(CH_2)_2PPh_2\}.CH_3COCH_3$ are 2.618Å (trans to CO) and 2.500Å (trans to Br) [7], and in $Et_3P(OC)_3Mo(\mu\text{-}PMe_2)_2Mo(CO)_3PEt_3$ Mo(0)-P is 2.477(5)Å [8], and in $Mo(Ntol)Cl2(Me_3P)_3$ Mo(IV)-P is 2.471(1)Å and 2.509(1)Å [9]. A Mo(V)-P bond is also known in $MoCl_4(NPPh_3)(PPh_3)$ and $Mo(NTol)Cl_3(Me_3P)_2$ [9], but no structural data are available. It appears that the Mo-P bond length is not very sensitive to the change of Mo oxidation state, or in other words, the Mo-P bond length

is not correlated to the Mo oxidation state. Based on this argument, we estimate the Mo(VI)-P single bond length to be between 2.5 and 2.6Å. This suggests that the Mo-P (2.759Å) bond in $MoO_2(OSiPh_3)_2(PPh_3)$ is weaker than a single bond. This conclusion is supported by the following experimental fact: if $MoO_2(OSiPh_3)_2(PPh_3)$ is suspended and stirred in hexane, in which both $MoO_2(OSiPh_3)_2$ and $MoO_2(OSiPh_3)_2(PPh_3)$ are insoluble, some PPh_3 is found in the hexane, which must come from the decomposition of $MoO_2(OSiPh_3)_2(PPh_3)$. The ^{31}P NMR of pure $MoO_2(OSiPh_3)_2(PPh_3)$ is always accompanied by a band at -4.9ppm (PPh_3), which is also an indication of the decomposition of $MoO_2(OSiPh_3)_2(PPh_3)$.

Although the Mo-P bonding is not strong in $MoO_2(OSiPh_3)_2(PPh_3)$, the uptake of the PPh_3 by $MoO_2(OSiPh_3)_2$ greatly changes its IR spectrum (Figure 3-3). Figure 3-3 shows the IR spectra of $MoO_2(OSiPh_3)_2(PPh_3)$, $MoO_2(OSiPh_3)_2(OPPh_3)$, and a 1:1 mixture $MoO_2(OSiPh_3)_2$ with PPh_3. It can be seen in the Mo=O stretching region that the 1:1 mixture of $MoO_2(OSiPh_3)_2$ and PPh_3 still has the same Mo=O stretching as $MoO_2(OSiPh_3)_2$, which is not altered at all by the mixture with PPh_3. The IR spectrum of $MoO_2(OSiPh_3)_2(PPh_3)$, however, is quite different from its parent compound, and shows two well-defined Mo=O stretchings at 897 and 872 cm^{-1}. These Mo=O stretching frequencies are lower than that of its parent compound (948, 933, 887 cm^{-1}), and even lower that of compound $MoO_2(OSiPh_3)_2(OPPh_3)$ (925, 881cm^{-1}).

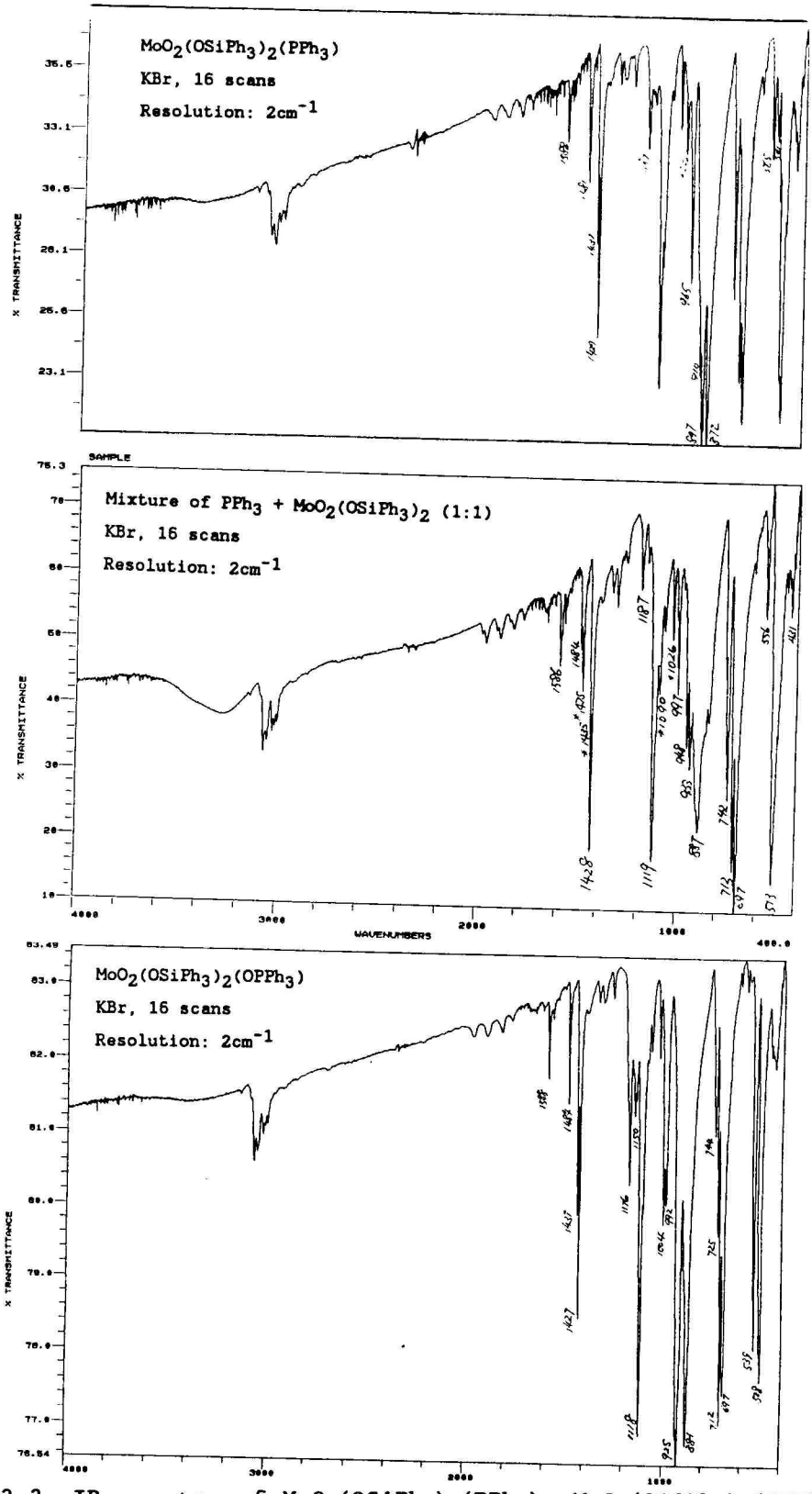

Figure 3-3. IR spectra of $MoO_2(OSiPh_3)_2(PPh_3)$, $MoO_2(OSiPh_3)_2(OPPh_3)$, and a 1:1 mixture of $MoO_2(OSiPh_3)_2$ with PPh_3

3-3. Implication of $MoO_2(OSiPh_3)_2(PPh_3)$ in the oxygen atom transfer reaction.

There are two models which have been discussed with respect to the initial step in the oxygen atom transfer reaction between a trialkylphosphine and a metal-oxo species. The first model, which involves the attack of the phosphine directly on the oxo moiety, is widely accepted [10,11]. The simplified scheme is shown below (eqn. 10), in which phosphine interacts with the π^* orbital of an Mo=O group.

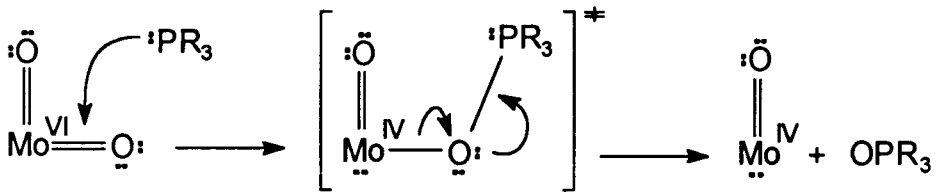

...(10)

In a classical paper [12] on the study of chromyl chloride oxidation of olefins, Sharpless and coworkers proposed for the first time that the initial step in the oxidation involved π coordination of the olefin to the Cr center. He postulated that the oxygen atom transfer reaction may undergo a similar initial process: direct coordination of the phosphine to the metal center followed by a 1,2-shift of the coordinated phosphine to an oxo group (see eqn. 11). Sharpless proposed that attack of a phosphine on a metal-oxo moiety (typically polarized M^+-O^-) was inconsistent with the notion of a charge-controlled process. It has been pointed out [1,11] that while there is no reason to believe the second model cannot exist there is no direct evidence to support it.

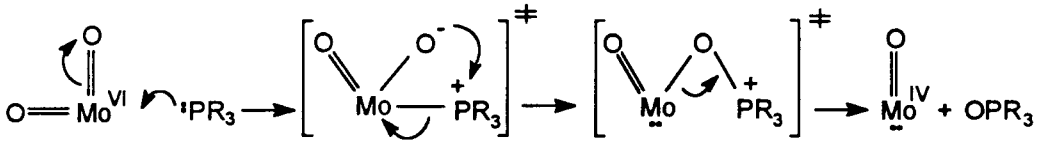

...(11)

The existence of compound $MoO_2(OSiPh_3)_2(PPh_3)$ is support for Sharpless's mechanism. It suggests that the initial interaction between phosphine and the Mo dioxo moiety is the coordination between the metal center and the phosphorus atom. The electron density of phosphine is redistributed into molybdenum-ligand bonds, which leads to a 1,2-shift of the phosphine to the electron-rich oxo atom.

3-4. Theoretical studies

In order to understand the stability of Mo-P bond and the bond length variation of $MoO_2(OSiPh_3)_2(PPh_3)$ in detail, we have performed an extended Hückel calculation [14]. $Mo(OH)_2O_2(PH_3)$ was chosen as a model system, where hydride models triphenylsilyl in Ph_3SiO^- and phenyl in PPh_3.

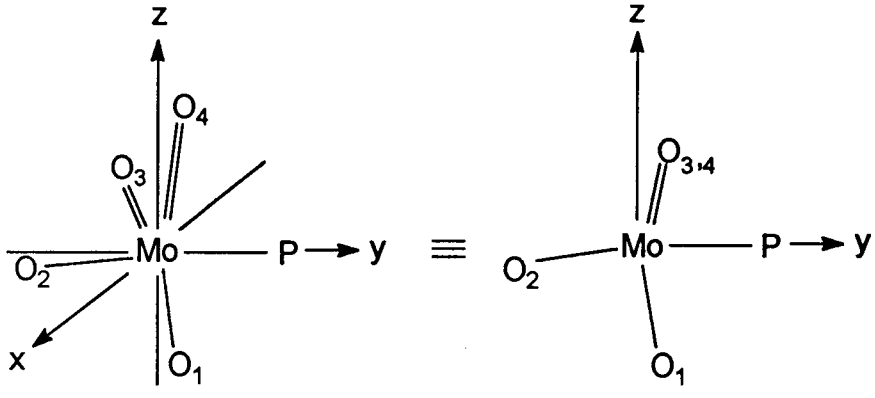

Scheme 1. The selection of coordinate system for $MoO_2(OH)_2(PH_3)$

The strategy used here was to vary the Mo-P distance while keeping all other parts of the model unchanged. The variation of the bond overlap population and in the energy of the molecular orbitals was studied as a function of Mo-P bond distance.

Figure 3-4 shows the total energy as a function of Mo-P distance. An energy well in the total energy vs. Mo-P distance curve shows that the EHMO method works well in modelling the bonding of Mo-P bond. The corresponding Mo-P distance in Figure 3-4 at the energy minimum is 3.2Å.

When the PH_3 fragment is completely separated from the Mo center (Mo-P = 10Å is used in the actual calculation), there is no overlap between Mo and P fragments), the d orbitals can be roughly divided into two groups: d_{z^2}, $d_{x^2-y^2}$, d_{xz} group with higher energy, and d_{xy}, d_{yz} (which is the LUMO) group at lower energy. As the PH_3 approaches the Mo center, the energy of the $d_{x^2-y^2}$ orbital is gradually raised due to σ bonding between $d_{x^2-y^2}$ and p_y of the P atom, while the other orbital's energy order remains the same. At the equilibrium position (Mo-P = 2.759Å), the order of d orbital energies is that expected from crystal field theory for a trigonal bipyramidal configuration. Recall the extensive π interactions between Mo d and O p orbitals, this result demonstrates that the Mo d orbital order is primarily determined by the σ bonding.

Figure 3-5 gives the overlap population of the Mo-P bond and Mo-O bonds as a function of Mo-P distance. It can be seen that a flat maximum

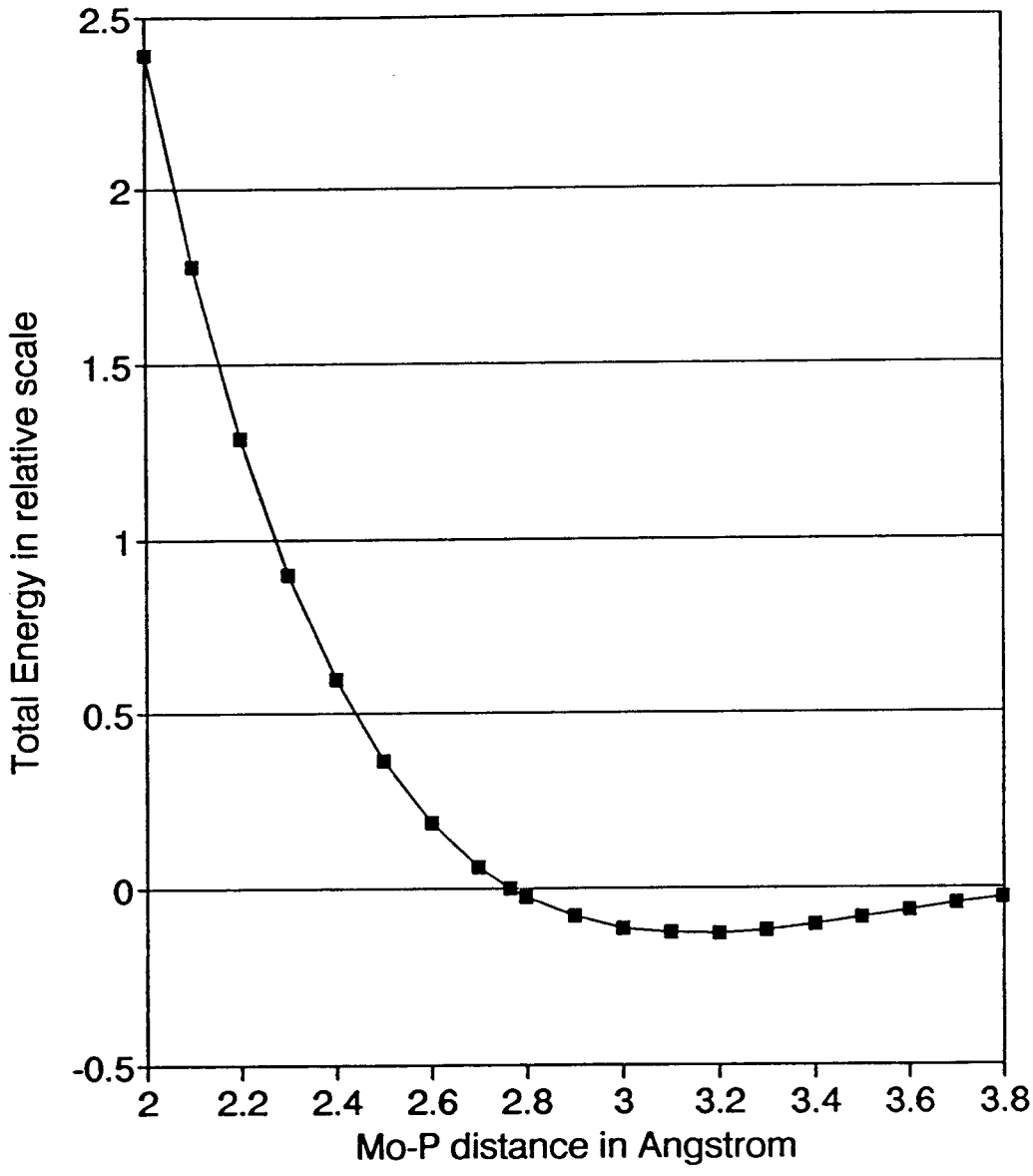

Figure 3-4. Total energy of $MoO_2(OH)_2(PH_3)$ vs. Mo-P distance.

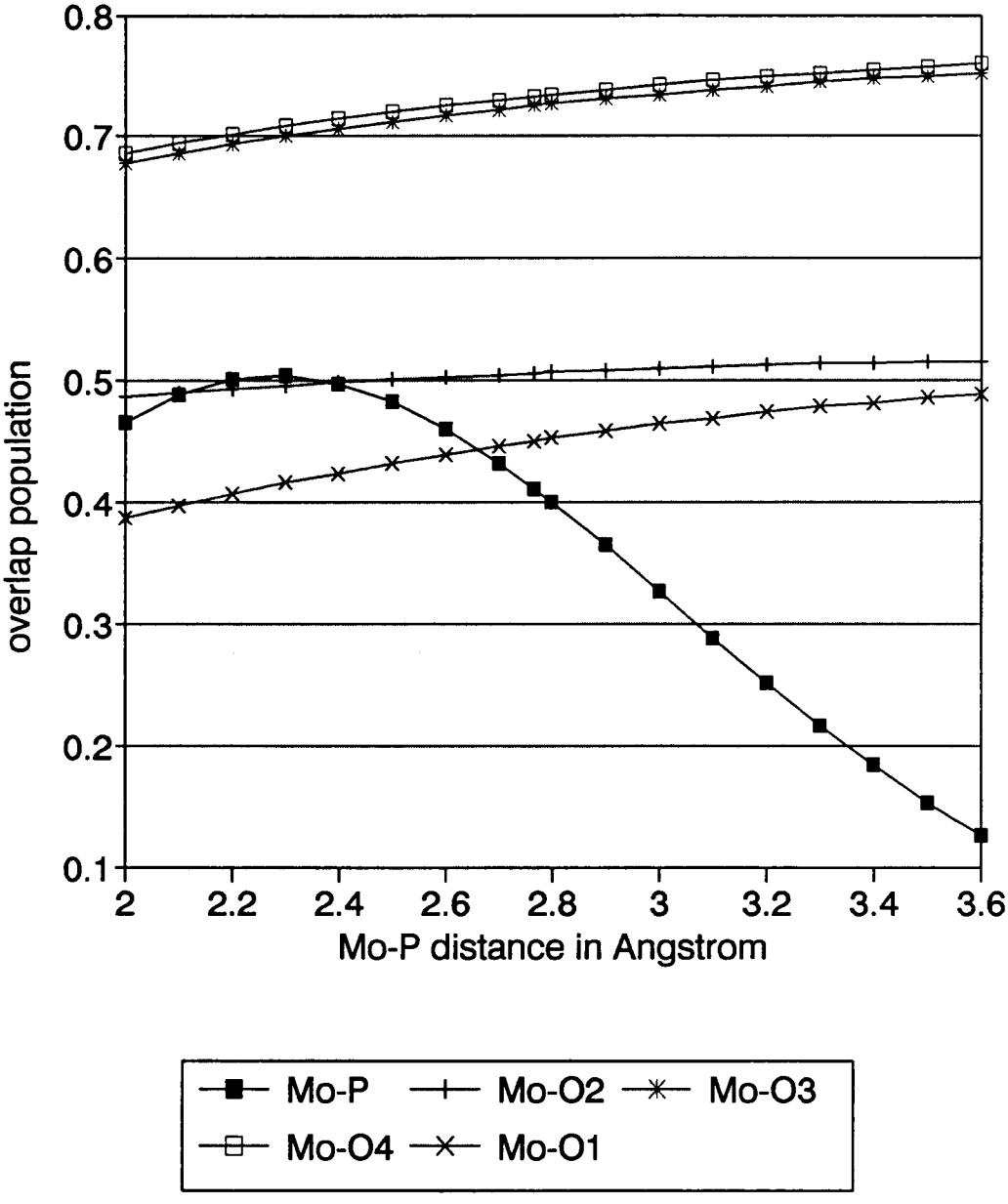

Figure 3-5. Overlap populations of the Mo-P bond and Mo-O bonds of $MoO_2(OH_3)_2(PH_3)$ as a function of Mo-P distance.

exists for the overlap population for Mo-P distances between 2.3-2.4Å. While this is far from the experimental bond length (2.759Å), it is reasonably close to a normal single bond length (~2.5Å). If we ascribe the maximum overlap population (0.5035) at 2.3Å to a full single bond, we might conclude that Mo-P at 2.759Å with an overlap population of 0.411 has a bond order of 0.8. The reason the Mo-P bond does not reach its maximum bond strength at ~2.5Å is presumably due to steric repulsion between PPh_3 and Mo fragments, not accounted by this model.

The decrease in the overlap population of Mo=O3 bond from 0.7605 at Mo-P = 10Å to 0.7240 at Mo-P = 2.759Å is consistent with the infrared result that ν(Mo=O) in $MoO_2(OSiPh_3)_2(PPh_3)$ (925, 881 cm^{-1}) is lower than in its parent compound $MoO_2(OSiPh_3)_2$ (948, 932, 885 cm^{-1}), which indicates Mo=O bonds are weakened by the coordination of phosphine.

It is of interest to note that the overlap population of Mo-O1 (equatorial Ph_3SiO) decreases faster than that of Mo-O2 (axial Ph_3SiO) as the P approaches Mo. This result is consistent with the fact that the Mo-O1 bond length is longer than the Mo-O2 bond length.

Figure 3-6 shows the π interaction between metal d orbitals and oxygen p orbitals [15]. Data given beside the bonds are the orbital by orbital overlap population, and the data in the square parentheses are that of the model compound at the Mo-P distance of 10Å. For d_{yz}, the orbital by orbital overlap populations between d_{yz} and p_y of oxo (π interaction) increase as PH_3 approaches the Mo center, which is opposite

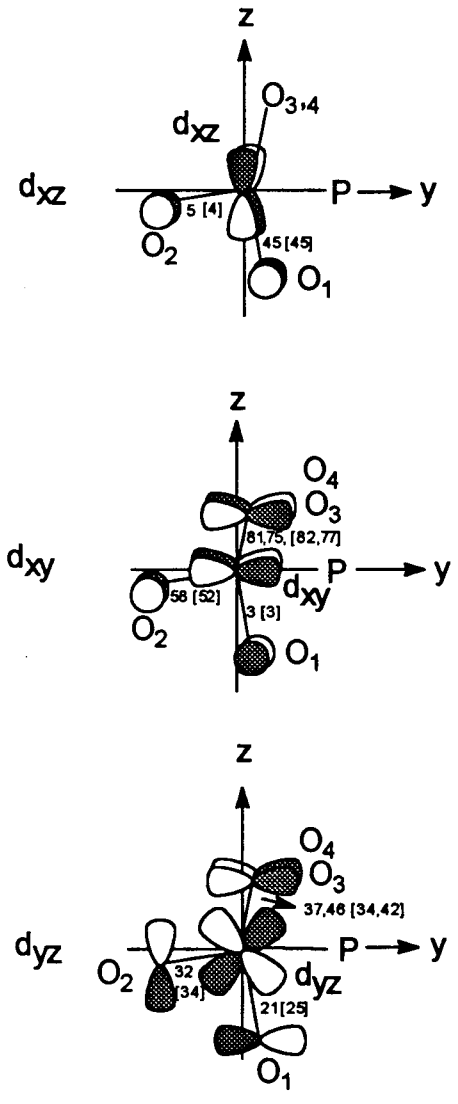

Figure 3-6. π interactions between Mo d orbitals and O p orbitals. Data beside the bond are the orbital overlap population ($x10^3$). Data in square parentheses are for the model compound at Mo-P = 10.0Å. Molecular orbital coefficients are also given in parentheses besides the orbitals.

to the trend shown in Fig. 3-5. Further analysis of other π interactions in FIgure 3-6 also show that considering π interaction only is not sufficient to account for the weakening of Mo-O and Mo=O bonds as PH_3 approaches the Mo center (Fig. 3-5).

The detailed analysis of the EHMO calculation result reveals that the decrease of Mo=O double bond overlap population as Mo-P distance becomes shorter should be primarily ascribed to the interaction shown in Figure 3-7. The interaction between p_y(Mo) and p_y(P) reduces the overlap between p_y(Mo) and p_y of the oxo atoms. For Mo-O single bonds, the trend of Mo-O1 and Mo-O2 overlap populations in Figure 3-5 cannot simply be ascribed to a pair of orbitals, as in the case of Mo=O double bonds. In fact, the change of Mo-O1 and Mo-O2 overlap population as a function of Mo-P distance is a subtle compromise of many opposite effects. For example, as PH_3 approaches the Mo center, while the overlap populations of p_y(O2)-s(Mo), s(O2)-$d_{x^2-y^2}$(Mo) and p_y(O2)-$d_{x^2-y^2}$(Mo) are reduced by 8%, 14%, and 27%, respectively, the overlap populations of s(O2)-p_y(Mo) and p_y(O2)-p_y(Mo) increase by 8% and 17%, respectively.

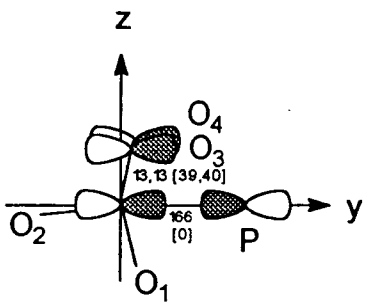

Figure 3-7. Orbital overlap population (x10^3, given beside the bonds) of Mo=O bonds become smaller as P atom approaches to Mo center. Data in square parentheses is for the model at Mo-P = 10.0Å.

It should be pointed out that it is also the P_y(Mo)-P_y(P) ovelap that contributes the most to the Mo(VI)-P bond. The overlap population between the P atom and O1, O3, O4 atoms are all negligible at a Mo-P distance of 2.759Å.

The fact that the Mo-O1 bond is weakened faster than the Mo=O bonds as phosphine approaches the Mo center can be stated in another way: the electrons provided by the phosphine are largely redistributed into the Mo-O1(Si) bond instead of Mo=O bonds. It has been pointed out that the siloxy group has weaker π donating ability than that of alkoxy and amide [16], the triphenylsiloxy group should be even weaker due to the electron withdrawing nature of phenyl groups, which makes the Ph_3SiO groups a good place to store charge density instead of pushing the charge density back to the oxo group.

The steric repulsion between the PPh_3 and the Mo fragment may account for the stabilization of Mo(VI)-P since it prevents PPh_3 from making a close approach to the Mo center.

3-5. Experimental

See the previous chapter for general experimental conditions. The PEt_3 was prepared by thermal pyrolysis of PEt_3.AgI at 169°C into a cold trap in the vacuum line. The purity was confirmed by proton NMR. The PBu^n_3 was distilled under reduced pressure before use. Both crude PBu^n_3 and PEt_3.AgI were generously provided by Prof. John Yoke.

Synthesis of $MoO_2(OSiPh_3)_2(PPh_3)$. 207mg of $MoO_2(OSiPh_3)_2$ was dissolved in a small amount of dichloromethane, the solution was then cooled to -78°C. To this solution was slowly added about 1ml dichloromethane solution containing 96mg triphenylphosphine. The adduct was precipitated by the addition of 30ml of cold hexane. The adduct was recovered by cold cannula filtration to yield 148mg of a grey solid after drying under vacuum. IR (KBr, cm^{-1}): 3050m, 1590m, 1482m, 1437w, 1429s, 1187w, 1117s, 989w, 965w, 898vs (Mo=O), 873vs (Mo=O), 712s, 698s, 564w, 536w, 507s. ^{31}P nmr (in $CDCl_3$, 85% H_3PO_4 as external standard): 30.44 ($Mo-PPh_3$), 4.823 (PPh_3), Area ratio: 3:2, obtained by removing the NOE effect through a gated decoupling pulse sequence.

Crystallographic Studies: see previous chapter for the general experimental conditions for crystallographic studies.

$MoO_2(OSiPh_3)_2(PPh_3)$. Some crystals were obtained by recrystallization from a toluene/hexane solvent mixture at -15°C. One crystal, size ~0.2x0.2x0.4 mm, was carefully chosen under a microscope and coated with epoxy resin. Unit cell parameters were determined from a least-squares fit of 12 accurately centered reflections ($22 < 2\theta < 24.6°$). The structure was solved by a combination of the direct method (SHELXS-86 [18]) and difference Fourier synthesis. Anisotropic temperature factors were refined for all nonhydrogen atoms. Final structural factors R=5.2%; R_w=5.6. The final difference electron density map was featureless with maximum peak at 0.527 $eÅ^{-3}$. The crystallographic data and atomic positions are given in Tables 3-1 and 3-2, respectively.

Table 3-1. Crystallographic Data and experimental conditions for $MoO_2(OSiPh_3)_2(PPh_3)$

compound	$MoO_2(OSiPh_3)_2(PPh_3)$		
empirical formula	$MoSi_2O_4C_{54}H_{45}P$	temperature	23°C
formula weight	941.03 amu	$2\theta_{max}$	45°
dimension, mm	0.2x0.2x0.4	data collection speed	16.0° min^{-1} in ω
crystal system	monoclinic	scan method	ω
lattice parameters	a = 18.498(4)Å	h k l limits	-21,0,0 to 21,12,29
	b = 10.818(3)Å	total no.of measd data	6546
	c = 24.844(3)Å	no. observations (I>3σ(I))	12768
	β = 107.08(1)°	no. variables	559
V, Å^3	4753(2) Å^3	residuals: R; R_w	0.052; 0.056
space group	$P2_1/a$ (#14)	GOF	1.34
Z	4	maximum shift	0.02
D_{calc}, g cm-3	1.315	largest residual peak	0.527
F(000)	1944	μ (MoKα), cm^{-1}	3.9368
diffractometer	Rigaku AFC6R		

Table 3-2. Fractional positional parameters and B(eq) of non-Hydrogen atoms for $MoO_2(OSiPh_3)_2(PPh_3)$

atom	x	y	z	B(eq)
Mo	-0.00209(5)	0.0737(1)	0.26813(4)	4.23(4)
P	0.1009(2)	0.1266(3)	0.3708(1)	4.7(1)
Si(1)	0.0733(2)	-0.2011(3)	0.2564(1)	4.0(1)
Si(2)	-0.1273(2)	0.0291(3)	0.1401(1)	4.7(2)
O(1)	0.0558(3)	-0.0759(6)	0.2875(2)	4.4(3)
O(2)	-0.0603(4)	0.0017(6)	0.1991(3)	5.1(3)
O(3)	-0.0664(4)	0.1092(7)	0.3019(3)	7.2(4)
O(4)	0.0317(4)	0.2035(7)	0.2474(3)	7.2(4)
C(1)	-0.0069(6)	-0.311(1)	0.2454(4)	4.3(5)
C(2)	-0.0007(7)	-0.430(1)	0.2244(5)	5.8(6)
C(3)	-0.0606(9)	-0.515(1)	0.2158(5)	6.7(7)
C(4)	-0.1230(8)	-0.485(1)	0.2294(6)	6.6(7)
C(5)	-0.1294(7)	-0.372(1)	0.2512(6)	6.7(8)
C(6)	-0.0715(7)	-0.285(1)	0.2594(5)	5.3(6)
C(11)	0.1601(6)	-0.2753(9)	0.3048(5)	4.2(5)
C(12)	0.1678(7)	-0.286(1)	0.3626(5)	5.4(6)
C(13)	0.228(1)	-0.343(1)	0.3981(5)	7.4(8)
C(14)	0.2829(8)	-0.393(1)	0.3782(7)	7.7(8)
C(15)	0.2781(7)	-0.384(1)	0.3217(7)	7.3(8)
C(16)	0.2151(6)	-0.328(1)	0.2857(5)	5.5(6)
C(21)	0.0938(6)	-0.160(1)	0.1898(4)	4.3(5)
C(22)	0.0568(7)	-0.212(1)	0.1386(6)	6.9(7)
C(23)	0.078(1)	-0.182(2)	0.0910(6)	8(1)
C(24)	0.132(1)	-0.099(2)	0.0926(7)	10(1)
C(25)	0.1698(8)	-0.044(2)	0.1422(7)	10(1)
C(26)	0.1485(7)	-0.076(1)	0.1901(5)	7.4(7)
C(31)	-0.2166(6)	0.064(1)	0.1562(5)	4.9(6)
C(32)	-0.2211(7)	0.163(1)	0.1901(6)	6.8(8)
C(33)	-0.287(1)	0.193(1)	0.2021(5)	7.7(8)
C(34)	-0.3501(8)	0.126(2)	0.1793(7)	7.5(9)
C(35)	-0.3482(8)	0.026(1)	0.1451(7)	7.9(8)
C(36)	-0.2811(9)	-0.006(1)	0.1348(5)	6.9(7)
C(41)	-0.1015(7)	0.166(1)	0.1046(5)	4.9(6)
C(42)	-0.0299(8)	0.185(1)	0.1019(5)	7.5(8)
C(43)	-0.013(1)	0.283(2)	0.0709(8)	10(1)
C(44)	-0.070(1)	0.356(2)	0.0421(7)	9(1)
C(45)	-0.142(1)	0.339(1)	0.0422(7)	9(1)
C(46)	-0.1562(7)	0.243(1)	0.0739(6)	6.8(7)
C(51)	-0.1392(6)	-0.108(1)	0.0926(5)	4.7(6)
C(52)	-0.1319(7)	-0.097(1)	0.0397(6)	6.9(7)
C(53)	-0.1401(8)	-0.197(2)	0.0035(5)	8.2(8)
C(54)	-0.1539(9)	-0.311(1)	0.0210(6)	8.3(9)
C(55)	-0.1620(8)	-0.325(1)	0.0733(7)	7.8(8)
C(56)	-0.1531(7)	-0.224(1)	0.1093(5)	6.5(7)
C(61)	0.1959(6)	0.138(1)	0.3647(4)	4.4(5)
C(62)	0.2254(6)	0.253(1)	0.3577(4)	5.0(6)
C(63)	0.2962(8)	0.260(1)	0.3489(5)	6.5(7)
C(64)	0.3353(7)	0.157(2)	0.3466(5)	6.9(8)
C(65)	0.3078(7)	0.044(1)	0.3536(5)	6.3(7)
C(66)	0.2385(8)	0.033(1)	0.3635(5)	6.1(7)
C(71)	0.0865(6)	0.271(1)	0.4035(5)	4.9(6)
C(72)	0.1086(7)	0.290(1)	0.4596(6)	6.9(8)
C(73)	0.099(1)	0.401(2)	0.4837(6)	9(1)
C(74)	0.063(1)	0.498(2)	0.4488(8)	9(1)
C(75)	0.0397(8)	0.481(1)	0.3924(8)	8.0(8)
C(76)	0.0502(7)	0.368(1)	0.3673(6)	6.6(7)
C(81)	0.1022(7)	0.012(1)	0.4237(4)	4.5(5)
C(82)	0.1666(7)	-0.026(1)	0.4658(5)	5.6(6)
C(83)	0.162(1)	-0.115(1)	0.5047(5)	7.4(8)
C(84)	0.093(1)	-0.165(1)	0.5024(6)	8(1)
C(85)	0.0301(8)	-0.131(1)	0.4609(6)	7.7(8)
C(86)	0.0330(7)	-0.043(1)	0.4226(5)	6.1(7)

3-6. References

1. Nugent, W.A. and Mayer J.M. *"Metal-Ligand Multiple Bonds, The Chemistry of Transition Metal Complexes Containing Oxo, Nitrido, Imido, Alkylidene, or Alkylidye Ligands"*, **1988**, John Wiley & Sons, Inc.

2. Holm, R.H. and Berg, J.M. *Acc Chem. Res.* **1986**, *19*, 363-70.

3. Watt, G.D.; McDonald, J.W.; Newton, W.E. *J. Less-Common Met.* **1977**, *54*, 415-423.

4. Reynolds, M.S.; Berg, J.M.; Holm, R.H. *Inorg. Chem.* **1984**, *23*, 3057-3062,

5. Harlan, E.W.; Berg, J.M.; Holm, R.H. *J. Am. Chem. Soc.* **1986**, *108*, 6992-7000.

6. Manojlović-Muir, L. *J. Chem. Soc.* (A) **1971**, 2769.

7. Drew, M. G. B. *J. Chem. Soc. Dalton Trans.* **1972**, 1329-1333.

8. Mais, R.H.B.; Owston, P.G.; Thompson, D.T. *J. Chem. Soc. (A)*, **1967**, 1735.

9. Chou, C.Y.; Decore, D.D.; Huckett, S.C.; Maatta, E.A.; *Polyhedron* **1986**, *5*, 301.

10. Holm, R.H. *Chem. Rev.* **1987**, 87, 1401. Craig, J.A.; Harlan, E.W.; Snyder, B.S.; Whitener, M.A.; Holm, R.H. *Inorg. Chem.*, **1989**, *28*, 2082.

11. Holm, R.H. *Coord. Chem. Rev.* **1990**, *100*, 183-219.

12. Sharpless, K.B.; Teranishi, A.Y.; Backvall, J.-E. *J. Am. Chem. Soc.*, **1977**, *99*, 3120.

14. Hoffmann, R. *J. Chem. Phys.* **1963**, *39*, 1397-1412. Parameters for Mo were taken from: Hughbanks, T. and Hoffmann, R. *J. Am. Chem. Soc.* **1983**, *105*, 3528-3537.

15. Tatsumi, K.; Hoffmann, R. *Inorg. Chem.* **1980**, *19*, 2656.

16. Feher, F.J.; Budzichowski, T.A. *J. Organomet. Chem.* **1989**, *379*, 33. Chisholm, M.H.; Budzichowski, T.A.; Feher, F.A.; Ziller, J.W., *Polyhedron* **1992**, *11*, 1575.

17. Lai, R; Le Bot, S.; Baldy, A.; Poerrot, M.; Arzoumanian, H. *J. Chem. Soc., Chem. Commun.* **1986**, 1208.

18. Sheldrick, G.M. in *Crystallographic Computing 3*, (Eds. G.M. Sheldrick, C. Kruger, and R. Goddard); Oxford University Press, pp175-89.

Chapter 4

Reactions of $MoO_2(OSiPh_3)_2$ With Alkylating Agents

4-1. Introduction

This chapter reports the reactions of $MoO_2(OSiPh_3)_2$ with two metal alkyls, $SnMe_4$ and $ZnEt_2$, and the crystal structure of a product of one of the above reactions, $(C_2H_5)Zn(\mu\text{-}OSiPh_3)_2Zn(\mu\text{-}OSiPh_3)_2Zn(C_2H_5)$ (1), which has some interesting structural features: (1) a Zn trimer with two three-coordinate Zn atoms and (2) two Zn-C bonds that are stable in air. The detailed analysis of the structure reveals the origin of the air-stability of the Zn-C bonds.

Some examples of alkylation of metal complexes that lead to some interesting results are discussed below.

(a) **Alkylation on Metal Ligand Multiple Bonds**. The preparation of $MoO_2(OSiPh_3)_2$ is an example in which two Mo=O double bonds of silver molybdate are silylated by the triphenylchlorosilane. Further silylation of the other two Mo=O double bonds does not happen with triphenylchlorosilane as a silylating agent. Perhaps stronger silylating agents are needed considering the molybdenum-oxo bonds in $MoO_2(OSiPh_3)_2$ are formally triple bonds. The complex $(dtc)_3Mo{\equiv}N$ (dtc = dimethyldithiocarbamate) contains a Mo≡N bond where the nitrido ligand is apparently electron-

rich. It can be alkylated even with methyl iodide to afford a cationic methylimido compound (eqn. 1). A number of other alkylating and acylating agents react similarly, including PhCOCl, $[R_3O]BF_4$, and $[Ph_3C]BF_4$ [1].

$$(dtc)_3Mo{\equiv}N + MeI \longrightarrow [(dtc)_3Mo{=}NMe]^+.I^- \quad ...(1)$$

Dirhenium heptaoxide and tetramethyl tin, $SnMe_4$, are effective catalyst/cocatalyst components in olefin metathesis, even catalyzing metathesis of industrially important unsaturated carboxylic acids and nitriles under quite mild conditions [2]. It was found by Herrmann's group that the alkylation of Re_2O_7 with $SnMe_4$ in boiling THF quantitatively affords CH_3ReO_3 (eqn. 2), which contains a Re(VII)-C bond and is completely air stable and water soluble. CH_3ReO_3 catalyzes some metathesis reactions with the coexistence of $AlCl_3$ and $SnMe_4$, and is considered to be a key in the $Re_2O_7/SnMe_4/Al_2O_3$ catalyst system. Starting from this compound and $[C_5(CH_3)_5]ReO_3$, a whole series of high-valent organorhenium oxides have been exploited, and many interesting structures found.

$$Re_2O_7 + SnMe_4 \longrightarrow Me_3SnOReO_3 + CH_3ReO_3 \quad ...(2)$$

$MoO_2(OR)_2/AlEt_3$ is also an effective catalyst system for olefin metathesis. For the above reasons a study of the reaction of $MoO_2(OSiPh_3)_2$ with alkylating agents was undertaken.

(b) **Alkylation of M-OR Bonds.** It is possible to attack M-OR bonds (Mo-$OSiPh_3$ bonds for $MoO_2(OSiPh_3)_2$) by alkylating agents. The following is an example [3]:

$$M(NBu^t)_2(OSiR_3)_2 + 2MgR'Br \xrightarrow{\text{hexane, r.t.}} M(NBu^t)_2R'_2 + 2'Mg(OSiR_3)Br' \quad \ldots(3)$$

(M=Cr or Mo, R=Me; M=W, R=Ph; R'=$C_6H_2Me_3$-2,4,6 or $C_6H_3Me_2$-2,6)

4-2. Results and Discussion

4-2-1. Reaction with tetramethyl tin, $SnMe_4$

Tetramethyl tin is considered to be a very selective and non-reductive alkylation (methylation) reagent [2]. There is no reaction found between $MoO_2(OSiPh_3)_2$ and $SnMe_4$ in some inert organic solvents, e.g., 1,2-dichloroethane and toluene.

In THF solvent, however, $MoO_2(OSiPh_3)_2$ reacts with $SnMe_4$ at 58°C and leads to the decomposition of $MoO_2(OSiPh_3)_2$ to form Ph_3SiOH and an unexpected ether, Ph_3SiOPr^i containing an orthopropoxy group, which is easily soluble in hexane. The existence of this ether was confirmed by FTIR, NMR and Mass spectra.

$$MoO_2(OSiPh_3)_2 + SnMe_4 \xrightarrow{\text{THF, 58°C}} Ph_3SiOH + Ph_3SiOPr^n + \{MoO_x\} + \ldots \quad \ldots(4)$$

It seems that the orthopropoxy group in $Ph_3SiOCH_2CH_2CH_3$ comes from the decomposition (or dissociation) of the THF solvent. THF decomposition/dissociation under various conditions has been known for many years:

$$THF + BuLi.TMEDA \xrightarrow{r.t.} CH_2{=}CHOLi + CH_2{=}CH_2 \quad ...(5)$$

$$[(C_5Me_5)_2Sm(THF)_2](BPh_4] + KC_5Me_5 \xrightarrow{-KBPh_4} (C_5Me_5)_2Sm[O(CH_2)_4C_5Me_5](THF) \quad ...(6)$$

Eqn. 5 [4] shows that the β-H of THF is abstracted by a strong Lewis base, and leads to a (2 + 2) decomposition. The $-O(CH_2)_4-$ unit in the product of eqn. 6 [5] was formed from the ring-opening of THF. The decomposition of the THF was considered to involve the formation of an oxonium ion initiated by the Lewis acid (Sm^{3+}) , which is then opened by the nucleophilic attack of $C_5Me_5^-$.

The molybdenum-containing species left as precipitate was soluble in water but not in organic solvents. FTIR of this species showed the existence of ν(Mo=O) at 859cm^{-1}, and no υ(C-H) bands for methyl groups were found. It seems this species contains mainly oxomolybdate, and no methylation on Mo=O bonds.

No further efforts were made to explore the origin and/or the mechanism for the formation of Ph_3SiOPr^n containing a three-carbon chain.

4-2-2. Reaction with $ZnEt_2$

The reaction of $MoO_2(OSiPh_3)_2$ with $ZnEt_2$ again leads to the decomposition of $MoO_2(OSiPh_3)_2$ and no alkylation on Mo=O bonds. Two identified products are Ph_3SiOH and $(C_2H_5)Zn(\mu\text{-}OSiPh_3)_2Zn(\mu\text{-}OSiPh_3)_2Zn(C_2H_5)$ (1). The molybdenum-containing component shows strong bands for Mo=O and the Ph_3SiO- group, and is soluble in 1,2-dichloroethane. It is reasonable to suggest that it is a triphenylsiloxy complex of oxomolybdenum or a mixture of these kind of complexes. Further workup failed to give a well-defined compound.

$$MoO_2(OSiPh_3)_2 + ZnEt_2 \xrightarrow{\text{toluene}} Ph_3SiOH + \{MoO_x(OSiPh_3)_y\} + \\ + (C_2H_5)Zn(\mu\text{-}OSiPh_3)_2Zn(\mu\text{-}OSiPh_3)_2Zn(C_2H_5)\ (1) + \ldots \ldots (7)$$

4-2-3. Structure of $(C_2H_5)Zn(\mu\text{-}OSiPh_3)_2Zn(\mu\text{-}OSiPh_3)_2Zn(C_2H_5)$ (1)

The structure of compound 1 was determined by an X-ray diffraction study. It has several interesting structural features: a Zn trimer; two three-coordinate Zn atoms; and two Zn-C bonds that are stable in air.

Although no definite Mo compounds were found from the alkylation reaction of $MoO_2(OSiPh_3)_2$, the Zn compound 1 is of interest since the compounds with three-coordinate Zn atoms are very rare [6], especially for the compounds that contains the Zn-C bond. Usually very bulky

ligands, e.g., Tpsi (tris(dimethylphenylsilyl)methyl, $[(MePh_2)Si]_3C$-) [6], are used to stabilize the three-coordinate Zn and/or Zn-C bonds.

The structure of 1 consists of a discrete Zn trimer with a 2-fold symmetric axis passing through the Zn atom and bisecting the O2-Zn-O1A and O2A-Zn-O1 angles (Figure 4-1 and 4-2). The central Zn atom is four-coordinate with a distorted tetrahedral configuration, bond angles O1A-Zn-O1 = 112.8(4)°, O1A-Zn-O2 = 117.7(4)°, and O1-Zn-O2 = 86.2(5)°. The other two Zn atoms are symmetrically equivalent, and both have a three-coordinate environment. While the planes Zn-O1-O2 and Zn-O1A-O2A are almost perpendicular to each other (85.7°), the planes Zn-O1-O1A and Zn-O2-O2A have an angle of 110.1°. Zn, O1, O2, and Zn1 are almost coplanar with an average of 0.0487Å deviation from the least square planes defined by these atoms. C1 is 0.322Å off the Zn-O1-O2-Zn1A plane. The Zn1-ethyl plane, Zn1-C1-C2, is almost perpendicular (88.1°) to the plane Zn-O1-O2-Zn1. The central Zn atom and the other two Zn atoms are bridged by the triphenylsiloxy ligands.

Bridging triphenylsiloxy groups are commonly found in the compounds containing large radii metal centers, e.g., lanthanides [7] and Pb [8], presumably because of the steric bulkiness of the triphenylsiloxy group. Compounds with relatively small metal centers bridged by a triphenylsiloxy group are rare, the only other example, besides 1, is $[Co(OSiPh_3)_2(THF)]_2$ [9]. It is worthwhile to note an observation: while the O atoms in the triphenylsiloxy groups that bridge two large radii metal centers are almost sp^3 hybridized with M-O-M′ and M-O-Si angles close to

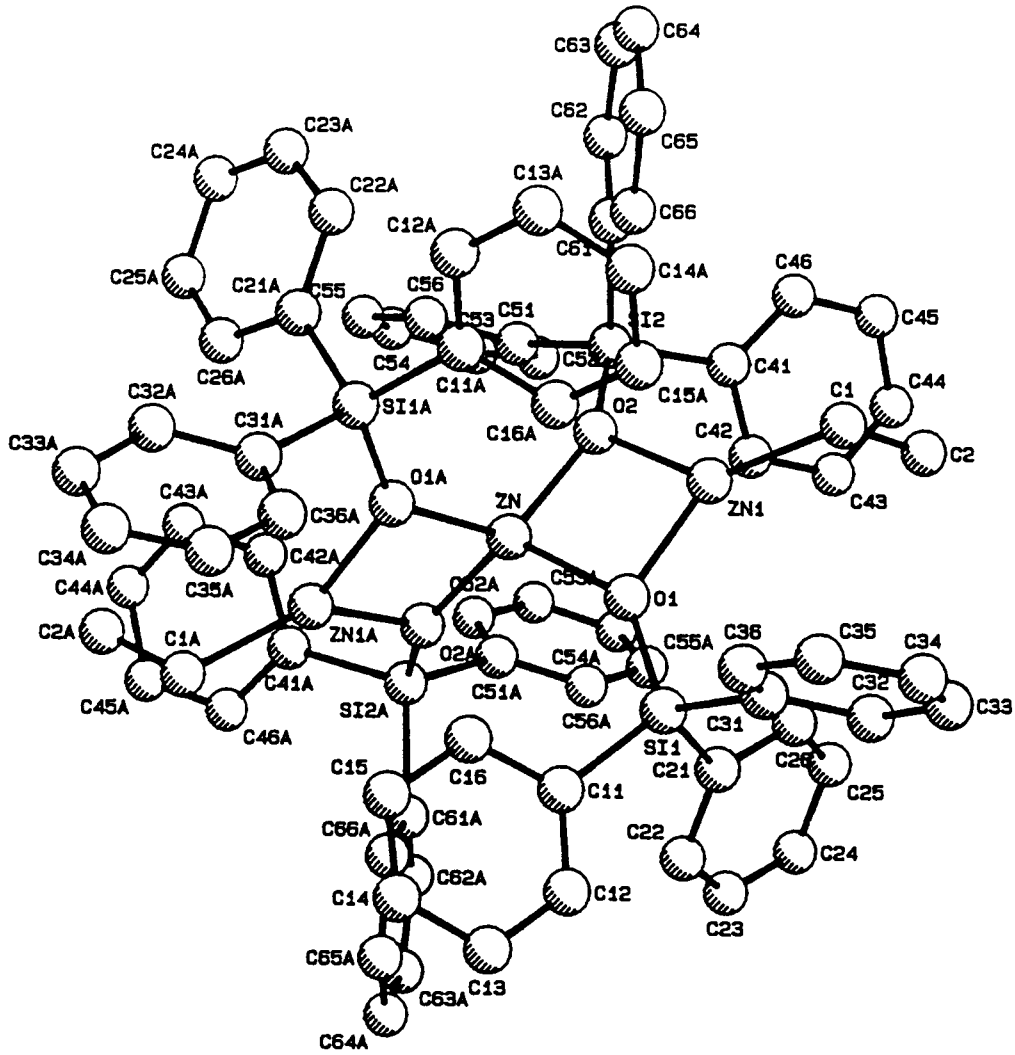

Figure 4-1. The structure of $(C_2H_5)Zn(\mu\text{-}OSiPh_3)_2Zn(\mu\text{-}OSiPh_3)_2Zn(C_2H_5)$ showing the labelling of non-Hydrogen atoms. The Hydrogen atoms are omitted for clarity. Selected bond lengths and angles (in Å or deg): Zn-O1 1.94(1), Zn-O2 2.01(1), Zn1-O1 2.03(1), Zn2-O2 1.93(1), Zn1-C1 2.00(3), C1-C2 1.41(4), Si1-O11.61(1), Si2-O2 1.62(1), O1-Zn-O2 86.2(5)°, O1-Zn1-O2 85.9(5)°, Zn-O1-Zn1 94.3(6)°, Zn-O2-Zn1 93.0(5)°, Zn1-C1-C2 116(2)°, Zn-O1-Si1 135.9(8)°, Zn1-O1-Si1 127.9(8)°, Zn-O2-Si2 144.4(8)°, Zn1-O2-Si2 120.3(7)°.

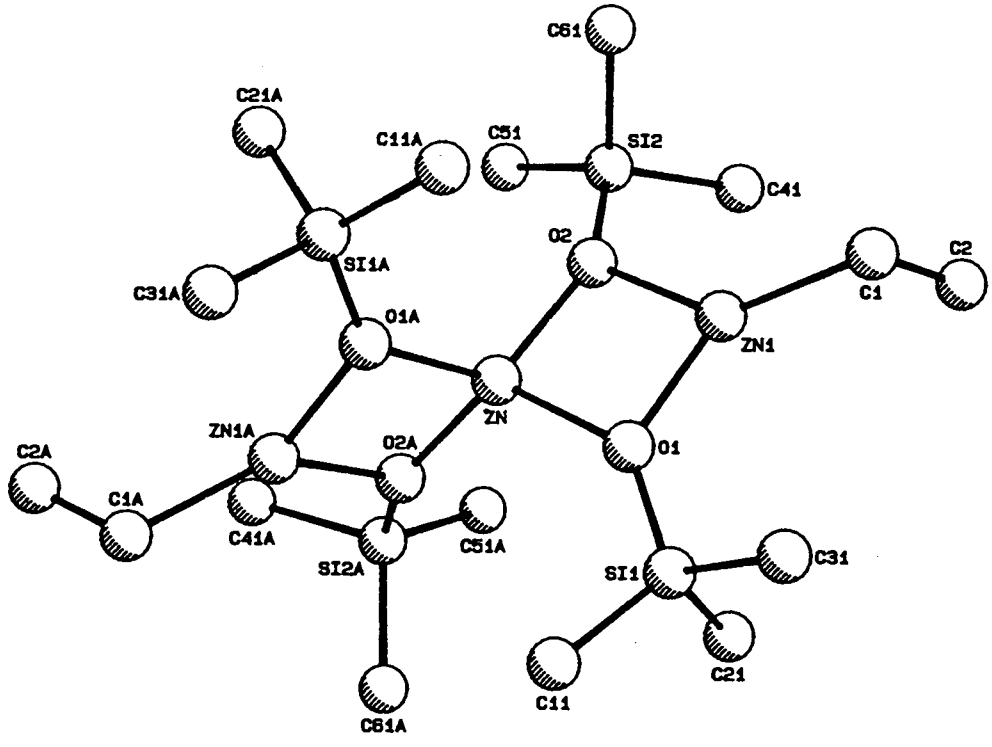

Figure 4-2. Partial structure of $(C_2H_5)Zn(\mu\text{-}OSiPh_3)_2Zn(\mu\text{-}OSiPh_3)_2\text{-}Zn(C_2H_5)$.

109° [7], the O atoms of 1 (and also $[Co(OSiPh_3)_2(THF)]_2$) with small metal centers are highly strained with Zn-O2-Zn1, Zn-O2-Si2 and Zn1-O2-Si2 angles of 94.3°, 144.4° and 120.3°, respectively. Another characteristic of 1 is that O atoms of the triphenylsiloxy group are almost coplanar with Zn, Zn1 and Si atoms, e.g., Zn, Zn1, O2 and Si2 has only 0.0271Å mean deviation from their least-squares plane, and Zn, Zn1, O1 and Si1 have only 0.0491Å mean deviation from their least-squares plane.

The average bond lengths of both three- and four-coordinate Zn atoms with the bridging oxygen atoms of the triphenylsiloxy group in 1 are the same within experimental error. The Zn-μ_2-O bond length (1.98(1)Å) of 1 is relatively long compared to Zn-μ_2-O (1.899(9)Å) in $[(Tpsi)Zn(\mu\text{-}OH)]_2$ [6], presumably due to the electron withdrawing nature of phenyl groups in triphenylsiloxy ligands. It is not surprising that this distance is shorter than Zn-μ_3-O bond lengths in the cubane structure containing four-coordinate Zn: 2.08(1)Å in $(MeZnOMe)_4$ [10] and 2.06(2)Å in $(MeZnOBu^t)_4$ [11].

The Zn-Zn (2.887(3)Å) and Zn-C (2.00(3)Å) bond lengths are in the normal range.

Air-stable Zn-C compounds are rare [6]. In $[(Tpsi)Zn(\mu\text{-}OH)]_2$ [6] bulky ligands, Tpsi, are used to protect Zn-C bonds and stabilize the three-coordinate Zn atom. A space-filling drawing of 1 (Figure 4-3) shows that an ethyl group is buried by the phenyl groups of the triphenylsiloxy ligands, which may account for the air stability of the Zn-C bonds.

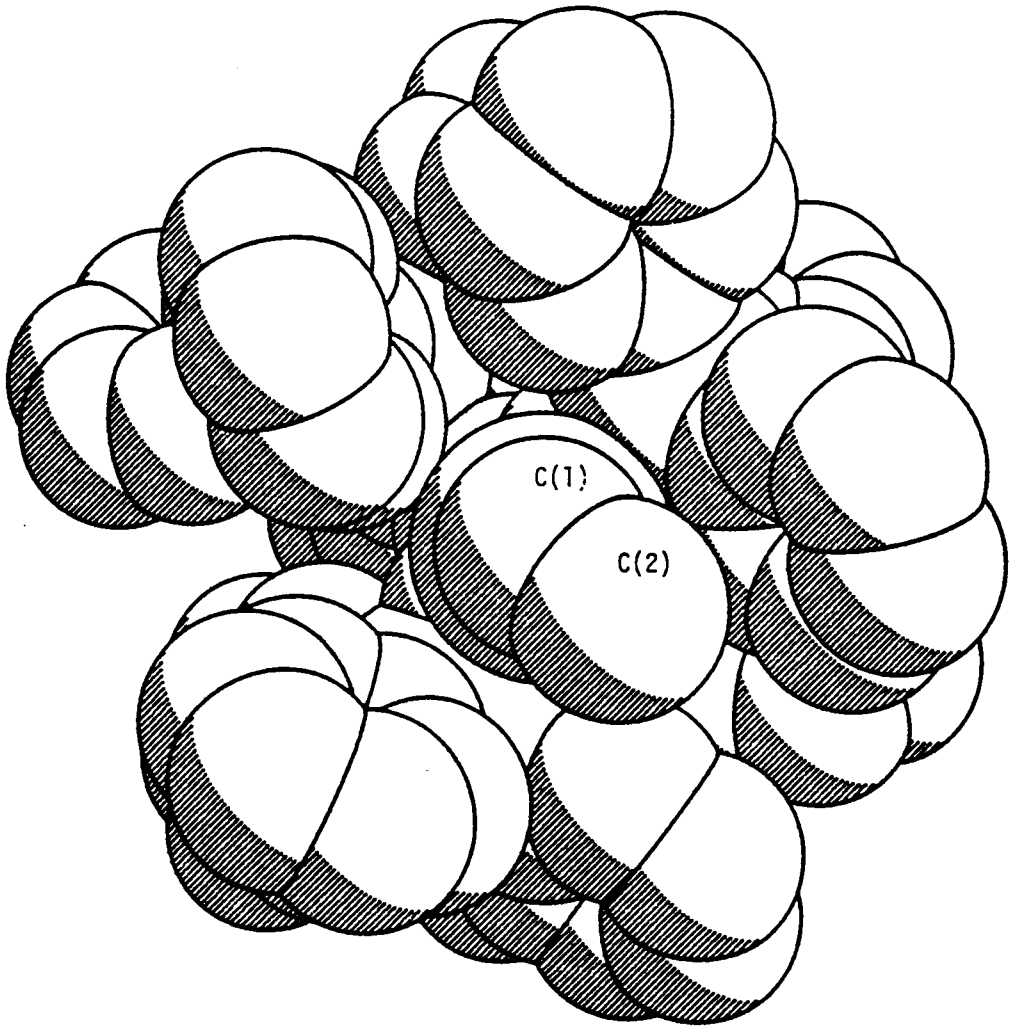

Figure 4-3. Space filling drawing of $(C_2H_5)Zn(\mu\text{-}OSiPh_3)_2Zn(\mu\text{-}OSiPh_3)_2$-$Zn(C_2H_5)$ viewed along C1-Zn1 bond showing that an ethyl group is buried by the phenyl groups of triphenylsiloxy ligands. Hydrogen atoms are omitted for clarity.

4-3. Experimental

General considerations: The operations were carried out under an atmosphere of purified nitrogen (see Chapter 1). Et_2O was freshly distilled from calcium hydride prior to use. THF was distilled first from KOH and then from sodium benzophenone ketyl before use. Toluene was distilled over sodium benzophenone. Deuterated solvents were purchased from Cambridge Isotope Laboratory. $CDCl_3$ was filtered through a neutral alumina column before use. Benzene-d^6 was stored over sodium metal. $ZnEt_2$ (1.0M in hexane) and $SnMe_4$ were reagent grade from Aldrich and used without further purification. Infrared spectra were recorded with a Nicholet 510P FTIR spectrometer, and NMR spectra with an AC-300 Bruker instrument.

Reaction of $MoO_2(OSiPh_3)_2$ with $SnMe_4$ in THF:

In a dry box, $MoO_2(OSiPh_3)_2$ (785mg, 1.12mmol) was dissolved in about 30ml freshly distilled THF solvent in a greaseless Schlenk flask equipped with a stirrer. While stirring, 218mg (1.22mmol) of $SnMe_4$ was added to the above mixture. The clear solution was then heated and stirred at 58°C for about 24 hours. The color of the mixture gradually darkened to a final bluish color. To work up the reaction, the solvent was stripped off at the Schlenk line. The dry residue (2) in the flask was first was washed twice with about 20ml cold hexane. The hexane solution, while immersed in an ice bath, was then filtered under pressure through a cannula tube equipped with a tiny filter head. A white powder (285mg) was

recovered from the hexane solution by pumping off the hexane solvent. The white solid was identified to be an ether $Ph_3SiOCH_2CH_2CH_3$. Two experiments gave the same yield:34% based on $MoO_2(OSiPh_3)_2$. FTIR (KBr, in cm^{-1}): 3067m , 2999w (aromatic C-H stretching); 2960m, 2923m, 2871m (aliphatic C-H stretching), 1587w, 1484w, 1429s (Si-Ph stretching), 1390w, 1110vs (Si-Ph stretching), 1085m, 1010m, 997m, 830w, 737m, 713s, 698s, 514s, 481w. NMR ($CDCl_3$, TMS, ppm): 7.64 (m, 6H), 7.44 (m, 9H), 3.75 (t, J=6.7Hz, 2H), 1.60 (sextet, J=6.7Hz, 2H), 0.902 (t, J=7.4Hz, 3H), Mass data [EI, m/z (% int), assign]: 183(87%), Ph_2SiH^+; 199(100%), Ph_2SiOH^+; 241(86%), $Ph_2SiOCH_2CH_2CH_3^+$; 259(58%), Ph_3Si^+; 289(8%), $Ph_3SiOCH_2^+$; 318(42%), $Ph_3SiOCH_2CH_2CH_3^+$.

After hexane washing, the dry residue, **2**, was again washed with 2x20ml anhydrous Et_2O. The Et_2O washing affords 285mg of Ph_3SiOH after stripping off the solvent. FTIR (KBr, cm^{-1}): 3266m (O-H stretching); 855, 835s (Si-O). NMR ($CDCl_3$, TMS): 2.50ppm (s, 1H, Ph_3SiOH).

The remaining residue, after hexane and Et_2O washing, was bluish, weight 241mg. It is soluble in water and not soluble in organic solvents. FTIR only gave an ill-defined broad band centered at $859cm^{-1}$. Other areas of the IR spectrum were almost blank except some very weak bands of $Ph_3SiOCH_2CH_2CH_3$.

Reaction of $MoO_2(OSiPh_3)_2$ with $SnMe_4$ in THF: The preparation of $(C_2H_5)Zn$-$(\mu$-$OSiPh_3)_2Zn(\mu$-$OSiPh_3)_2Zn(C_2H_5)$ (1):

In a dry box, 345mg (0.509mmol) of $MoO_2(OSiPh_3)_2$ was dissolved in 12ml of dry toluene. 1.0ml (1.0mmol) of $ZnEt_2$ was then slowly added to the above $MoO_2(OSiPh_3)_2$ solution while stirring. The color of the mixture gradually darkened to a deep brown. The mixture was stirred for an hour, then the solvent was pumped out to get a black solid residue. The proton NMR in C_6D_6 of the solid, after washing with 2x10ml of hexane, showed the existence of the Ph_3SiO group at 7.70ppm and Zn-Et at 0.75 (t, J=8Hz) and 0.15ppm (q, J=8Hz). The solid was then dissolved in 1,2-dichloroethane and the solid that was not dissolved was filtered out. Layered carefully with hexane solution on the top of 1,2-dichloroethane solution for a day, the 1,2-dichloroethane solution afforded two kinds of crystals. Many of the crystals were white needles and were identified by FTIR to be Ph_3SiOH. The other crystals were transparent plates, which proved to be $(C_2H_5)Zn(\mu$-$OSiPh_3)_2Zn(\mu$-$OSiPh_3)_2Zn(C_2H_5)$ (1) by an X-ray diffraction study. The solid of the 1 is stable in air. FTIR (KBr, cm^{-1}): 3068m, 3047m (aromatic C-H), 2953w, 2926m, 2859m (ethyl C-H stretching), 1589m, 1485m, 1428vs (Si-Ph), 1116vs (Si-Ph); 880m; 887vs; 544m, 513s.

184mg of grayish solid was recovered after hexane and 1,2-dichloroethane washing. FTIR (film on KBr plate, cm^{-1}): 3067m, 3047m (aromatic C-H stretching), 2929m, 2895w, 2857m (ethyl C-H stretching); 1428vs (Si-Ph), 1114vs (Si-Ph), 908m, 880w, 743m 699vs, 510s. The solid was soluble

in 1,2-dichloroethane. Further workup failed to give a definite Mo-containing compound.

Crystallographic Studies of (1): X-ray reflection data were collected at 23°C using a Rigaku AFC6R diffractometer equipped with graphite monochromated Mo K_α (λ = 0.71073Å) radiation. First, a ZIGZAG search was used to find 17 low angle reflections at 2θ = 9.69-13.94° range. The average diffracting intensity of the crystal was 1990±936cps (at the range of 706 to 3447cps) at X-ray rotating anode tube current = 120mA and voltage = 60KV. The average of the full width at half height of these 17 reflections was 0.566±0.156°ω with some widths as high as 0.775°. This means the reflection peaks are relatively weak and wide compared to that of other crystals. A preliminary orientation matrix of the crystal was then calculated from these 17 reflections. Secondly, a small set of data (300 reflections) at 2θ range of 23.6 and 26.9° was then quickly collected at a data collection speed of 32°min^{-1} in ω and without rescanning the weak peaks. All the 300 reflections were flagged as weak at the F(obs)>10ΔF criterion with all intensities less than 300cps. From these 300 reflections, 21 strong reflections were selected and their angles refined. Only 11 reflections among these 21 reflections were successfully refined. Their intensities were in a range of 197 and 506cps with average at 323cps. These reflections were then used to refine the orientation matrix and cell parameters. The refined and idealized cell parameters were: a = 13.922(3)Å, b = 19.374(5)Å, c = 25.053(4)Å, α=β=γ=90°, V = 6757(2)$Å^3$.

Finally the full reflection data were collected. The data collection speed was 16°min^{-1} in ω. Three reflections (intensities 4891, 5481, 675 at 2θ = 12.9, 9.1, 23.2°) were monitored every 300 reflections to check stability. No significant intensity loss was found. The whole data was divided into four shells with 2θ from 2, 30, 36, 41, and to 45°. The weak reflections in the first two shells were allowed to rescan three times to increase the signal-to-noise ratio. The tolerances for the reorientation of the crystal were set to $\Delta\omega$=0.250° and $\Delta\chi$=0.348°. Reorientation measurement for the last two shells was disabled. Also the rescan number for the last two shells was increased to four times considering that the high angle reflections were relatively weak. Of all 4925 reflections measured, only 27% (1328 reflections) was flagged as observed with intensity $I > 3\sigma(I)$, which reflects the weak diffracting power of the crystal and accounts for the somewhat large error for final structural parameters.

The structure was solved by direct methods SHELXS-86 [12], which gave a few benzene rings and two heavy atoms, and so suggested the right result. Further structure expanding (different Fourier synthesis) and least-square refinement was done by using the TEXSAN program [13] installed on a microVAX. All non-hydrogen atoms were set to anisotropical temperature factors and refined successfully, except C1, C2, and C15 becoming non-positively defined. These three atoms were set back to isotropical temperature factors in the final cycle of refinement and gave good results. All hydrogen atoms were included in a calculated position and not updated after the final cycle of refinement. Considering only

1328 reflections were available for the least-square refinement, a strategy that fixed all benzene rings into the rigid groups in order to reduce the number of variables was tried but gave no better results. Final R = 6.72%; R_w = 7.04%, and final differential Fourier is featureless with maximum peak of 0.469 e/Å^3. The selected crystallographic data are given in Table 4-1. The fractional coordinates of all atoms are given in Table 4-2.

Table 4-1. Selected Crystal Data and Experimental Conditions for $(C_2H_5)Zn(\mu\text{-}OSiPh_3)_2Zn(\mu\text{-}OSiPh_3)_2Zn(C_2H_5)$ (1)

compound	$(C_2H_5)Zn(\mu\text{-}OSiPh_3)_2Zn(\mu\text{-}OSiPh_3)_2Zn(C_2H_5)$
empirical formula	$C_{38}H_{35}O_2Si_2Zn_{1.5}$
formula weight	677.9343amu
dimension, mm	0.2x0.2x0.4
crystal system	orthorhombic
lattice parameters	a = 13.922(3)Å
	b = 19.374(5)Å
	c = 25.053(4)Å
μ (MoKα), cm^{-1}	11.99 cm^{-1}
V, Å^3	6757(4) Å^3
space group	Pccn (#56)
Z	8
$D_{calc,\ g\ cm\text{-}3}$	1.3326 g/cm^3
temperature	23°C
$2\theta_{max}$	45°
data collection speed	16.0° min^{-1} in ω
diffractometer	Rigaku AFC6R
scan method	ω
h k l limits	0,0,0 to 20,26,14
F(000)	2816.00
total no.of measd data	4925
no. observations (I>3σ(I))	1328
no. variables	378
residuals: R; R_w	0.0672; 0.0704
GOF	1.7
maximum shift	0.01
largest residual peak	0.469

Table 4-2. Positional parameters and B(eq) for the non-hydrogen atoms of $(C_2H_5)Zn(\mu\text{-}OSiPh_3)_2Zn(\mu\text{-}OSiPh_3)_2Zn(C_2H_5)$ (1)

atom	x	y	z	B(eq)
Zn(1)	0.0564(2)	0.2949(1)	0.0771(1)	4.7(2)
Zn	1/4	1/4	0.0994(1)	3.1(2)
Si(1)	0.1032(4)	0.1467(3)	0.0275(3)	4.1(4)
Si(2)	0.1467(5)	0.3738(3)	0.1751(3)	3.5(4)
O(1)	0.137(1)	0.2182(6)	0.0545(6)	4.1(8)
O(2)	0.1643(8)	0.3197(6)	0.1268(5)	4.1(8)
C(1)	-0.068(2)	0.338(1)	0.054(1)	8.2(8)
C(2)	-0.151(2)	0.314(2)	0.080(1)	13(1)
C(11)	0.203(2)	0.102(1)	-0.009(1)	5(2)
C(12)	0.197(2)	0.038(1)	-0.030(1)	6(2)
C(13)	0.271(2)	0.008(1)	-0.058(1)	7(2)
C(14)	0.355(2)	0.044(2)	-0.062(1)	7(2)
C(15)	0.365(2)	0.108(1)	-0.044(1)	4.9(6)
C(16)	0.289(2)	0.138(1)	-0.017(1)	4(1)
C(21)	0.045(2)	0.091(1)	0.079(1)	4(1)
C(22)	0.077(2)	0.024(1)	0.090(1)	6(2)
C(23)	0.030(3)	-0.013(2)	0.127(1)	8(2)
C(24)	-0.044(3)	0.008(2)	0.156(1)	9(3)
C(25)	-0.076(2)	0.076(2)	0.148(1)	7(2)
C(26)	-0.034(2)	0.116(1)	0.111(1)	6(2)
C(31)	0.016(2)	0.172(1)	-0.027(1)	3(1)
C(32)	-0.085(2)	0.155(1)	-0.019(1)	5(2)
C(33)	-0.147(2)	0.176(2)	-0.064(2)	7(2)
C(34)	-0.114(3)	0.204(2)	-0.106(1)	7(2)
C(35)	-0.020(3)	0.217(1)	-0.110(1)	7(2)
C(36)	0.042(2)	0.201(1)	-0.072(1)	6(2)
C(41)	0.023(2)	0.356(1)	0.2065(8)	4(1)
C(42)	-0.001(2)	0.288(2)	0.211(1)	8(2)
C(43)	-0.090(3)	0.271(1)	0.234(2)	10(3)
C(44)	-0.151(2)	0.320(2)	0.245(2)	10(3)
C(45)	-0.132(2)	0.388(2)	0.235(1)	8(2)
C(46)	-0.043(2)	0.405(1)	0.216(1)	6(2)
C(51)	0.240(2)	0.367(1)	0.229(1)	4(1)
C(52)	0.217(2)	0.349(2)	0.279(2)	8(2)
C(53)	0.281(3)	0.347(2)	0.320(1)	10(3)
C(54)	0.372(2)	0.367(2)	0.311(1)	7(2)
C(55)	0.401(2)	0.382(1)	0.261(1)	6(2)
C(56)	0.334(2)	0.386(1)	0.220(1)	6(2)
C(61)	0.149(1)	0.466(1)	0.149(1)	4(1)
C(62)	0.153(2)	0.521(2)	0.183(1)	6(2)
C(63)	0.143(2)	0.587(2)	0.165(1)	5(2)
C(64)	0.128(2)	0.599(1)	0.110(1)	5(2)
C(65)	0.124(2)	0.545(2)	0.077(1)	7(2)
C(66)	0.131(2)	0.477(1)	0.095(1)	6(2)

4-4. **Reference:**

1. Bishop, M.W.; Chatt, J.; Dilworth, J.R.; Neave, B.D.; Dahlstrom, P.; Hyde, J.; Zubieta, J. *J. Organomet. Chem.* **1981**, *213*, 109-124.

2. Herrmann, W.A. *Angew. Chem. Int. Ed. Engl.* **1988**, *27*, 1297-1313. A review paper entitled "High Oxidation State Organometallic Chemistry, A Challenge - the Example of Rhenium".

3. Sullivan, A. and Wilkinson, G. *J. Chem. Soc. Dalton Trans.* **1988**, 53-60.

4. Brandsma, L. and Verkruijsse, H.D. "Preparative Polar Organometallic Chemistry", Vol 1, Springer-Verlag, Berlin, **1987**.

5. Evans, W.J.; Ulibarri, T.A.; Chamberlain, L.R.; Ziller, J.W.; Alvarez, D. Jr. *Organometallics*, **1990**, *9*, 2124-2130.

6. Al-Juaid, S. S.; Buttrus, N. H.; Eaborn, C.; Hitchcock, P. B.; Roberts, A.; Smith, J. D.; Sullivan, A., *J. Chem. Soc. Chem. Commun.*, **1986**, 908.

7. Evans, W. J.; Golden, R. E.; Ziller, J. W., *Inorg. Chem.*, **1991**, *30*, 4963. Coan, P. S., McGeary, M. J.; Lobkovsky, E. B.; Caulton, K. G. *Inorg. Chem.* **1991**, *30*, 3570.

8. Gaffney, C.; Harrison, P. G.; King, T., *J. Chem. Soc., Chem. Commun.*, **1980**, 1251.

9. Sigel, G. A.; Bartlett, R. A.; Decker, D. Olmstead, M. M.; Power, P. P. *Inorg. Chem.* **1987**, *26*, 1773.

10. Shearer, H. M. M.; Spencer, C. B., *Acta Crystallogr., Sect. B*, **1980**, *36*, 2046.

11. Herrmann, W. A.; Bogdanovic, S.; Behm, J.; Denk, M., *J. Organomet. Chem.*, 19892, 430, C33.

12. Sheldrick, G. M. in *Crystallographic Computing 3*, (Eds. G. M. Sheldrick, C. Kruger, and R. Goddard); Oxford University Press, pp175-189.

13. TEXSAN: *Single crystal structure analysis software*. Version 5.0; Molecular Structure Corporation; The Woodlands, TX 77381, **1989**.

Chapter 5

Reactions with Phosphorus Ylides

5-1. Introduction

Phosphorus ylides, $R_3P^+CR'_2^-$, are highly reactive compounds, and can be represented by two limiting Lewis structures: ylide and ylene:

$$\underset{\text{ylide}}{R_3P^+\text{-}CR'_2^-} \longleftrightarrow \underset{\text{ylene}}{R_3P\text{=}CR'_2}$$

Phosphorus ylides are an important group of nucleophilic carbon species. The most common use of ylide is found in the Wittig reaction, where a phosphorus ylide reacts with an aldehyde or ketone to provide a means of introducing a carbon-carbon double bond in place of a carbon-oxygen double bond [1] (eqn. 1):

$$R_3P^+\text{-}CR'_2^- + R''_2C\text{=}O \longrightarrow R''_2C\text{=}CR'_2 + R_3P\text{=}O \qquad \ldots(1)$$

The mechanism of the reaction is one of nucleophilic addition of the ylide carbon to the carbonyl group to yield a dipolar intermediate (a betaine), followed by elimination of phosphine oxide. The elimination might be concerted, or it might take place via a four-member oxaphosphetane intermediate [2].

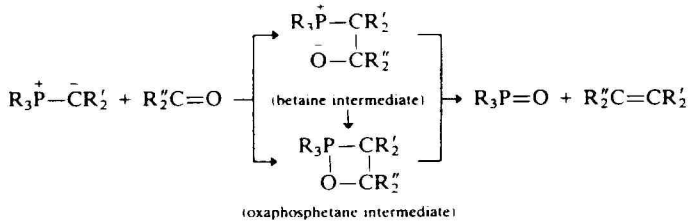

...(2)

The inorganic-version of the Wittig reaction, i.e., the conversion of a metal oxo double bond to a metal carbon double bond, is a potentially very useful reaction [3]. Actually a similar reaction has often been used in inorganic synthesis, where a phosphinimine, $R_3P{=}NR'$, (similar to $R_3P^+\text{-}CR'_2{}^-$) reacts with a metal oxo moiety to replace an oxo ligand by an organoimido ligand. Eqn. 3 gives an example of this kind of reaction [4]: one Mo=O bond in a hexamolybdate was replaced by an Mo=NR (R = tolyl, p-$CH_3C_6H_5$-) bond. By the way, isocyanates, RN=C=O, are also frequently used in this transformation.

$$[(n\text{-}Bu)_4N]_2[Mo_6O_{19}] + Ph_3P{=}Ntol \rightarrow [(n\text{-}Bu)_4N]_2[Mo_5O_{18}(Mo{=}Ntol)] + Ph_3P{=}O \quad ...(3)$$

The direct conversion of M=O to $M{=}CH_2$ has been observed in a gas phase reaction. Such reaction involves naked oxometal cations and ethylene as shown in eqn. 4. The example of a gas phase reaction in which a d^0 oxo species reacts with an olefin to form an alkylidene bond is also known (eqn. 5) [4].

$$[MO]^+ + CH_2{=}CH_2 \longrightarrow [MCH_2]^+ + CH_2{=}O \quad ...(4)$$

$$[ClCrO_2]^+ + CH_2{=}CH_2 \longrightarrow [ClCrOCH_2]^+ + CH_2{=}O \quad \ldots(5)$$

Arzoumanian and his coworkers attempted to achieve the formation of metal-alkylidene compounds by treating $MoO_2(mesityl)_2$ (mesityl = 2,4,6-$C_6H_2Me_3$) with various ylides in solution phase [6-8]. Unfortunately, their attempts failed. Transient peaks in the range 165-238 ppm in the $^{13}C\{^1H\}$ NMR spectra were observed in several cases, which were assigned to metal-alkylidene carbon atoms. Their reactions have either afforded stable adducts (eqn. 6) [6] or alternatively have resulted in a variety of interesting rearrangements (eqns. 7-9) [7-8] rather than discrete alkylidene complexes.

$$MoO_2(mesityl)_2 + Bu_3P^+CH_2^- \xrightarrow{THF,\ 0°C} MoO_2(mesityl)_2CH_2PBu_3 \quad \ldots(6)$$

$$MoO_2(mesityl)_2 + 2\ Bu_3P^+CH_2^- \xrightarrow{py,\ 20°C} (mesityl)O_2Mo{=}C(mesityl)PBu_3 \quad \ldots(7)$$

$$MoO_2(mesityl)_2 + Ph_3P^+CHR^- \xrightarrow{CH_2Cl_2,\ 20°C} (Ph_3PCH_2R)_2Mo_6O_{19} \quad \ldots(8)$$
(R = Ph, COOEt, H)

$$MoO_2(mesityl)_2 + Ph_3P^+CHR^- \xrightarrow{CH_2Cl_2,\ 20°C} (Ph_3PCH_2R)_4(\beta\text{-}Mo_8O_{24}) \quad \ldots(9)$$
(R = OCH_3, COOEt)

In the eqns 7-9, Mo-mesityl bonds are broken upon Wittig reagents' attack to form various products including an interesting compound $(mesityl)O_2Mo{=}C(mesityl)PBu_3$.

In this thesis work, $MoO_2(OSiPh_3)_2$ has been used to react with Wittig reagents. The hope was that the Mo-siloxy bonds in $MoO_2(OSiPh_3)_2$ will be more robust than Mo-mesityl bonds of $MoO_2(mesityl)_2$ to a reduced rearrangement reaction, and yet the coordination around molybdenum is still unsaturated to allow the direct attack of Wittig reagents on the molybdenum center.

5-2. Reactions of $MoO_2(OSiPh_3)_2$ with $Ph_3P{=}CH_2$ and $Ph_3P{=}CR_2$

In an attempt to prepare the adduct of $MoO_2(OSiPh_3)_2$ with a Wittig reagent, stoichiometric amount of $Ph_3P^+C(CH_3)_2^-$ was added to a saturated solution of $MoO_2(OSiPh_3)_2$. The reaction was based on solubility considerations: the adduct should have a lower solubility than the parent compound since it has a higher molecular weight. Indeed, some YELLOWISH crystals were precipitated out quickly ($Ph_3P^+C(CH_3)_2^-$ is also yellowish). The NMR of the crystals in CD_2Cl_2 showed that the doublet of $Ph_3P^+CH_2^-$ at 1.4ppm shifted to 2.54ppm. Based on these arguments, the crystals were tentatively identified as an adduct $MoO_2(OSiPh_3)_2.Ph_3P^+C(CH_3)_2^-$. Unfortunately, several attempts to do an X-ray diffraction study on the crystals of the adduct failed.

Lai et. al. successfully prepared a similar adduct (eqn. 6) $MoO_2(mesityl)_2.CH_2PBu_3$ at 0°C and obtained a crystal structure of the complex. The structure of the adduct shows some interesting features. The five-coordinate Mo center is in a distorted bipyramidal configuration. Two oxo atoms and one mesityl group occupy the equatorial plane with Mo-C(mesi-

tyl) bond length at 2.224Å. Another mesityl group and the ylide occupy the axial position with Mo-C(ylide) = 2.249(7)Å. The P-C bond length of the ylide is 1.765Å, showing some ylidic character for the P-C bond. The Mo=O bond lengths are 1.688 and 1.706Å. The bond length difference between Mo=O bonds is not significant enough to account for greater electron density on one oxo atom than on another one. The author concluded that the adduct is better described as a dioxo ylide complex (A) rather than an "oxo-metallobetain" intermediate, (B).

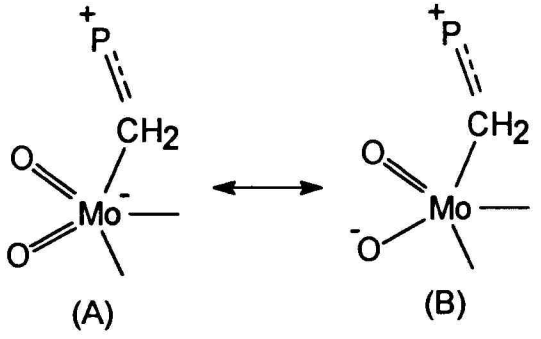

In Arzoumanian and his coworkers' study of the reaction of $MoO_2(mesityl)_2$ with various ylides (eqns. 8 and 9), polyoxomolybdates and phosphonium cations were found as major products. The occurrence of a transylidation reaction was used to explained the presence of phosphonium in the products (Scheme 2). The transylidation is often encountered in ylide-transition metal chemistry [9]. Compounds of type (5) can be thought of as being the first step in the formation of an isopolymolybdate anion, in a manner similar to that in the usual aqueous isopolymolybdate synthesis [10].

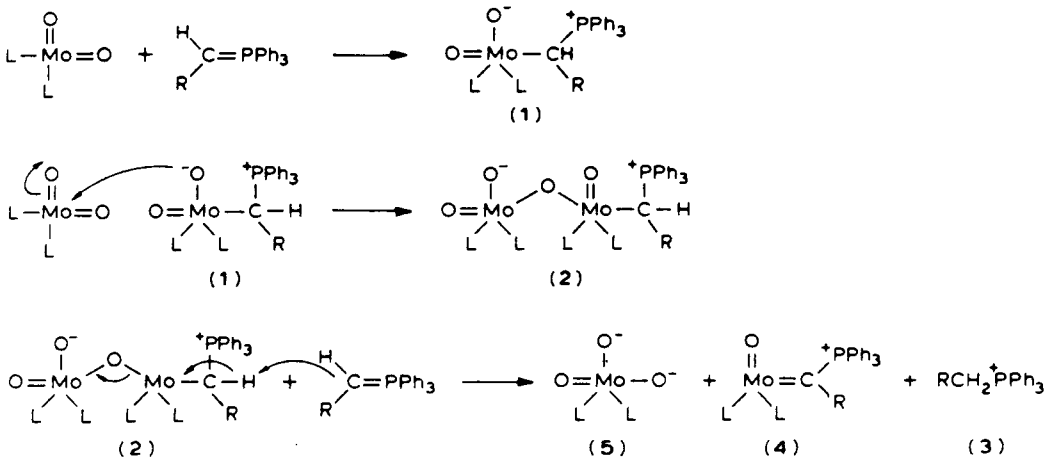

In this thesis work, an ylide $Ph_3P^+C(CH_3)_2^-$ was used in a Wittig-like reaction in the hope that the transylidation reaction would be reduced. The results of the reaction between $MoO_2(OSiPh_3)_2$ and $Ph_3P^+C(CH_3)_2^-$ for an extended period, however, still gave a hexamolybdate $[Ph_3PCH(CH_3)_2]_2(Mo_6O_{19})$ as the major product. The source of the proton that accounts for the formation of phosphonium is not clear.

Besides the hexamolybdate $[Ph_3PCH(CH_3)_2]_2(Mo_6O_{19})$ as a major product, $(Ph_3Si)_2O$ was also frequently found in the products. The appearance of $(Ph_3Si)_2O$ in the products of the reaction of $MoO_2(OSiPh_3)_2$ indicates the easy decomposition of $MoO_2(OSiPh_3)_2$ (eqn. 10) through either intra- or inter-molecular elimination of triphenylsiloxy groups.

$$MoO_2(OSiPh_3)_2 \longrightarrow (Ph_3Si)_2O + \{MoO_3\} \qquad \ldots(10)$$

5-3. Crystal Structure of $[Ph_3PCH(CH_3)_2]_2(Mo_6O_{19})$ and $Ph_3PCH(CH_3)_2Cl$

The structures $[Ph_3PCH(CH_3)_2]_2(Mo_6O_{19})$ and $Ph_3PCH(CH_3)_2Cl$ were determined in the thesis work through an X-ray diffraction study. The structure of the anion of $[Ph_3PCH(CH_3)_2]_2(Mo_6O_{19})$ is shown in Figure 5-1. The structures of the cations of $[Ph_3PCH(CH_3)_2]_2(Mo_6O_{19})$ and $Ph_3PCH(CH_3)_2Cl$ are the same and is shown in Figure 5-2. Selected bonds lengths and angles are given in Tables 5-3 and 5-4, respectively.

$[Ph_3PCH(CH_3)_2]_2(Mo_6O_{19})$ crystallizes in the C2/c space group with four molecules per unit cell. The $[Mo_6O_{19}]^{2-}$ anion is flanked by two $[Ph_3PCH(CH_3)_2]^+$ cations. The central oxygen atom of the $[Mo_6O_{19}]^{2-}$ anion is at a special position (½,½,0), which is also the symmetric center of the whole molecule. Each molybdenum atom is six-coordinate and forms a somewhat distorted octahedra with six surrounding oxygen atoms. Six such $\{MoO_6\}$ octahedra stack together and share the same central oxygen atom to construct the structure of the anion $[Mo_6O_{19}]^{2-}$. Unlike the parent compound $MoO_2(OSiPh_3)_2$ that contains a $\{MoO_2\}$ unit, the hexamolybdate contains only mono (terminal oxo) $\{MoO\}$ units. The mean Mo-O bond lengths are terminal Mo-O_t = 1.674(5)Å, central Mo-O_c = 2.314(1)Å, and bridging Mo-O_b = 1.924(53)Å, which are very close to literature values [10].

Many structures of hexamolybdates with different cations have been determined by the X-ray diffraction method [10-11]. The number of structures has increased recently partly because of the interest in *organo donor-inorganic acceptor* (ODIA) charge transfer salts, where

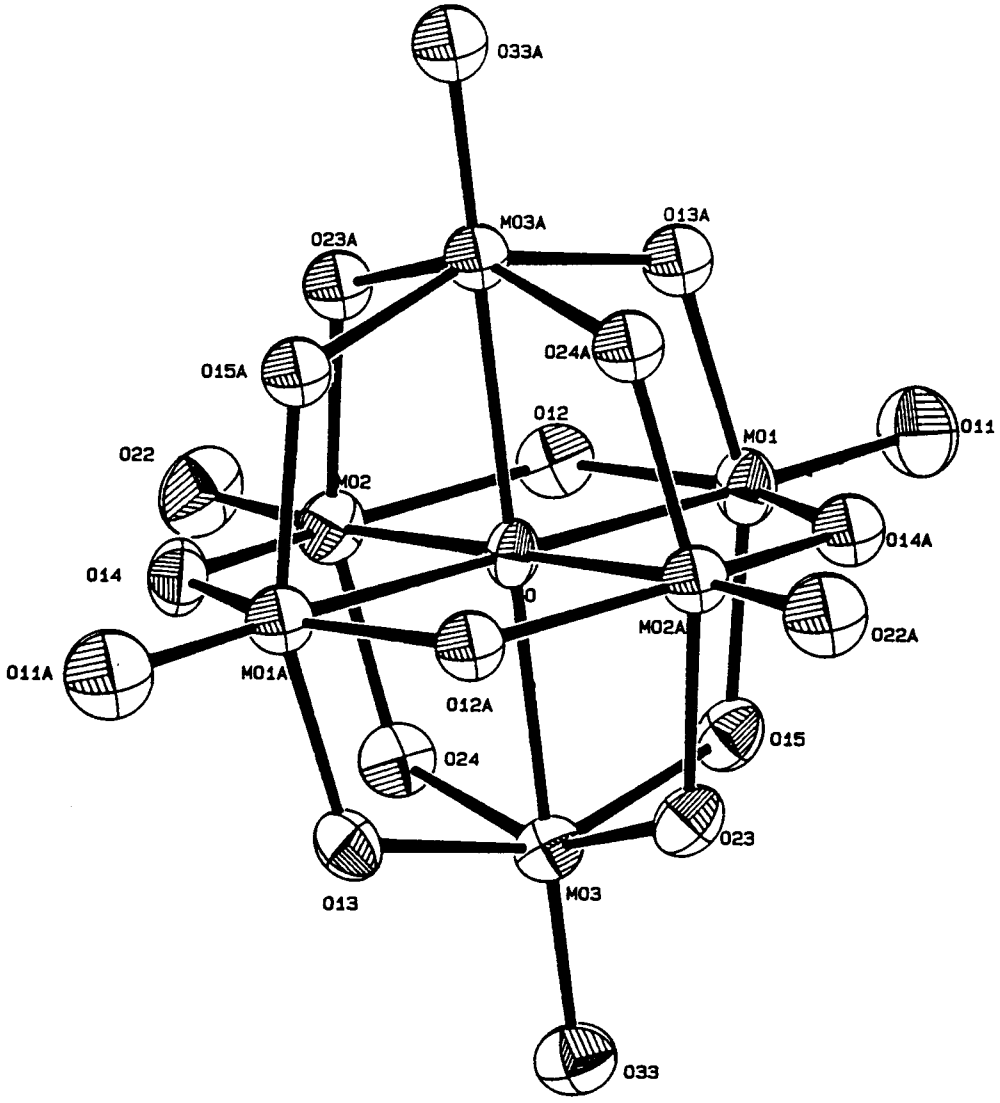

Figure 5-1. The ORTEP drawing of the structure of $(Mo_6O_{19})^{2+}$ in $[Ph_3PCH(CH_3)_2]_2(Mo_6O_{19})$.

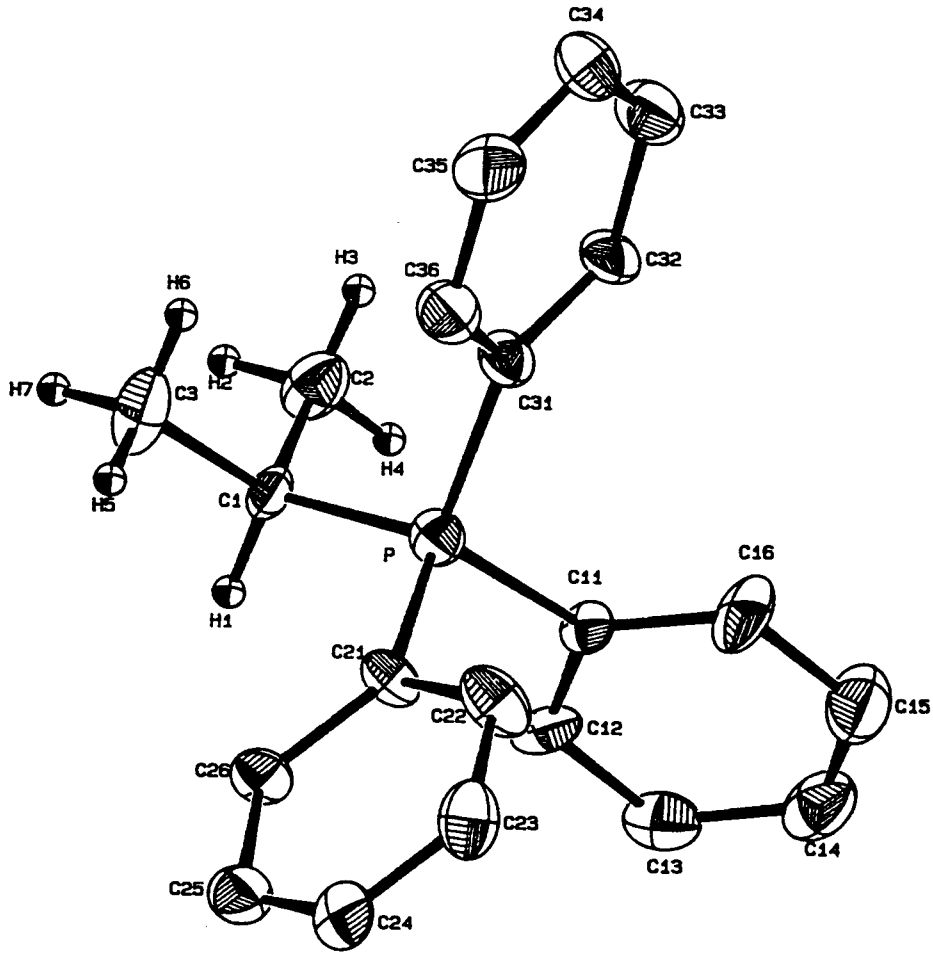

Figure 5-2. The ORTEP drawing of the structure of $(Ph_3PCH(CH_3)_2)^+$ in $Ph_3PCH(CH_3)_2Cl$.

hexamolybdate is used as an inorganic anion and tetrathiafulvalene (TTF) and tetracyanoquinodimethane (TCNQ) derivatives are used as organic cations [12]. All hexamolybdates have similar anion structures and the bond lengths are in good agreement.

The salt $Ph_3PCH(CH_3)_2Cl$ was isolated during a reaction between $MoO_2(OSiPh_3)_2$, $Ph_3P^+C(CH_3)_2^-$ and $Al(OEt)_3$. The finding of chloride anion is interesting since the reaction system did not contain Cl except that the solvent 1,2-dichloroethane was used for product workup.

5-4. Experimental

General considerations: The operations were carried out under an atmosphere of purified nitrogen. Anhydrous 1,2-dichloroethane and acetonitrile were used as purchased from Aldrich, and purged with Ar for 15 minutes before use. 1,2-dichloromethane was distilled from P_2O_5 powder. THF was distilled first from KOH and then from sodium benzophenone ketyl before use. Toluene was distilled over sodium benzophenone. Pyridine was first soaked in KOH for a few days and then distilled from calcium hydride. Deuterated solvents were purchased from Cambridge Isotope Laboratory. $CDCl_3$ was filtered through a neutral alumina column before use. Benzene-d^6 was stored over sodium metal. "Instant Ylides" [13] were purchased from Fluka and used as received. Infrared spectra were recorded with a Nicholet 510P FTIR spectrometer, and NMR spectra with an AC-300 Bruker instrument.

Preparation of ylides (1,1'-dimethylmethylene)triphenylphosphorane ($Ph_3P^+C(CH_3)_2^-$) [and methylenetriphenylphosphorane ($Ph_3P^+CH_2^-$)] [13]: In a dry box, instant ylide (1,1'-dimethylmethylenetriphenylphosphonium + sodium bromide) [or methylenetriphenylphosphonium + sodium bromide] was dissolved in a solvent (usually THF) at room temperature and then stirred for an hour. The color of the mixture turned to deep reddish (yellowish for $Ph_3P^+CH_2^-$). The mixture was filtered through a Pasteur pipette tightly filled with some glass wool. The clear filtrate contained mainly ylide. Only a trace amount of the phosphonium salt was found by proton NMR in C_6D_6. If a solvent other than THF was to be used, THF was pumped off in the vacuum line and the solvent added. Both ylides are air sensitive. The color discharged upon air exposure. NMR of $Ph_3P^+C(CH_3)_2^-$ (C_6D_6/TMS, ppm): 7.62(m, aromatic C*H*), 7.08(m, aromatic C*H*), 2.17(d, J=16.5Hz, PCH_3). NMR of $Ph_3P^+CH_2^-$ ($CD_3C_6D_5$, ppm): 7.6(m), 7.0(m), 1.49(d, J=13.2Hz, PCH_2). For comparison, the NMR of the corresponding phosphonium salts: $Ph_3PCH(CH_3)_2^+$, 3.95(m, PC*H*), 0.88(dd, J=18, 7Hz, CH_3); $Ph_3PCH_3^+$, 3.05(d, J=13Hz, PCH_3).

Reaction of $MoO_2(OSiPh_3)_2$ with $Ph_3P^+C(CH_3)_2^-$: 784mg (1.16mmol) of $MoO_2(OSiPh_3)_2$ was dissolved in 15ml of freshly distilled THF in a dry box to give a pale bluish solution. Five ml of THF solution that contained 1.16mmol of $Ph_3P^+C(CH_3)_2^-$ were then added to the above solution, and led to the discharge of the red color of $Ph_3P^+C(CH_3)_2^-$. The mixture was then stirred for an hour to yield a greenish solution with some bluish silk-like solid. The following day, the solvent was removed and the greenish sticky solid residue was dissolved in toluene to remove the bluish solid. 230mg of pale yellowish solid was recovered from the toluene solution and

was crystallized by dichloromethane layered with hexane. A crystal (orthorhombic, 0.2x0.3x0.4mm) was chosen for X-ray analysis. The formula of the compound was found to be $[Ph_3PCH(CH_3)_2]_2(Mo_6O_{19})$ by X-ray analysis. FTIR ($CD_3C_6D_5$ film on KBr, cm^{-1}): 1653m, 1428s, 1115vs, 913vs (Mo=O stretching), 709s, 511s. Proton NMR ($CD_3C_6D_5$): 7.0-8.0(m, aromatic C*H*), 4.3(m, PC*H*), 0.7(dd, J=18, 7Hz, CH_3).

Reaction of $MoO_2(OSiPh_3)_2$ with $Ph_3P^+CH_2^-$: In a dry box, 1ml of yellowish THF solution containing 0.151mmol of $Ph_3P^+CH_2^-$ was slowly added to a 2.4ml acetonitrile solution saturated with 102.8mg (0.152mmol) of $MoO_2(OSiPh_3)_2$. The mixture was yellowish and clear. One hour later, solid was precipitated out of the mixture, which was isolated and washed with 2x5ml of hexane to afford some tiny yellowish crystals. The crystals, however, did not give satisfactory X-ray diffraction profiles. Proton NMR ($CD2Cl_2$, ppm), 7.7-7.0(m, Phenyl C*H*), 2.54(d, J=13.2Hz, $MoO_2(OSiPh_3)_2$.-$Ph_3P^+CH_2^-$), 1.42(d, J=13.7Hz, weak, $Ph_3P^+CH_2^-$).

Crystallographic studies: see previous chapters for the general experimental conditions for X-ray diffraction studies. All H atoms were included in the calculated positions (C-H = 0.95Å) in the structure factor calculation. The atomic coordinates, selected bond lengths and bond angles for $[Ph_3PCH(CH_3)_2]_2(Mo_6O_{19})$ (and $Ph_3PCH(CH_3)_2Cl$) are given in Tables 5-2, 5-3, 5-4, respectively.

$[Ph_3PCH(CH_3)_2]_2(Mo_6O_{19})$. Some selected crystallographic data are given in Table 5-1. The structure was solved by a Patterson deconvolution program (PHASE) in a SHELXS-86 [14] software package. The structure was refined to final R=4.27% and R_w=5.04%. Final difference Fourier map was featureless with largest peak at 0.796 e/Å^3.

$Ph_3PCH(CH_3)_2Cl$. A transparent crystal with size 0.2x0.2x0.4 mm was chosen for X-ray diffraction studies. The structure was easily solved by direct methods. The structure was refined to final R=5.84% and R_w=6.074%. Final difference Fourier map was featureless with largest peak at 0.251 e/Å^3. Some selected crystallographic data are given in Table 5-1.

Table 5-1. Selected Crystal Data and Experimental Conditions for $[Ph_3PCH(CH_3)_2]_2(Mo_6O_{19})$ and $Ph_3PCH(CH_3)_2Cl$

	$[Ph_3PCH(CH_3)_2]_2(Mo_6O_{19})$	$Ph_3PCH(CH_3)_2Cl$
empirical formula	$Mo_3C_{22}H_{24}O_{9.5}PCl_2$	$C_{21}H_{22}PCl$
formula weight	830.1257 amu	340.8316 amu
crystal form	orthorhombic	cube
crystal dimension	0.2x0.3x0.4 mm	0.2x0.2x0.4 mm
crystal system	monoclinic	monoclinic
lattice parameters	a = 20.018(12)Å	a = 10.521(5)Å
	b = 13.359(5)Å	b = 12.231(5)Å
	c = 21.606(5)Å	c = 14.240(8)Å
	β = 102.98(3)°	β = 93.53(5)°
space group	C2/c (#15)	$P2_1/n$ (#14)
Z	8	4
D_{calc}	1.958 g/cm^3	1.229g/cm^3
F(000)	3256.00	720.0000
μ (MoKα)	15.809 cm^{-1}	2.8833cm^{-1}
diffractometer	Rigaku AFC6R	Rigaku AFC6R
radiation	MoKα (λ = 0.710690Å), monochromated	
temperature	23°C	23°C
$2\theta_{max}$	53°	53°
hkl limit	0,0,0,-25,-17,-27	0,0,-18,-13,-15,-18
standard reflections	1,-3,-2; 4,-2,0; 2,0,4	1,3,-2; 2,3,0; 0,1,-4
scan method	ω	ω
data collection speed	16.0° min^{-1} in ω	32.0° min^{-1} in ω
total no.of measd data	6295	2860
no. observations (I>3σ(I))	4002	919
no. variables	340	208
residuals: R; R_w	4.27%; 5.04%	5.84%; 6.07%
GOF	1.6	1.5
max. shift in final cycle	0.24	0.18
largest peak in diff. map	0.796	0.251 e/Å^3

Table 5-2. Positional parameters and B(eq) for $[Ph_3PCH(CH_3)_2]_2(Mo_6O_{19})$ and $Ph_3PCH(CH_3)_2Cl$

	For $[Ph_3PCH(CH_3)_2]_2(Mo_6O_{19})$				For $Ph_3PCH(CH_3)_2Cl$				
atom	x	y	z	B(eq)	atom	x	y	z	B(eq)
Mo(1)	0.50397(3)	0.64837(4)	-0.05424(3)	3.82(2)	Cl	1.1143(3)	-0.0971(2)	0.8167(2)	3.6(2)
Mo(2)	0.49531(3)	0.41192(4)	-0.09311(3)	3.72(2)	P	0.7706(3)	0.0659(2)	0.6485(2)	3.1(2)
Mo(3)	0.61840(3)	0.49052(4)	0.02248(3)	3.50(2)	C(1)	0.9132(9)	0.1102(9)	0.7128(7)	2.9(5)
P	0.72888(8)	0.5361(1)	0.29131(7)	3.25(6)	C(2)	0.888(1)	0.214(1)	0.7693(8)	4.5(7)
O	1/2	1/2	0	2.9(2)	C(3)	1.020(1)	0.131(1)	0.6487(8)	5.1(7)
O(11)	0.5041(3)	0.7578(4)	-0.0924(3)	6.5(3)	C(11)	0.646(1)	0.0451(8)	0.7250(7)	2.6(6)
O(12)	0.4926(2)	0.5514(3)	-0.1197(2)	3.9(2)	C(12)	0.675(1)	0.003(1)	0.8122(9)	3.7(6)
O(13)	0.5933(2)	0.3700(3)	0.0559(2)	4.1(2)	C(13)	0.578(1)	-0.029(1)	0.8701(8)	4.6(8)
O(14)	0.4897(2)	0.3100(3)	-0.0333(2)	4.2(2)	C(14)	0.452(1)	-0.018(1)	0.835(1)	5.3(8)
O(15)	0.5979(2)	0.6125(3)	-0.0288(2)	3.9(2)	C(15)	0.424(1)	0.023(1)	0.747(1)	5.6(8)
O(22)	0.4857(3)	0.3507(4)	-0.1620(2)	5.7(3)	C(16)	0.521(1)	0.056(1)	0.6942(8)	4.8(7)
O(23)	0.6029(2)	0.5626(3)	0.0914(2)	3.8(2)	C(21)	0.794(1)	-0.0626(8)	0.5934(7)	2.8(6)
O(24)	0.5888(2)	0.4239(3)	-0.0619(2)	4.1(2)	C(22)	0.703(1)	-0.098(1)	0.5260(9)	4.7(7)
O(33)	0.7039(2)	0.4847(4)	0.0354(2)	4.7(2)	C(23)	0.713(1)	-0.202(1)	0.4880(8)	4.6(8)
C(1)	0.6575(3)	0.4746(5)	0.2401(3)	3.6(3)	C(24)	0.808(1)	-0.270(1)	0.5176(8)	4.0(7)
C(2)	0.6818(4)	0.3806(6)	0.2121(3)	5.3(4)	C(25)	0.897(1)	-0.236(1)	0.5862(9)	4.3(7)
C(3)	0.6016(4)	0.4500(6)	0.2753(4)	5.3(4)	C(26)	0.892(1)	-0.132(1)	0.6246(7)	3.3(6)
C(11)	0.7910(3)	0.5770(5)	0.2480(3)	3.5(3)	C(31)	0.725(1)	0.165(1)	0.5611(8)	3.2(6)
C(12)	0.7734(4)	0.5919(6)	0.1834(3)	4.8(3)	C(32)	0.650(1)	0.256(1)	0.5822(8)	3.5(6)
C(13)	0.8217(5)	0.6296(7)	0.1536(4)	6.5(5)	C(33)	0.627(1)	0.336(1)	0.517(1)	4.7(7)
C(14)	0.8848(5)	0.6543(7)	0.1856(4)	6.3(4)	C(34)	0.676(1)	0.328(1)	0.430(1)	4.9(8)
C(15)	0.9026(4)	0.6414(7)	0.2498(4)	6.1(4)	C(35)	0.746(1)	0.237(1)	0.4063(9)	5.1(8)
C(16)	0.8563(4)	0.6038(6)	0.2813(3)	5.0(3)	C(36)	0.770(1)	0.157(1)	0.473(1)	4.3(7)
C(21)	0.7024(3)	0.6453(5)	0.3274(3)	3.8(3)	H(1)	0.9401	0.0530	0.7572	3.5
C(22)	0.6465(4)	0.6990(6)	0.2958(4)	5.4(4)	H(2)	0.9651	0.2373	0.8015	5.4
C(23)	0.6309(5)	0.7914(7)	0.3214(5)	6.9(5)	H(3)	0.8584	0.2694	0.7271	5.4
C(24)	0.6718(6)	0.8251(7)	0.3770(6)	7.2(5)	H(4)	0.8261	0.1998	0.8129	5.4
C(25)	0.7263(5)	0.7734(7)	0.4087(4)	6.6(5)	H(5)	1.0379	0.0663	0.6163	6.1
C(26)	0.7426(4)	0.6821(6)	0.3841(3)	5.1(4)	H(6)	0.9932	0.1868	0.6058	6.1
C(31)	0.7684(3)	0.4486(5)	0.3508(3)	3.5(2)	H(7)	1.0939	0.1547	0.6846	6.1
C(32)	0.7420(4)	0.4349(5)	0.4045(3)	4.3(3)	H(12)	0.7626	-0.0054	0.8346	4.4
C(33)	0.7690(4)	0.3611(6)	0.4462(3)	5.5(4)	H(13)	0.5992	-0.0558	0.9308	5.4
C(34)	0.8215(4)	0.3018(6)	0.4363(4)	5.9(4)	H(14)	0.3861	-0.0399	0.8752	6.4
C(35)	0.8466(4)	0.3140(6)	0.3832(4)	5.8(4)	H(15)	0.3371	0.0269	0.7253	6.6
C(36)	0.8201(4)	0.3872(5)	0.3404(3)	4.5(3)	H(16)	0.5001	0.0855	0.6350	5.8
H(1)	0.7285	0.5773	0.1610	5.7	H(22)	0.6345	-0.0513	0.5053	5.6
H(2)	0.8094	0.6377	0.1087	8.1	H(23)	0.6513	-0.2245	0.4409	5.5
H(3)	0.9174	0.6799	0.1643	7.8	H(24)	0.8142	-0.3406	0.4912	4.7
H(4)	0.9470	0.6596	0.2740	7.4	H(25)	0.9629	-0.2835	0.6074	5.2
H(5)	0.8677	0.5972	0.3269	6.1	H(26)	0.9536	-0.1087	0.6710	4.1
H(6)	0.6181	0.6743	0.2576	6.4	H(32)	0.6159	0.2612	0.6421	4.0
H(7)	0.5931	0.8306	0.2994	8.4	H(33)	0.5768	0.3965	0.5324	5.5
H(8)	0.6617	0.8877	0.3934	8.6	H(34)	0.6609	0.3849	0.3858	5.8
H(9)	0.7538	0.7982	0.4471	8.1	H(35)	0.7772	0.2295	0.3462	6.0
H(10)	0.7813	0.6456	0.4057	6.2	H(36)	0.8190	0.0943	0.4574	4.9
H(11)	0.7061	0.4764	0.4125	5.3					
H(12)	0.7507	0.3504	0.4837	6.5					
H(13)	0.8389	0.2515	0.4680	7.0					
H(14)	0.8820	0.2720	0.3774	7.1					
H(15)	0.8374	0.3951	0.3030	5.4					
H(21)	0.6422	0.5195	0.2069	2.4					
H(22)	0.6459	0.3508	0.1799	6.2					
H(23)	0.5635	0.4219	0.2475	7.2					
H(24)	0.6180	0.4122	0.3107	7.2					
H(25)	0.7199	0.3934	0.1931	6.2					
H(26)	0.6964	0.3295	0.2443	6.2					
H(27)	0.5859	0.5157	0.2893	7.2					
Cl(1)	0.4928(2)	0.0338(4)	0.6221(3)	18.0(4)					
Cl(2)	0.3991(3)	0.0363(5)	0.5052(3)	19.0(4)					
C	0.4692(8)	0.099(1)	0.5515(8)	13(1)					
H(28)	0.4580	0.1681	0.5581	15.0					
H(29)	0.5071	0.1017	0.5294	15.0					

Table 5-3. Selected Intramolecular Distances for $[Ph_3PCH(CH_3)_2]_2(Mo_6O_{19})$ and $Ph_3PCH(CH_3)_2Cl$

atom	atom	distance	ADC(*)
MO1	O	2.313(1)	1
MO1	O11	1.678(5)	1
MO1	O12	1.893(4)	1
MO1	O13	1.955(5)	66503
MO1	O14	1.949(5)	66503
MO1	O15	1.897(5)	1
MO2	O	2.314(1)	1
MO2	O12	1.947(5)	1
MO2	O14	1.897(4)	1
MO2	O22	1.671(4)	1
MO2	O23	2.004(4)	66503
MO2	O24	1.848(4)	1
MO3	O	2.314(2)	1
MO3	O13	1.879(4)	1
MO3	O15	1.961(4)	1
MO3	O23	1.857(4)	1
MO3	O24	1.996(4)	1
MO3	O33	1.672(5)	1
P	C1	1.798(7)	1
P	C11	1.802(6)	1
P	C21	1.789(7)	1
P	C31	1.785(6)	1
C1	C2	1.520(9)	1
C1	C3	1.521(9)	1
C11	C12	1.374(9)	1
C11	C16	1.389(8)	1
C12	C13	1.37(1)	1
C13	C14	1.34(1)	1
C14	C15	1.36(1)	1
C15	C16	1.36(1)	1
C21	C22	1.376(9)	1
C21	C26	1.395(8)	1
C22	C23	1.41(1)	1
C23	C24	1.37(1)	1
C24	C25	1.34(1)	1
C25	C26	1.40(1)	1
C31	C32	1.390(8)	1
C31	C36	1.378(9)	1
C32	C33	1.362(9)	1
C33	C34	1.37(1)	1
C34	C35	1.36(1)	1
C35	C36	1.37(1)	1

*** For $Ph_3PCH(CH_3)_2Cl$ ***

atom	atom	distance
P	C1	1.80(1)
P	C11	1.78(1)
P	C21	1.78(1)
P	C31	1.78(1)
C1	C2	1.54(1)
C1	C3	1.52(1)
C11	C12	1.37(1)
C11	C16	1.37(1)
C12	C13	1.41(1)
C13	C14	1.40(2)
C14	C15	1.37(2)
C15	C16	1.37(1)
C21	C22	1.38(1)
C21	C26	1.39(1)
C22	C23	1.39(2)
C23	C24	1.35(1)
C24	C25	1.38(1)
C25	C26	1.38(1)
C31	C32	1.41(1)
C31	C36	1.38(1)
C32	C33	1.37(1)
C33	C34	1.37(1)
C34	C35	1.39(2)
C35	C36	1.38(1)

Distances are in angstroms. Estimated standard deviations in the least significant figure are given in parentheses.

Table 5-4. Selected Intramolecular Bond Angles for $[Ph_3PCH(CH_3)_2]_2(Mo_6O_{19})$ and $Ph_3PCH(CH_3)_2Cl$

atom	atom	atom	angle
O	MO1	O11	177.6(2)
O	MO2	O22	175.7(2)
O	MO3	O33	177.5(2)
O12	MO1	O14	153.0(2)
O13	MO1	O15	153.0(2)
O12	MO2	O14	152.3(2)
O23	MO2	O24	153.6(2)
O13	MO3	O15	152.8(2)
O23	MO3	O24	153.5(2)
MO1	O	MO2	89.69(3)
MO1	O	MO3	89.82(3)
MO2	O	MO3	89.68(3)
MO1	O13	MO3	116.8(2)
MO1	O14	MO2	117.1(2)
MO2	O23	MO3	116.3(2)
C1	P	C11	111.4(3)
C1	P	C21	111.6(3)
C1	P	C31	107.8(3)
C11	P	C21	106.6(3)
C11	P	C31	109.1(3)
C21	P	C31	110.3(3)
P	C1	C2	109.9(5)
P	C1	C3	111.3(5)
C2	C1	C3	110.9(6)
P	C11	C12	121.5(5)
P	C11	C16	119.1(5)
C12	C11	C16	119.0(6)
C11	C12	C13	118.9(7)
C12	C13	C14	122.0(7)
C13	C14	C15	119.8(7)
C14	C15	C16	120.2(8)
C11	C16	C15	120.1(7)
C22	C21	C26	119.8(7)
C21	C22	C23	119.1(8)
C22	C23	C24	119.3(8)
C23	C24	C25	122.4(8)
C24	C25	C26	119.2(9)
C21	C26	C25	120.2(8)
P	C31	C32	119.8(5)
P	C31	C36	120.0(5)
C32	C31	C36	119.8(6)
C31	C32	C33	118.6(7)
C32	C33	C34	121.3(7)
C33	C34	C35	120.1(7)
C34	C35	C36	119.6(7)
C31	C36	C35	120.5(7)

**** For $Ph_3PCH(CH_3)_2Cl$ ****			
atom	atom	atom	angle
C1	P	C11	110.5(5)
C1	P	C21	111.2(5)
C1	P	C31	109.8(5)
C11	P	C21	105.8(5)
C11	P	C31	110.6(6)
C21	P	C31	108.9(5)
P	C1	C2	110.9(7)
P	C1	C3	111.6(7)
C2	C1	C3	109.4(9)
P	C11	C12	119.1(9)
P	C11	C16	121.3(9)
C12	C11	C16	119(1)
C11	C12	C13	121(1)
C12	C13	C14	118(1)
C13	C14	C15	120(1)
C14	C15	C16	120(1)
C11	C16	C15	122(1)
C22	C21	C26	120(1)
C21	C22	C23	120(1)
C22	C23	C24	121(1)
C23	C24	C25	119(1)
C24	C25	C26	121(1)
C21	C26	C25	119(1)
P	C31	C32	121.1(9)
P	C31	C36	120(1)
C32	C31	C36	119(1)
C31	C32	C33	120(1)
C32	C33	C34	121(1)
C33	C34	C35	121(1)
C34	C35	C36	118(1)
C31	C36	C35	122(1)

Angles are in degrees. Estimated standard deviations in the least significant figure are given in parentheses.

5-5. References

1. Carey, F.A.; Sundberg, R.J. *"Advanced Organic Chemistry"*, Part B, 2nd Ed., 1983, Plenum Press, New York.

2. Trindle, C.; Hwang, J.-T.; Carey, F.A. *J. Org. Chem.* **1973**, *38*, 2664.

3. Nugent, W.A.; Mayer, J.M. *"Metal-Ligand Multiple Bonds"*, John-Wiley & Sons, 1988.

4. Du, Y.H.; Rheinggold, A.L.; Maatta, E.A. *J. Am. Chem. Soc.* **1992**, *114*, 345-346.

5. Walba, D.M.; DePuy, C.H.; Grabowski, J.J.; Bierbaum, V.M. *Organometallics* **1984**, *3*, 498-499.

6. Lai, R., Le Bot, S., Baldy, A., Pierrot, M., Arzoumanian, H. *J. Chem. Soc., Chem. Commun.* **1986**, 1208-1209.

7. Arzoumanian, H.; Baldy, A.; Lai, R.; Metzger, J. Peh, M.-L.N.; Pierrot, M. *J. Chem. Soc., Chem. Commun.* **1985**, 1151-1152.

8. Arzoumanian, H.; Baldy, A.; Lai, R.; Odreman, A. Metzger, J.; Pierrot, M. *J. Organomet. Chem.* **1985**, *295*, 343-352.

9. Kaska, W.C., *Coord. Chem. Rev.* **1983**, *48*, 1.

10. Pope, M.T. *"Heteropoly and Isopoly Oxometallates"*, Spinger-Verlag, **1983**.

11. Lu, S.F.; Huang, J.Q.; Huang, Z.X.; Huang, J.L. *Jiegou Huaxue*, **1989**, *8(1)*, 27-30. Colton, R.; Hoskins, B.F.; Panagiotidou, P. *Aust. J. Chem.* **1988**, *41*, 1295-303.

12. Triki, S.; Ouahab. L.; Grandjfean, D. *Acta Crystallogr.* **1991**, *C47*, 645-647 and 1371-1373. Triki, S.; Ouahab, L.; Padiou, J.; Grandjean, D. *J. Chem. Soc., Chem. Commun.* **1989**, 1068-1070.

13. Pike, R.M.; Mayo, D.W.; Butcher, S.S; Hinkle, R.J. *J. Chem. Edu.* **1986**, *63(10)*, 2917-918.

14. Sheldrick, G.M. in *Crystallographic Computing 3*, (Eds. G.M. Sheldrick, C. Kruger, and R. Goddard); Oxford University Press, pp175-89.